

Durham E-Theses

Functionalization of solid surfaces by pulsed plasma polymerization

Cinzia Tarducci

How to cite:

Tarducci, Cinzia (2002) Functionalization of solid surfaces by pulsed plasma polymerization. Doctoral thesis, Durham University.

Use policy

The full-text may be used and/or reproduced, and given to third parties in any format or medium, without prior permission or charge, for personal research or study, educational, or not-for-profit purposes provided that:

- a full bibliographic reference is made to the original source
- a <https://etheses.durham.ac.uk/id/eprint/4157/> is made to the metadata record in Durham E-Theses
- the full-text is not changed in any way

The full-text must not be sold in any format or medium without the formal permission of the copyright holders.

Please consult the [full Durham E-Theses policy](#) for further details.

FUNCTIONALIZATION OF SOLID SURFACES BY PULSED PLASMA POLYMERIZATION

Cinzia Tarducci

Department of Chemistry
University of Durham

**A copyright of this thesis rests
with the author. No quotation
from it should be published
without his prior written consent
and information derived from it
should be acknowledged.**

A Thesis Submitted for the Degree of Doctor of Philosophy

2002



1 2 DEC 2003

ABSTRACT

Pulsed plasma polymerization provides a direct method for the functionalization of solid surfaces. Compared to low power continuous wave plasma conditions, it provokes very little monomer fragmentation and leads to high levels of structural retention.

The monomers investigated in this thesis contained a polymerizable double bond and either a perfluoro, epoxide, cyano, hydroxyl or furan functionality. Under pulsed conditions activation of the double bond occurs during the time on period and conventional intermolecular propagation reactions occur during the time off. In the case of dienes, cyclic structures are formed, via intramolecular propagation. The plasma polymers were investigated using X-ray photoelectron, infrared, ultraviolet/visible and secondary ion mass spectroscopies, nuclear magnetic resonance, contact angle and gel permeation chromatography.

Epoxide and hydroxyl functionalized solid surfaces could be further functionalized via conventional chemistry reactions. Furan functionalized solid surfaces were capable of undergoing Diels-Alder reactions. The cyano functionalized layers were found to readily complex silver ions from solution. Epoxide and cyano functionalized surfaces exhibited adhesive behavior.

DECLARATION

The work described herein was carried out in the Department of Chemistry, University of Durham, between October 1998 and September 2001. All the work is my own and no part of it has been submitted for a degree at this or any other university.

STATEMENT OF COPYRIGHT

The copyright of this thesis rests with the author. No quotation from it should be published without prior written consent and information derived from it should be acknowledged.

PUBLICATIONS

Tarducci, C.; Kinmond, E. J.; Badyal, J. P. S.; Brewer, S. A.; Willis, C. Epoxide Functionalized Solid Surfaces *Chemistry of Materials*, **2000**, *12*, 1884.

Tarducci, C.; Schofield, W. J.; Badyal, J. P. S.; Brewer, S. A.; Willis, C. Cyano Functionalization of Solid Surfaces *Chemistry of Materials*, **2001**, *13*, 1800.

Tarducci, C.; Badyal, J. P. S.; Brewer, S. A.; Willis, C. Diels-Alder Chemistry at Furan Ring Functionalized Solid Surfaces, Submitted for Publication.

Tarducci, C.; Badyal, J. P. S.; Brewer, S. A.; Willis, C. Catalytic Rhodium Centres at 2-Hydroxyethyl Methacrylate Plasma Polymer Surfaces, Submitted for Publication.

CONFERENCE ATTENDED

Gordon Research Conference on *Plasma Processing Science*, 13-18 August 2000 Tilton School, NH, USA.

ACKNOWLEDGEMENTS

Many thanks also to everyone in lab CG 98: Iain, Paul, Tom and Stephen for the AFM images, Wayne for the thickness measurements, Vincent for the Raman spectra and the help with the grazing angle, Christos for keeping me informed on the status of his car and computer, Corinne for the time spent together in Boston, Luke for his culture on cinema, and finally Declan, Elinor, Gisle, Ste, Simon G., Simon H. and Jonathan for all the time spent together.

Many thanks also to the glassblowers for mending the things I broke and creating odd devices, and the mechanical and the electrical workshop for contributing in various ways to my work.

A special thanks to Dr. Kenwright and all the NMR service for the NMR analysis and to Doug for the GPC measurements.

I would also like to thank my whole family in Italy for sustaining and constantly visiting me in Durham during these three years. I would also like to thank Fiorenza, Gigi, Cala and Valerio for constantly writing e-mails thus keeping me informed on what was going on in Florence.

Many thanks also to Edoardo, Claudia and Andrea, who were always by my side at the lunch table.

And finally an extremely special thanks to Dimitri, who helped me to never give up and without whom this thesis would not exist.

A mio nonno

To my granddad

Considerate la vostra semenza:
Fatti non foste a viver come bruti,
Ma per seguir virtute e conoscenza.

Dante Alighieri, La Divina Commedia,
Canto XXVI, 118

FUNCTIONALIZATION OF SOLID SURFACES BY PULSED PLASMA POLYMERIZATION.

1.	Scope of the Thesis	1
1.1.	Scope of the Thesis	1
1.2.	References	3
2.	Surface Functionalization by Plasma Polymerization	4
2.1.	Plasma Polymerization	4
2.1.1.	What is a Plasma	4
2.1.2.	Generation of a Glow Discharge	7
2.1.3.	Mechanism of Plasma Polymerization	8
2.1.4.	Continuous Wave versus Pulsed Plasma Polymerization	10
2.2.	Analysis of Plasma Polymers	11
2.2.1.	X-Ray Photoelectron Spectroscopy	11
2.2.2.	Infrared Spectroscopy	12
2.2.3.	Nuclear Magnetic Resonance	13
2.2.4.	Contact Angle	13
2.2.5.	Secondary Ion Mass Spectroscopy	14
2.2.6.	Atomic Force Microscopy	14
2.3.	References	15
3.	Experimental	16
3.1.	Plasma Polymerization	16
3.2.	Plasma Polymer Analysis	16
3.2.1.	X-ray Photoelectron Spectroscopy	16
3.2.2.	Infrared Spectroscopy	18
3.2.3.	Contact Angle	18
3.2.4.	Nuclear Magnetic Resonance	18
3.2.5.	Deposition Rate and Film Thickness	18
3.2.6.	Atomic Force Microscopy	18
3.2.7.	Raman Spectroscopy	18

3.2.8.	Ultraviolet-Visible Spectroscopy	18
3.2.9.	Gel Permeation Chromatography	19
3.3.	Adhesion	19
4.	Plasma Polymerization of 2,2,3,4,4,4-Hexafluorobutyl Methacrylate	20
4.1.	Introduction	20
4.2.	Experimental	20
4.3.	Results and Discussion	21
4.4.	Conclusions	26
4.5.	References	26
5.	Epoxide Functionalized Solid Surfaces	27
5.1.	Introduction	27
5.2.	Materials and Methods	28
5.3.	Results and Discussion	29
5.3.1.	Butadiene Monoxide Plasma Polymerization	29
5.3.2.	Allyl Glycidyl Ether Plasma Polymerization	30
5.3.3.	Glycidyl Methacrylate Plasma Polymerization	33
5.3.4.	Glycidyl Methacrylate Plasma Polymer Coatings	
Derivatization Reactions		40
5.3.4.1.	Carboxylic Acids	41
5.3.4.2.	Amines	43
5.3.4.3.	Dendrimers	45
5.3.5.	Adhesion	48
5.4.	Conclusions	50
5.5.	References	51
6.	Functionalization of Solid Surfaces with Cyano Groups	53
6.1.	Introduction	53
6.2.	Materials and Methods	54
6.3.	Results	54
6.3.1.	Plasma Polymerization of Fumaronitrile	54
6.3.2.	Plasma Polymerization of 2-Cyanoethyl Acrylate	56

6.4.	Discussion	60
6.5.	Conclusions	62
6.6.	References	62
7.	Plasma Deposition of 2-Hydroxyethyl Methacrylate	64
7.1.	Introduction	64
7.2.	Materials and Methods	65
7.3.	Results and Discussion	66
7.3.1.	Plasma Polymerization of 2-Hydroxyethyl Methacrylate	66
7.3.2.	Derivatization Reactions	72
7.3.2.1.	Reaction with Trifluoroacetic Anhydride	72
7.3.2.2.	Diethylchlorophosphite and Rh Absorption	75
7.3.2.3.	Zirconium tert- Butoxide and Multilayer Assemblies	78
7.4.	Conclusions	82
7.5.	References	82
8.	Plasma Polymerization of Difunctional Monomers	85
8.1.	Introduction	85
8.2.	Experimental	86
8.3.	Results and Discussion	87
8.3.1.	Ethylene Glycol Dimethacrylate Plasma Polymerization	87
8.3.2.	Methacrylic Anhydride Plasma Polymerization	89
8.3.3.	Diallyl Amine Plasma Polymerization	92
8.4.	Conclusions	95
8.5.	References	96
9.	Diels-Alder Chemistry at Furan Ring Functionalized Solid Surfaces	97
9.1.	Introduction	97
9.2.	Materials and Methods	98
9.3.	Results and Discussion	98
9.4.	Conclusions	103
9.5.	References	104

1. SCOPE OF THE THESIS

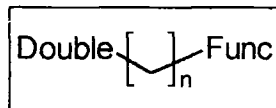
1.1. Scope of the thesis

The interaction between a material and the surrounding environment depends on its outermost layer, i.e. its surface. Surface related properties include wettability, adhesion and catalysis. Materials with desirable bulk mechanical characteristics often do not possess surfaces suitable for the needed applications. Tailoring surfaces at a molecular level allows the improvement of substrate performance without affecting the overall properties. This is fundamental for adhesion technology, biomedical applications, microelectronics, packaging, etc.

Plasma polymerization consists on the deposition of a thin polymeric film onto a substrate in contact with an ionized gas (plasma).¹ Other methods to produce polymeric thin films are spin coating and graft polymerization. The latter consists of the activation of the substrate by plasma, ion beam, electron beam, ultraviolet radiation, followed by immersion into a monomer solution for polymer growth. Compared to graft polymerization, plasma polymerization has the advantages to be solventless, single step, and above all substrate independent. However, the principal drawback is the lack of chemical control. Traditionally plasma polymers differ from conventional polymers since the monomer undergoes extensive fragmentation under plasma conditions and its chemical functionalities are not retained in the polymer films.¹ However, in recent years it has been shown that pulsing²⁻⁵ the electric discharge in the μs -ms timescale improves retention of monomer functionalities. Perfluoroalkyl,⁶⁻⁸ anhydride,⁹ alcohol,¹⁰ and amino¹¹ functionalized surfaces have been achieved under these conditions.

In this thesis plasma polymerization is investigated as a method to tailor surface properties by introducing on the surface specific functionalities. Plasma polymerization of monomers of the kind described in Structure 1.1 is investigated.





Structure 1.1.

General chemical structure of the monomer employed for plasma polymerization.

They possess a double bond in the form of allyl (Double = (CH₂=CH-CH₂-)), vinyl (Double = (CH₂=CH-)), acrylate (Double = (CH₂=CH-(C=O)O)) or methacrylate (Double = (CH₂=C(CH₃)-(C=O)O)) moiety and a functionality (Func) to be retained. In Table 1.1 a list of the functionalities and the monomer investigated is presented.

Table 1.1. Functionalities to be retained and monomers employed in this thesis.

Chapter 4	Fluoroalkyl	2,2,3,4,4,4-Hexafluorobutyl methacrylate
Chapter 5	Epoxide	Glycidyl methacrylate
		Butadiene monoxide
		Allyl glycidyl ether
Chapter 6	Cyano	2-Cyanoethyl acrylate
		Fumaronitrile
Chapter 7	Hydroxyl	2-Hydroxyethyl methacrylate
Chapter 8	Double bond	Ethylene glycol dimethacrylate
		Diallyl amine
		Methacrylic anhydride
Chapter 9	Furan	Furfuryl methacrylate

It has been observed that the lower the power applied in the plasma under continuous wave conditions the higher the retention of the original monomer structure. So in order to assess the effectiveness of the pulsed plasma polymerization as a method to selectively functionalize surfaces, a comparison between the lowest power continuous wave and the pulsed plasma conditions is made. Unless otherwise stated, the continuous wave experiments are performed at the lowest power achievable by the reactor, i. e. 3W, and the pulsed plasma experiments are performed at a duty cycle of 20 μs time on and 20 ms time off, with a peak power of 40 Watts. This duty cycle has been found to give the best results in terms of functionality retention for perfluoroacrylates,¹² and the possibility to apply it to other monomers is here investigated. The plasma polymer

coatings are fully characterized by a variety of analytical techniques (X-ray photoelectron spectroscopy, Fourier transform infrared spectroscopy, contact angle, etc). Plasma polymer modified surfaces are further investigated for their possible derivatization via conventional chemistry pathways or for the possibility to promote adhesion.

1.2.References

- [1] Yasuda, H. *Plasma Polymerization*; Academic Press: New York, 1985.
- [2] Savage, C. R.; Timmons, R. B. *Chem. Mater.* **1991**, *3*, 575.
- [3] Panchalingam, V.; Chen, X.; Savage, C. R.; Timmons, R. B.; Eberhart, R. C. *J. Appl. Polym. Sci.* **1994**, *54*, 123.
- [4] Han, L. M.; Timmons, R. B.; Bagdal, D.; Pielichowski *Chem. Mater.* **1998**, *10*, 1422.
- [5] Han, L. M.; Timmons, R. B. *J. Polym. Sci., Part A: Polym. Chem.* **1998**, *36*, 3121.
- [6] Coulson, R. S.; Woodward, I.; Badyal, J. P. S.; Brewer, S. A.; Willis, C. *Chem. Mater.* **2000**, *12*, 2031.
- [7] Coulson, R. S.; Woodward, I.; Badyal, J. P. S.; Brewer, S. A.; Willis, C. *Langmuir* **2000**, *16*, 6287.
- [8] Coulson, R. S.; Woodward, I.; Badyal, J. P. S.; Brewer, S. A.; Willis, C. *J. Phys. Chem. B* **2000**, *104*, 8836.
- [9] Ryan, M. E.; Hynes, A. M.; Badyal, J. P. S. *Chem. Mater.* **1996**, *8*, 37.
- [10] Rimsch, C. L.; Chem, X. L.; Panchalingam, V.; Eberhart, R. C.; Wang, J. H.; Timmons, R. B. *Langmuir* **1996**, *12*, 2995.
- [11] Rimsch, C. L.; Chem, X. L.; Panchalingam, V.; Savage, C. R.; Wang, J. H.; Eberhart, R. C.; Timmons, R. B. *Abstr. Pap. Am. Chem. Soc. Polym.* **1995**, *209*, 141.
- [12] Coulson, S. R. *Liquid Repellent Surfaces*; University of Durham: Durham, 1999.

2. SURFACE FUNCTIONALIZATION BY PLASMA POLYMERIZATION

2.1. Plasma Polymerization

2.1.1. What is a Plasma

A plasma is an ionized gas in which the concentrations of positive and negative charge carriers are approximately equal.¹ Other than ions, a plasma is constituted of photons, radicals, electrons and neutral molecules. These species are chemically active and can react producing new compounds. Plasma chemistry deals with the occurrence of these reactions.

The state of plasma can be created by strong electric and magnetic fields.² The electric field transfers energy to free electrons (e^-) and accelerates them. These electrons transmit their energy to neutral gas species through collisions. If the energy transferred is higher than the ionization potential of the molecule (M) ionization occurs:



This process produces an avalanche of electrons, thus igniting the plasma.

Ionization competes with recombination of ions and free electrons:



The gas must receive constant inputs of energy to offset the recombination of the charged particles and to remain ionized.

Other than ionization collisions can cause excitation and dissociation.

- Excitation



The molecules excited to a higher electronic level (M^*) can return to their

fundamental energy by emission of a photon



- Dissociation:



where M_i and M_j represent two different fragments of the original molecule M .

Because the energy of plasma electrons is much higher than a chemical bond energy, the molecules in a plasma are essentially randomized, breaking down into all conceivable fragments. Fragments can be either radicals or ions.

The physical and chemical properties of a plasma depend on the conditions employed for its production. Figure 2.1 illustrates the characteristics for a number of “plasmas” in terms of electron density and temperature.

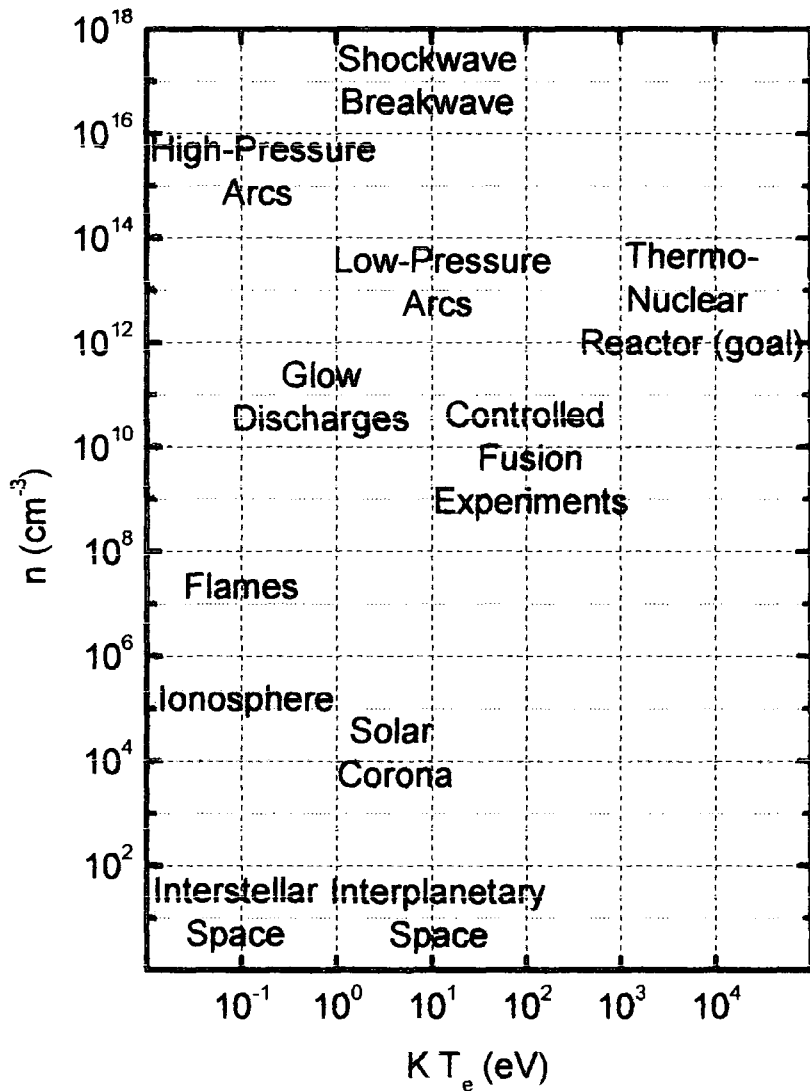


Figure 2.1.

Typical plasmas characterized by their electron energy and density³

The plasma in the region of “glow discharge” (1-10 eV of electron energy and electron densities of 10^9 - 10^{12} per cm^3) is characterized by electrons which are sufficiently energetic to induce ionization in the gas molecules and thus to sustain the plasma. However, the gas temperature remains near the ambient value. For these reasons glow discharges are also termed cold or non-equilibrium plasmas. Glow discharges are well suited for the promotion of chemical reactions involving thermally sensitive materials and are the ones of greatest importance for surface modification.³

2.1.2. Generation of a Glow Discharge

As already stated a glow discharge is produced by transfer of electric power to primary electrons in a gas. The gas is usually maintained at low pressure in order to minimize the recombination process. To have a stable and continuous plasma an AC discharge must be employed. A DC discharge would in fact rapidly extinguish because of the rapid charging of any insulating material in contact with it.² In order to maximize the collisions between electrons and gas molecules, high frequencies must be employed. Under these conditions in fact the electrons will move rapidly only near their position without hitting the walls of the reactor. Such collisions would in fact extinguish the electron energy without causing any ionization.

Most common generators have fixed frequencies and variable power. The frequency used is usually 13.56 MHz. This value was alluded by international authorities as “ the one at which it is possible to radiate a certain amount of energy without interfering with communications”.²

The energy is usually transferred by inductive coupling (Figure 2.2.). For high frequencies direct contact between the electrodes and the gas is no longer required, so a coil wrapped around the glass vessel is usually employed. A matching network between the RF generator and the glow discharge must be used for maximizing the power dissipation in the discharge. The matching network is a load that can be varied to match the output impedance of the generator.

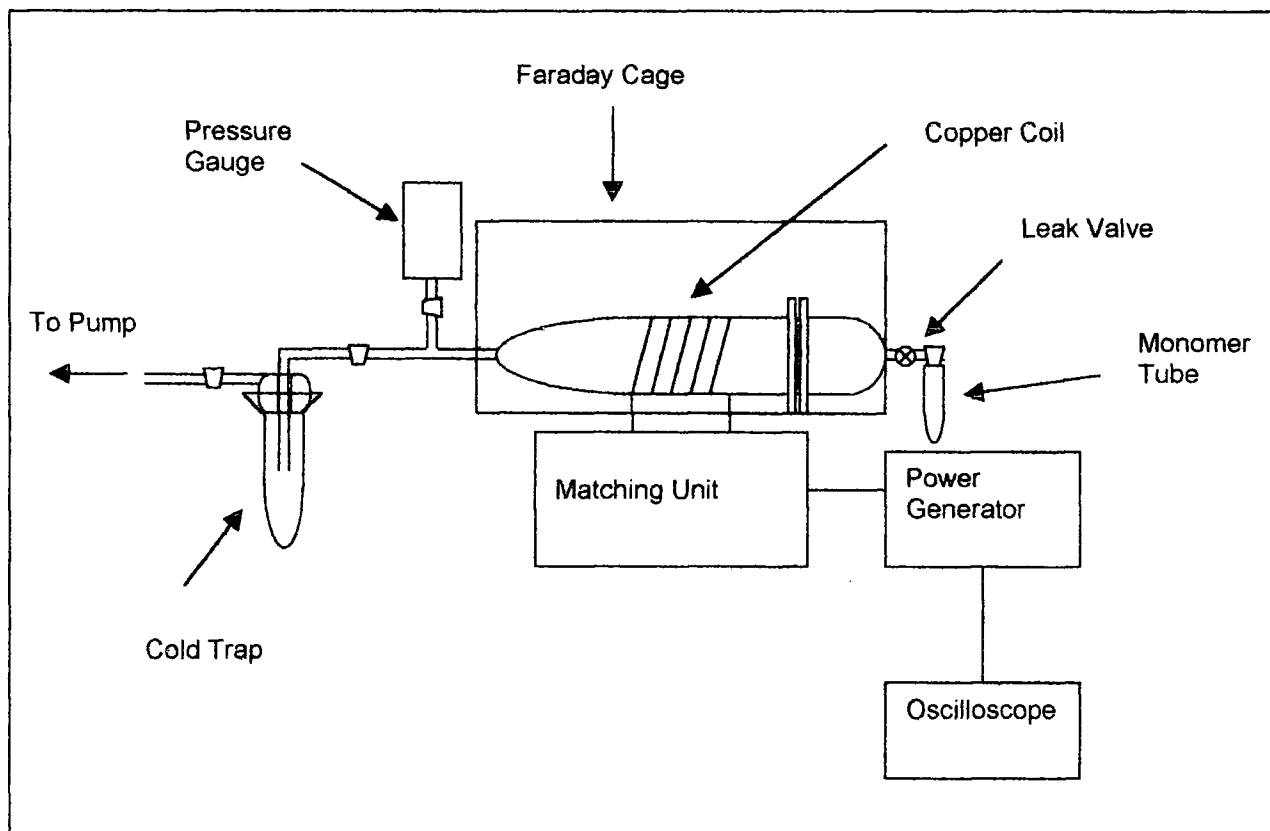


Figure 2.2.

Schematic representation of a typical reactor for the production of glow discharges

2.1.3. Mechanism of Plasma Polymerization

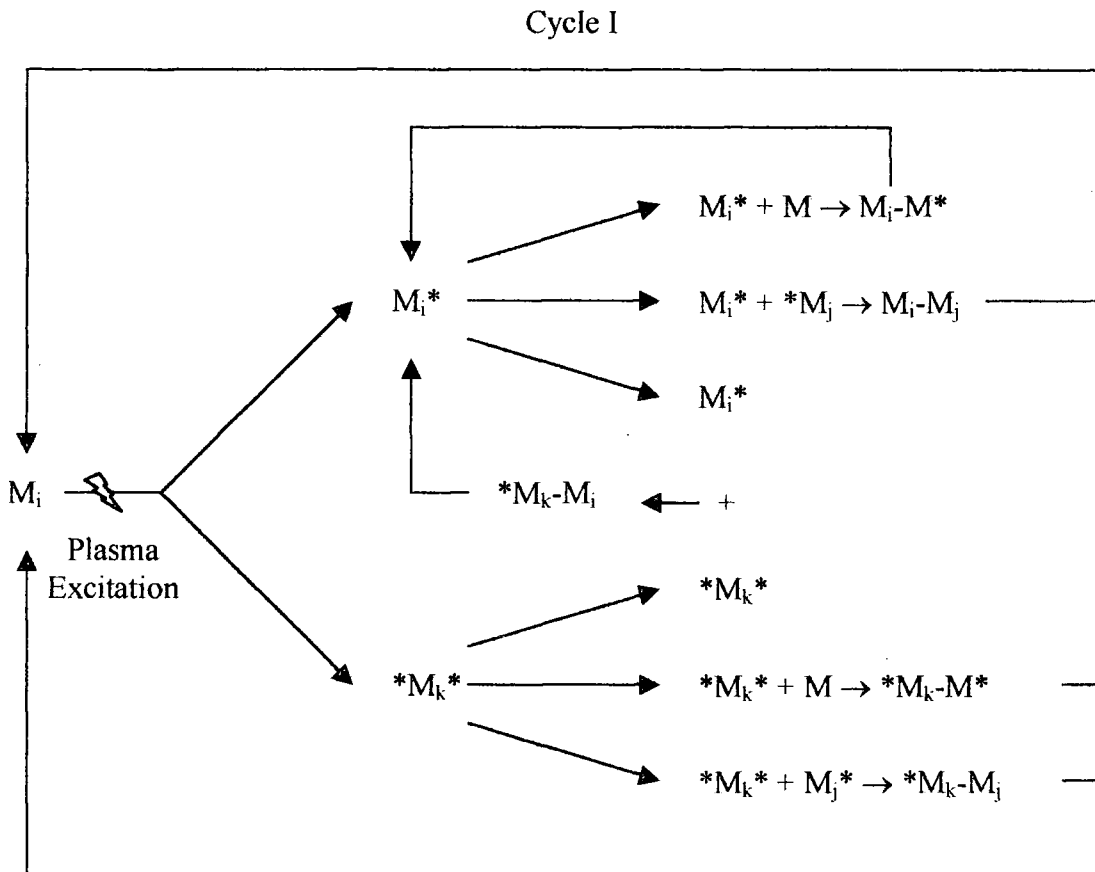
Plasma polymerization is a complex process involving:⁴

- Reactions between plasma species;
- Reactions between plasma and surface species;
- Reactions between surface species.

Traditionally two mechanisms of plasma polymerization are described: plasma induced polymerization and plasma state polymerization.¹ The first refers to a conventional polymerization mechanism in which the plasma acts as “initiator”. The reaction occurs via breakage of an active bond (e.g. C=C) and successive chain growth polymerization. The second refers to a mechanism involving active species produced by breakage of any bond, Scheme 2.1. Plasma state polymerization can be described as a step-growth polymerization: any active species produced in the plasma react and

produce species that are further activated by the plasma. Unconventional monomers such as alkanes and benzene originate high molecular weight material during this process. Due to the low-pressure environment plasma induced polymerization is believed to provide only a small contribution to the overall process.

Scheme 2.1. Mechanism of plasma state polymerization.¹



In Scheme 2.1 M_x ($x = i, j, k$) refers to a neutral species (original monomer or any of the dissociation products), M^* is any activated species (radical or ion) capable of participating to a chemical reaction to create covalent bonds, and $*M^*$ is a di-functional active specie. The subscripts i, j and k indicate a difference in the size of species involved.

Plasma polymerization is highly dependent on a variety of parameters:⁴

- Frequency of exciting potential.
- Excitation power (W).
- Monomer flow rate.
- Plasma pressure.

- Geometry (reactor shape and dimensions, positioning of samples, etc).
- Temperature.

Variation of any of these leads to coatings with different properties.

2.1.4. Continuous Wave versus Pulsed Plasma Polymerization

The polymers produced under plasma state mechanism differ from conventional polymers because they lack a repeat unit. Extensive monomer fragmentation in the plasma produces highly cross-linked materials. Another characteristic of plasma polymers is that they usually contain trapped free radicals.¹

Higher retention of monomer structure can be achieved by limiting power input, working at relatively high pressures, cooling of the substrate, afterglow positioning of the substrates.⁴ However the best results achieved so far are by pulsing the electric discharge. Even linear polymers have been synthesized in this way.⁵

A mechanism that explains the reactions occurring under pulsed plasma conditions is not available yet. However, it is believed that three main factors play a key role in the process.

- Low power input^{5,6}

The average power ($\langle P \rangle$) delivered by the system during pulsing is given by the following expression:

$$\langle P \rangle = P_p \left(\frac{t_{on}}{t_{on} + t_{off}} \right)$$

(2.6.)

Where P_p is the power output of the power supply, t_{on} is the time that the plasma is on and t_{off} is the time that the plasma is off. It is clear that very low power output can be achieved during pulsing conditions.

- Kinetic⁷

Very short bursts of plasma provoke little monomer fragmentation. The species formed during the time on can undergo conventional polymerization reaction pathways during the time off.

- Ion bombardment^{8,9}

An insulating material in contact with a plasma (substrate) is biased to a negative potential (plasma sheath potential), which accelerates the ions in the plasma and causes a continuous bombardment. The plasma sheath potential produced during the time on dies off during the time off. Ion bombardment is thus drastically reduced during pulsed plasma polymerization.

2.2. Analysis of Plasma Polymers

Unlike conventional polymers, plasma polymers are in the form of highly cross-linked three-dimensional network coatings. Unless the plasma polymerization conditions lead to products that can be handled by conventional analytical tools (e.g. NMR, GPC, MS), the only possible approach is to rely on surface analysis.

2.2.1. X-Ray Photoelectron Spectroscopy

X-ray photoelectron spectroscopy (XPS) is a versatile surface sensitive technique. It consists on the irradiation of solid samples with soft X-ray and the monitoring of the kinetic energy of the emitted photoelectrons. The kinetic energy of the photoelectrons depends on the originating atom and can thus be used to obtain qualitative and quantitative information. Due to the loss in energy of the electrons emitted from the core of the sample, the technique is sensitive only to the outermost layer. Different depth sensitivities can be obtained by varying the angle between the substrate normal and the analyzer. In this way a vertical distribution of an element or functional group is obtained.¹⁰

Any element from the periodic table, with the exception of hydrogen, can be detected by XPS. Besides, it is sensitive to the chemical environment of atoms and can be used to identify functional groups. The binding energy of an electron in an atom is in fact influenced by the electron-withdrawing power of nearest neighboring atoms. Other

functional groups can be identified by reacting them with a specific reagent that contains an atom not present in the coating (label). Typical probes are bromine for C=C and trifluoroacetic anhydride for hydroxyl groups.¹¹

The principal drawback of the technique is the necessity to operate under ultra high vacuum conditions.¹² Particular care must also be taken on the cleanliness of the surface. In the case of organic polymers X-ray damage may limit the acquisition time and differential charging can give multiple peaks and make difficult the readability of the data. Differential charging is highly reduced in the case of thin films onto glass, where the secondary electrons from the substrate can neutralize the positive charge in the film.¹³

2.2.2. Infrared Spectroscopy

Infrared spectroscopy provides information on the chemical functionalities in the plasma polymer. It is complementary to XPS. For example, it can give evidence of carbon-carbon double bonds that are not distinguishable from carbon-carbon single bonds in the XPS signal. By comparison of the plasma polymer spectrum with that of the monomer and/or conventional polymer, information on the fragmentation and rearrangement of the monomer in the plasma can be obtained.

Transmission infrared spectra of plasma polymers can be obtained on coated NaCl or KBr discs. However, conventional transmission mode FT-IR can be unsuited for surface analysis. The total adsorption arising from changes at the surface could be too small to be measured. Infrared spectroscopy must be used in reflectance mode in order to be surface sensitive.

In attenuated total reflectance Fourier transform infrared spectroscopy (ATR-FT-IR) the sample is brought into intimate contact with a prism. The prism is made of infrared transmitting material of high refractive index. When the infrared radiation is passed through, it is totally reflected by the prism, but eventually attenuated by the sample. As a result the absorption spectrum is recorded. ATR is useful to analyze pure liquids or coated NaCl or KBr discs.¹⁴

The absorption spectrum of molecules in a thin layer on the metal surface can be measured with light coming at a grazing angle, going through the surface layer, being reflected at the metal and going back again through the layer. Grazing incidence angle

greatly amplifies the sensitivity of the instrument and even monolayers can be analyzed by this method.¹⁴

2.2.3. Nuclear Magnetic Resonance

Plasma polymers in the form of insoluble coatings can be analyzed only by solid state NMR. However, under pulsed conditions it has been shown that plasma polymerization leads to soluble linear polymers.⁵ The polymer, collected from the reactor vessel following polymerization, can be analyzed by liquid NMR.

The principal drawback of the technique is that it requires high deposition rates in order to obtain the amount of material necessary for the analysis.

2.2.4. Contact Angle

The contact angle (θ) is the angle between the solid surface and the tangent of the liquid/vapour interface of a sessile drop, Figure 2.3. It gives a measure of the affinity of the liquid for the solid.

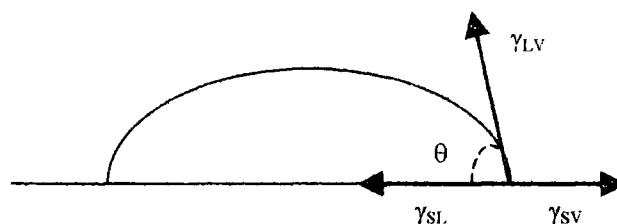


Figure 2.3.

Schematic representation of the contact angle of a liquid drop onto a solid substrate

The Young's equation (2.7.) relates the contact angle to the surface tensions between the solid and the liquid phase(γ_{SL}), between the solid and the vapour phase(γ_{SV}) and between the liquid and the vapour phase(γ_{LV}):¹⁵

$$\gamma_{SV} = \gamma_{SL} + \gamma_{LV} \cos \theta$$

(2.7.)

The surface tension (or surface free energy) is considered to be a measure of the attractive intermolecular forces at the interfaces. These forces are Van der Waals

interactions and can be divided into a dispersion component (forces arising from instant dipole moments) and a polar component (forces due to permanent dipoles):¹⁶

$$\gamma_s = \gamma_s^D + \gamma_s^P$$

(2.8.)

$$\gamma_L = \gamma_L^D + \gamma_L^P$$

(2.9.)

The measurement of the contact angle of minimum two liquids on a solid surfaces leads to the determination of the components of the surface tension of the solid via the Owens-Wedt equation. ¹⁶

$$(1 + \cos \theta) \gamma_L = 2 \left(\sqrt{\gamma_s^D \gamma_L^D} + \sqrt{\gamma_s^P \gamma_L^P} \right)$$

(2.10.)

2.2.5. Secondary Ion Mass Spectroscopy

Secondary Ion Mass Spectrometry (SIMS) consists on the bombardment of the sample with a primary ion beam. The material sputtered from the surface (elemental and cluster ions) is analyzed to produce positive and negative ions mass spectra. Peaks can derive from side chains, fragment of side chains and peaks due to multiple repeat unit. .

SIMS analysis of plasma polymer can provide valuable information on monomer retention and linearity of the chains produced.^{11, 17}

2.2.6. Atomic Force Microscopy

Atomic force microscopy (AFM) gives information on surface topology. It consists on scanning a sharp probe across the surface and measuring the interaction forces between the probe and the surface structural features. The probe is a cantilever placed parallel to the surface with a sharp force-sensing tip at its end. As the interaction forces between the tip and the surface vary, deflections are produced and measured.

In order to limit sample damagement, polymer are analysed in tapping or non contact mode. In this case the position of the cantilever is oscillated at high frequencies and the variation of oscillating frequency is detected.¹⁴

2.3. References

- [1] Yasuda, H. *Plasma Polymerization*; Academic Press: New York, 1985.
- [2] Chapman, B. *Glow Discharge Processes*; John Wiley & Sons: New York, 1980.
- [3] McTaggart, F. K. *Plasma chemistry in electrical discharges*, 1967.
- [4] Morosoff, N. In *Plasma Deposition, Treatment and Etching of Polymers*; R. D'Agostino, Ed.; Academic Press: New York, 1990.
- [5] Han, L. M.; Timmons, R. B. *J. Polym. Sci., Part A: Polym. Chem.* **1998**, *36*, 3121.
- [6] Han, L. M.; Timmons, R. B.; Bagdal, D.; Pielichowski, J. *Chem. Mater.* **1998**, *10*, 1422.
- [7] Mackie, N. M.; Castner, D. G.; Fisher, E., R. *Langmuir* **1998**, *14*, 1277.
- [8] Leich, M. A.; Mackie, N. M.; Williams, K. L.; Fisher, E., R. *Macromolecules* **1998**, *31*, 7618.
- [9] Panchalingam, V.; Chen, X.; Huo, H.-H.; Savage, C. R.; Timmons, R. B.; Eberhart, R. C. *ASAIO J.* **1993**, M305.
- [10] Prutton, M. *Surface Physics*; 2nd ed.; Oxford University Press: Oxford, 1983.
- [11] Briggs, D. In *Comprehensive Polymer Science*; G. C. Eastmond, A. Ledwith, S. Russo and P. Sigwalt, Ed.; Pergamon Press: Oxford, Vol. 1 ;1989.
- [12] Riviere, J. C. In *Practical Surface Analysis by Auger and X-ray Photoelectron Spectroscopy*; D. Briggs and M. P. Seah, Ed.; John Wiley & Sons: New York, 1983.
- [13] Beamson, G.; Briggs, D. *High resolution XPS of organic polymers: the Scienta ESCA300 database*; John Wiley & Sons: New York, 1992.
- [14] Riviere, J. C. In *Handbook of surface and interface analysis*, ; J. C. Riviere and S. Myhre, Eds.; Marcel Dekker: New York, 1998.
- [15] Padday, J. F. In *Handbook of Adhesion*; D. E. Peckham, Ed.; Longman, 1992.
- [16] Lee, L. H. In *Contact Angle, Wettability and Adhesion*; K. L. Mittal, Ed.; VSP: Utrecht, 1993.
- [17] Briggs, D.; Brown, A.; Vickerman, J. C. *Handbook of Static Secondary Ion Mass Spectrometry*; J. Wiley & Sons: New York, 1989.

3. EXPERIMENTAL

3.1. Plasma Polymerization

Plasma polymerization was carried out in a cylindrical glass reactor pumped by a mechanical rotary pump via a liquid nitrogen cold trap (base pressure = 10^{-2} torr, leak rate below 10^{-8} mol s⁻¹). A copper coil wrapped around the reactor was coupled to a 13.56 MHz radio frequency power supply via an LC matching network.

Prior to each experiment the chamber was cleaned with detergent and then using a 40 W air plasma at 0.2 torr for 30 min. The monomer, degassed using several freeze-pump-thaw cycles, was then introduced via a fine control needle valve followed by film deposition. Upon completion the reactor was purged with the monomer for 5 min. In the case of pulsed plasma polymerization, a signal generator was used to trigger the RF supply, and the pulse shape was monitored with an oscilloscope.

3.2. Plasma Polymer Analysis

3.2.1 X-Ray Photoelectron Spectroscopy

X-ray photoelectron spectroscopy (XPS) was performed using a Kratos ES 300 spectrometer equipped with a Mg K_α X-ray source and a hemispherical analyzer operating at a take-off angle of 30° from the substrate normal. Additional depth-profiling studies were undertaken by varying the take-off angle. The elemental composition was calculated using sensitivity factors derived from chemical standards, Table 3.1.

All binding energies were referenced to the C(1s) hydrocarbon peak at 285 eV. A Marquardt minimization computer program was used to fit core levels envelopes with fixed width gaussian peak shapes.

Table 3.1: Atomic sensitivity factors for Kratos ES 300 XPS spectrometer.

Peak	Sensitivity Factor
C (1s)	1
O (1s)	0.57
F (1s)	0.67
N(1s)	0.74
Si (2p)	1.02
Ag (3d _{5/2})	0.08
P (2p)	0.73
Cl (2p)	0.42
Zr (3d)	0.12
Rh (3d)	0.12

3.2.2. Infrared Spectroscopy

Infrared spectra were acquired on a Mattson Polaris (Chapters 4, 5, 6, 7, 8 (Figure 8.1)) or on a Perkin Elmer Spectrum One (Chapter 7, 8 (Figure 8.), 9) FT-IR instrument operating at a resolution of 4 cm⁻¹. The latter was equipped with both a DTGS and a liquid nitrogen cooled MCT detector.

Attenuated total reflectance (ATR) spectra were acquired using a diamond Graseby Specac Golden Gate accessory fitted to the spectrometer.

Reflectance absorption spectra were acquired using a grazing angle reflection accessory (Specac) fitted to the spectrometer.

3.2.3. Contact Angle

Sessile drop contact angle measurements were carried out at 20 °C using a video capture apparatus (A.S.T. Products VCA2500XE) and high purity water (B.S. 3978 Grade 1) or diiodomethane was employed as the probe liquid.

3.2.4. Nuclear Magnetic Resonance

NMR spectra of the deposited films were acquired using a Varian VXR-400S (Chapter 6) operating at 100.57 MHz for ^{13}C or a Bruker AM 250 (Chapter 6) spectrometer operating at 62.90 MHz and 250.13 MHz for ^1H and ^{13}C , respectively.

3.2.5. Deposition Rate and Film Thickness

Plasma polymer thickness was measured using a nkd-6000 spectrophotometer (Aquila Instruments Ltd). Transmission-reflectance curves (over the 350 – 1000 nm wavelength ranges) were fitted to a Cauchy model for dielectric materials using a modified Levenburg-Marquardt method.

Plasma polymer deposition rate (weight) was determined using a quartz crystal microbalance (Varian Model 985-7013).

3.2.6. Atomic Force Microscopy

Topographical images were acquired with a Digital Instrument Nanoscope III atomic force microscope. All images were acquired in air at room temperature using the tapping mode.

3.2.7. Raman Spectroscopy

Surface enhanced raman spectroscopy of plasma polymer films deposited onto rough silver was performed on a ISA LABRAM integrated raman system equipped with a HeNe laser (wavelength 632.8 nm, power 20 mW) a grating with 1800 grates per mm and a CCD detector.

3.2.8. Ultraviolet-Visible Spectroscopy

Uv/Visible spectra were acquired using a Unicam UV-4 spectrometer operating in absorbance mode.

3.2.9. Gel Permeation Chromatography

Gel permeation chromatography (GPC) was performed at 25°C using a Viscotek TDA 300 equipment, connected to a refractive-index detector. A series of three Plgel columns with pore sizes of 10^3 , 10^5 , and 100 Å was used for affecting the separation. Poly(ethylene oxide) standards were used for calibration, dimethyl fomamide (DMF) was used as an eluent (at 1 mL/min) and a volume of 100 µl of polymer dissolved in DMF was used for each measurements.

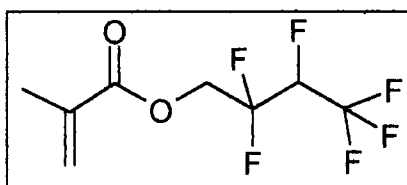
3.3. Adhesion

For adhesion measurements two strips of coated polymer (4 cm x 1 cm) were pressed together to form a joint (overlap about 1 cm²). Single lap and T-peel tests were carried out using an Instron 5543 tensilometer operating at a crosshead speed of 1 mm min⁻¹. For each value of maximum load reported, at least three measurements were averaged.

4. PLASMA POLYMERISATION OF 2,2,3,4,4,4-HEXAFLUOROBUTYL METHACRYLATE.

4.1. Introduction

In this study 2,2,3,4,4,4-hexafluorobutyl methacrylate (HFBMA), Structure 4.1, is chosen as the monomer since it contains the polymerizable acrylate group and a fluorocarbon functionality. Methacrylate plasma polymers have been successfully employed as electron beam resists for lithography processes¹ and conventional poly(fluoro methacrylates) have been shown to have better contrast than their unfluorinated homologues.^{2,3}



Structure 4.1.

2,2,3,4,4,4- Hexafluorobutyl methacrylate (HFBMA)

4.2. Experimental

Plasma polymerization of HFBMA (Lancaster, 97% purity) was carried out at a pressure of 2×10^{-1} torr. Glass slides were used for as substrate for XPS and contact angle analysis, NaCl discs were used for transmission infrared spectroscopy and a quartz slide was employed for UV/Vis absorption measurements.

Transmission infrared spectra were averaged over 100 scans for continuous wave plasma polymers and over 300 scans for the pulsed plasma polymer.

The values of contact angle reported were averaged on at least six measurements. The surface energy was calculated with the Owens Wedt equation (see Chapter 2)

4.3. Results and Discussion

XPS analysis of the deposited plasma polymer coating indicates the presence of carbon, oxygen and fluorine. No silicon could be detected from the underlying glass substrate.

A comparison between the lowest power continuous wave plasma polymer coating and the optimum pulsed conditions shows that, compared with the theoretical values, a higher fluorine concentration is present in the film deposited under pulsed plasma and an oxygen depletion occurs in the continuous wave plasma polymer coating (Table 4.1).

Table 4.1. XPS elemental percentage analysis of HFBMA plasma polymer coatings.

Coating	%F	%C	%O
Theoretical	37.5	50	12.5
Continuous Wave	35 ± 1	53 ± 1	9 ± 1
Pulsed	43 ± 1	41.4 ± 0.7	15 ± 1

The C(1s) envelope was deconvoluted into several peaks, each corresponding to a different carbon environment. (Table 4.2, Figure 4.1.).

Table 4.2. C(1s) peak assignments for the HFBMA pulsed plasma polymer ($t_{\text{on}} = 20\mu\text{s}$, $t_{\text{off}} = 20 \text{ ms}$, peak power = 40W).

Binding Energy (eV)	Carbon functionality
285.0	$\text{-}\underline{\text{C}}\text{H}_2^4$
285.8	$\underline{\text{C}}(\text{CH}_3)\text{C}=\text{O}^5$
287.4	$\text{O-}\underline{\text{C}}\text{H}_2\text{-CF}_2\text{-}^6$
288.8	$\underline{\text{C}}(=\text{O})\text{-O}^6$
289.8	$\underline{\text{C}}(\text{CF}_3)\text{-F}^7$
291.0	$\text{CH}_2\text{-}\underline{\text{C}}\text{F}_2\text{-CF}^7$
293.4	$\underline{\text{C}}\text{F}_3^7$

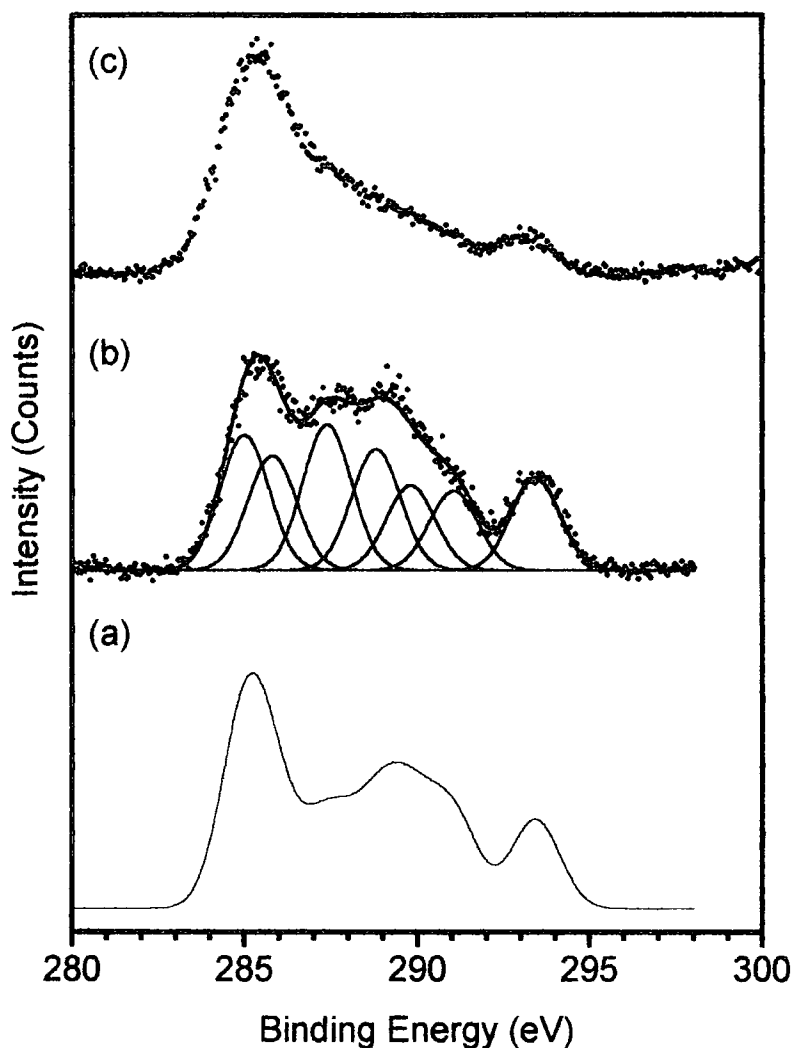


Figure 4.1.

XPS spectra of HFBMA plasma polymers deposited onto a flat glass substrate: (a) theoretical curve; (b) pulsed ($t_{\text{on}} = 20\mu\text{s}$, $t_{\text{off}} = 20\text{ ms}$, peak power = 40W); and (c) 3W continuous wave.

It is clear that the pulsed plasma polymer peak bears a stronger resemblance to the theoretically expected structure based on polymerization via the acrylate carbon-carbon double bond.

The CF_3 peak was well resolved and could be used to assess the degree of monomer functionality retention, Table 4.3.

Table 4.3. Percentage of carbon in CF₃ form as determined from the peak fitting

Coating	%C in CF ₃ form
Theoretical	6.2
Continuous wave	3.5 ± 0.8
Pulsed	6.1 ± 0.5

Transmission infrared spectra of the continuous wave and pulsed plasma polymer coatings are shown in Figure 4.2.

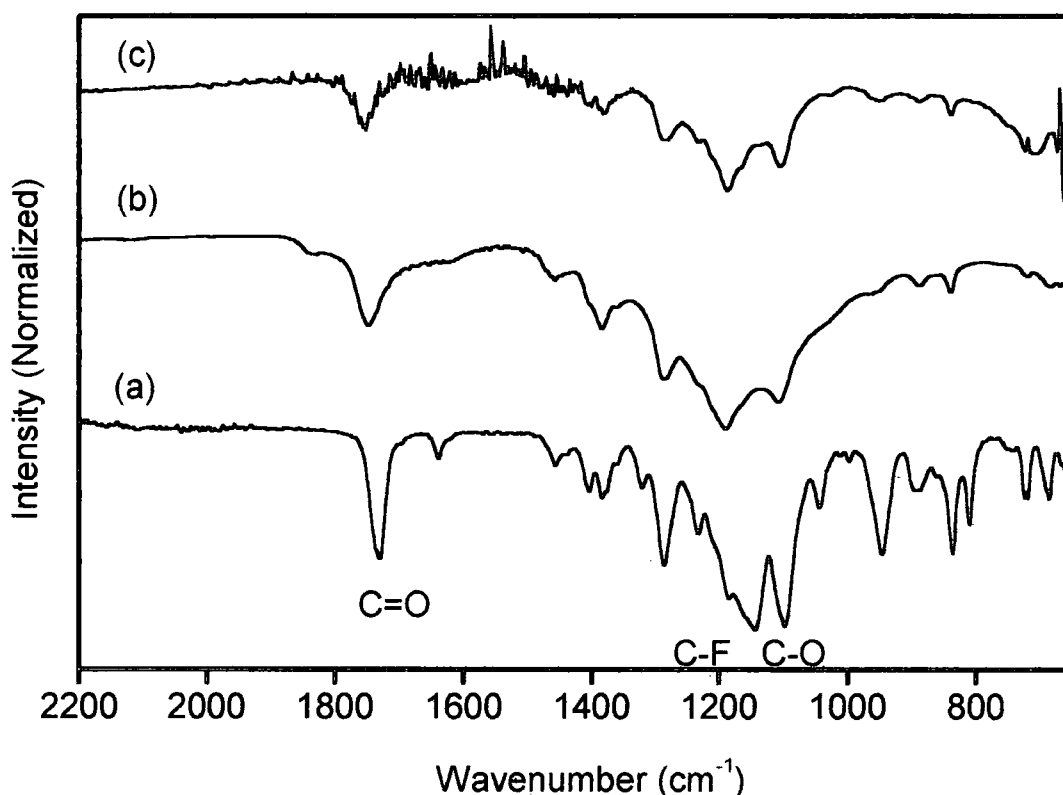


Figure 4.2.

Infrared spectra of: (a) HFBMA monomer, (b) HFBMA 3W continuous wave plasma polymer and (c) pulsed plasma polymer ($t_{\text{on}} = 20\mu\text{s}$, $t_{\text{off}} = 20\text{ ms}$, peak power = 40W)

The infrared spectrum of the HFBMA monomer showed the following assignments:⁸ C-H stretching (3000-2900 cm⁻¹), methacrylate C=O stretching (1730 cm⁻¹), methacrylate C=C stretching (1637 cm⁻¹), asymmetrical and symmetrical CH₃ bending modes (1456 cm⁻¹ and 1377 cm⁻¹) =CH₂ wagging (945 cm⁻¹), and =CH₂ twisting

(808 cm^{-1}). The multiple peaks in the 1300-1000 cm^{-1} region are the C-O and the C-F stretching.⁹

The 3 W continuous wave plasma polymer spectrum contained the following peaks: C-H stretching (3000-2900 cm^{-1}), C=O stretching (1830 cm^{-1} and 1749 cm^{-1}) C=C stretching(1627 cm^{-1}), CH₃ stretching (1451 and 1387 cm^{-1}). The region 1300-1000 cm^{-1} is less resolved than in the monomer spectrum and shows a strong and broad absorption peaks.

In the case of the pulsed plasma polymer the following band assignments could be made:C-H stretching (3000-2900 cm^{-1}), C=O stretching of unconjugated esters (1760 cm^{-1}), CH₃ bending at (1380 cm^{-1}). The 1300-1100 cm^{-1} region is better resolved than in the continuous wave plasma polymer spectrum

The plasma polymer coated samples were found to be hydrorepellent, Table 4.4.

Table 4.4. Contact angle and surface energy values for HFBMA plasma polymers.

Coating	Contact Angle with water (°)	Surface Energy (dyne/cm ²)
Continuous Wave	98 ± 2	36.3
Pulsed	89 ± 4	29.2

The higher concentration in fluorine in the pulsed plasma polymer coating should lead to a higher hydrophobicity (i.e. higher contact angle). Instead a lower value in contact angle compared to the continuous wave plasma polymer is observed. Further investigations on film morphology and thickness should be performed for a full understanding of this difference.

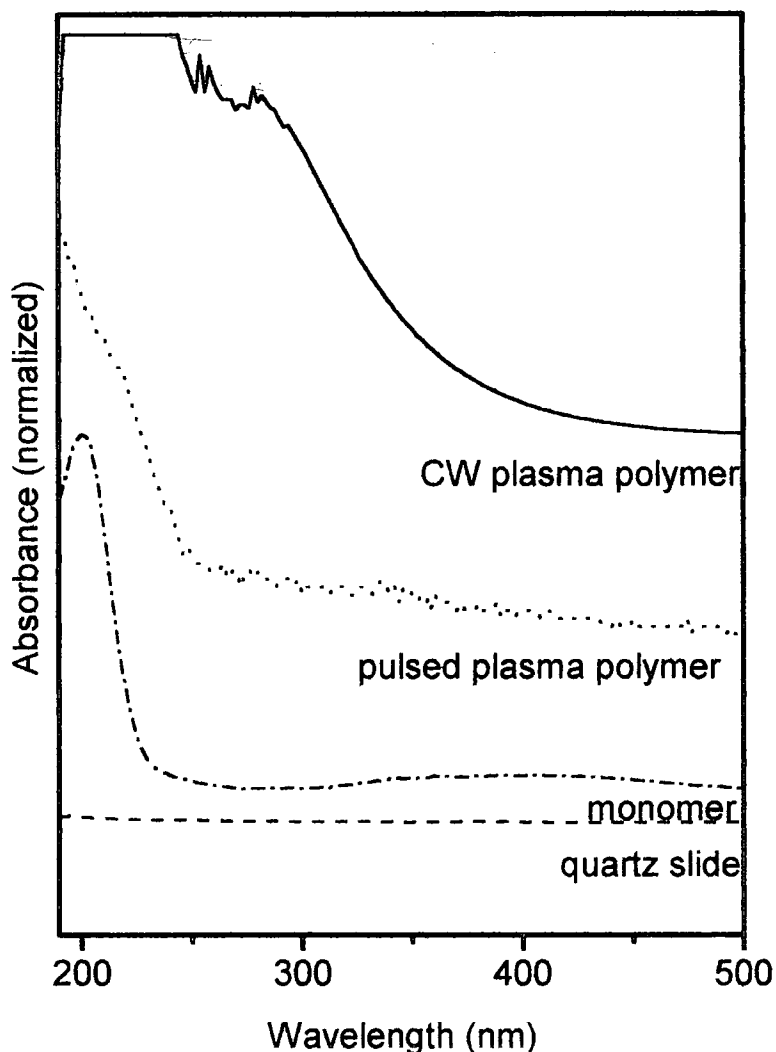


Figure 4.3.

UV/Vis spectra of HFBMA, HFBMA continuous wave plasma polymer and HFBMA pulsed plasma polymer

The absorption of the monomer at 200 nm is due to the $\pi \rightarrow \pi^*$ transition of the C=C bond conjugated to the C=O bond.¹⁰ The pulsed plasma polymer shows a maximum lower than 190 nm, which could be attributed to the $n \rightarrow \pi^*$ transition of the unconjugated carbonyl group.¹⁰ The very intense absorption of the CW plasma polymer around 200 nm is probably due to unsaturations, which can be present in methacrylates plasma polymers¹¹ as demonstrated by the infrared results.

4.4. Conclusions

XPS, IR and UV-Visible spectroscopies demonstrate that high levels of structural retention are obtained under pulsed conditions. Whereas, low power continuous wave plasma polymerisation leads to monomer fragmentation.

4.5. References

- [1] Morita, S.; Tamano, J.; Hattori, S.; Ieda, M. *J. Appl. Phys.* **1980**, *51*, 3938.
- [2] Kakuchi, M.; Sugawara, S.; Murase, K.; Matsuyama, K. *J. Electrochem. Soc.* **1977**, *124*, 1648.
- [3] Gokan, H.; Esho, S.; Ohnishi, Y. *J. Electrochem. Soc.* **1983**, *130*, 143.
- [4] Beamson, G.; Briggs, D. *High resolution XPS of organic polymers: the Scienta ESCA300 database*; John Wiley & Sons: New York, 1992.
- [5] Clark, D. T.; Thomas, H. R. *J. Polym. Sci.* **1976**, *14*, 1671.
- [6] Clark, D. T.; Thomas, H. R. *J. Polym. Sci.* **1976**, *14*, 1701.
- [7] Clark, D. T.; Feast, W. J.; Kilcast, D.; Musgrave, W. K. R. *J. Polym. Sci.* **1973**, *11*, 389.
- [8] Lin-Vien, D.; Colthup, N. B.; Fateley, W. G.; Grasselli, J. G. *The Handbook of Infrared and Raman Characteristic Frequencies of Organic Molecules*; Academic Press: New York, 1991.
- [9] Weiblen, D. G. In *Fluorine Chemistry*; J. H. Simmons, Ed., 1954; Vol. 2, pp 449.
- [10] Rao, C. N. R. *Ultraviolet and Visible Spectroscopy*; Butterworths: Markham, 1961.
- [11] Vickie, P. N.; Barrios, E. Z.; Denton, D. D. *J. Polym. Sci., Part A: Polym. Chem.* **1998**, *36*, 587.

5. EPOXIDE FUNCTIONALIZED SOLID SURFACES

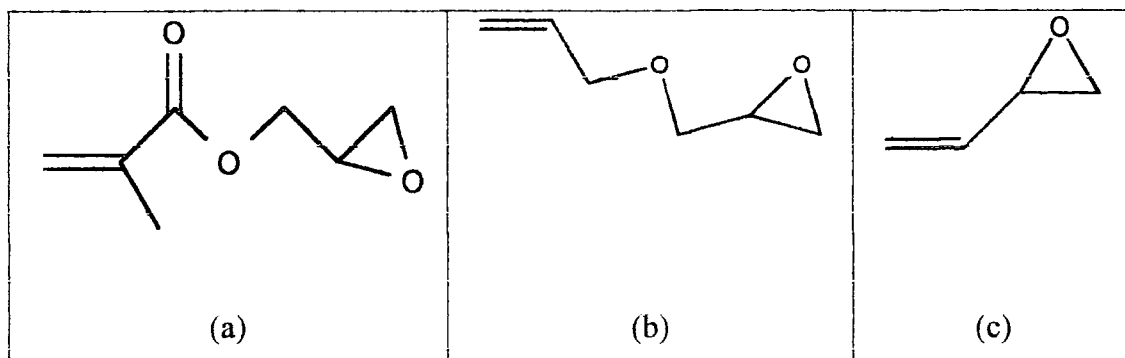
5.1. Introduction

An epoxide group is a three-membered ring cyclic ether. Due to the strain induced by the small ring an epoxide is highly reactive compared to linear ethers.¹

Epoxide rings containing molecules are fundamental in adhesion technology. Epoxy resins, for example, are composed of a primer, which contains reactive epoxide groups, and a curing agent or hardener. The latter is a compound, which has two or more reactive functional groups (typically a diamine) and upon reaction with the primer forms a rigid three-dimensional network.

Surface epoxide groups can provide binding sites for nucleophilic reagents,² such as amines.³⁻⁸ Important applications include biotechnology⁷⁻¹⁰ and adhesion.^{3, 11-14} Existing methods for incorporating epoxides onto solid surfaces involve UV^{5, 6, 9, 12} or electron beam irradiation⁷ of a substrate followed by immersion in a solution containing an initiator and a polymerizable epoxide monomer (e.g. glycidyl methacrylate) leading to polymer growth at the surface. Other possibilities comprise plasma activation of a substrate followed by solution phase grafting of a polymerizable epoxide monomer,^{4, 13} or alternatively the direct coupling of epoxysilanes onto silicon wafers.¹⁵ All of these approaches suffer drawbacks such as multistep processes, solution-phase chemistry, and a tendency for being substrate specific.

In this chapter the surface functionalization with epoxide groups by means of plasma polymerization is described. Unlike the existing methods this provides a solventless and one step route to surface modification. Three monomers have been investigated: glycidyl methacrylate (Structure 5.1.a), allyl glycidyl ether (Structure 5.1.b) and butadiene monoxide (Structure 5.1.c). They all present a polymerizable double bond and an epoxide group.



Structures 5.1.

Glycidyl methacrylate (a), allyl glycidyl ether (b) and butadiene monoxide(c)

5.2. Materials and Methods

Plasma polymerization of butadiene monoxide (Aldrich, 98% purity), allyl glycidyl ether (Aldrich, 98% purity) and glycidyl methacrylate (Aldrich, + 97 %), was carried out at a monomer pressure of 0.2 torr (glycidyl methacrylate flow rate: $1,2 \cdot 10^{-7} \text{ mol s}^{-1}$). In the case of glycidyl methacrylate films were deposited for 15 min. Flat glass substrates were employed for XPS and SIMS analysis and NaCl plates for transmission infrared analysis. In the latter case films were deposited for 1h. Butadiene monoxide films were deposited for 30 min, whereas allyl glycidyl ether films were deposited for 30 min and also for 1.5 h under pulsed conditions.

Vapour phase reactions with trifluoroacetic acid (Fluorochem Limited, + 99.5 %), ethylenediamine (Aldrich, + 99%) and diethylamine (Sigma, +98%) were performed by exposing the coated glass slides to the reagent vapour for 30 min followed by evacuation to remove any adsorbed remnants.

Solution phase derivatization was performed by immersing plasma polymer coated glass slides into a solution of the reagent in methanol (Fisher, +99 %) for 24 h. The samples were rinsed several times in pure methanol and the solvent eliminated under vacuum prior to analysis.

Reaction with generation 4 Pamam dendrimers (Aldrich, 10% w/v solution in methanol) were performed under nitrogen atmosphere by immersing the coated glass slides in a 1:1 dilution of the solution with methanol. The samples were rinsed several times in pure methanol and vacuum dried prior to analysis.

For the adhesion measurements a drop ($\sim 3 \mu\text{L}$) of a coupling agent solution (ethylenediamine, 0.5 M in 1,4-dioxane (Aldrich, +99 %)) was placed between two glycidyl methacrylate plasma polymer coated strips of polymer film (polyethylene, PE,

ICI, 0.08 mm thickness, or polytetrafluoroethylene, PTFE, Goodfellow, 0.25 mm thickness), and then cured in the oven at 60° for 18 h.

5.3. Results and Discussion

5.3.1. Butadiene Monoxide Plasma Polymerization

XPS analysis of butadiene monoxide plasma polymer coatings (Table 5.1.) showed that none of the deposited films possessed molecular structures that one would expect from the monomer when it undergoes conventional polymerization.

Table 5.1. Elemental analysis of the butadiene monoxide plasma polymers as determined by XPS.

Conditions	%C	%O	%Si
Theoretical	80	20	0
CW 3W	89 ± 2	11 ± 2	0
Pulsed	54 ± 4	35 ± 2	11 ± 2
Glass slide	23 ± 2	53 ± 1	24 ± 2

The film deposited by continuous wave method showed a depletion in oxygen content with respect to the theoretical value. No Si(2p) peak was observed from the glass substrate. The pulsed plasma technique produced very slow deposition rates, evidenced by the presence of Si in the XPS spectrum.

The following infrared band assignments could be made in the case of the monomer (Figure 5.1.):¹⁶ vinyl C-H stretching (3095 cm⁻¹ and 2996 cm⁻¹), epoxide C-H stretching (3054 cm⁻¹), saturated C-H stretching (2926 cm⁻¹), C=C stretching (1646 cm⁻¹), epoxide ring breathing (1250 cm⁻¹), antisymmetric epoxide deformation (909 cm⁻¹), symmetric epoxide deformation (824 cm⁻¹). The infrared spectrum of the continuous wave plasma polymer, indicated the presence of C=O groups (1730 cm⁻¹).¹⁶ It is difficult to determine whether a small amount of epoxide functionality is retained. The infrared spectrum of the pulsed plasma polymer layer was very weak. This is consistent with the existence of a very thin coating.

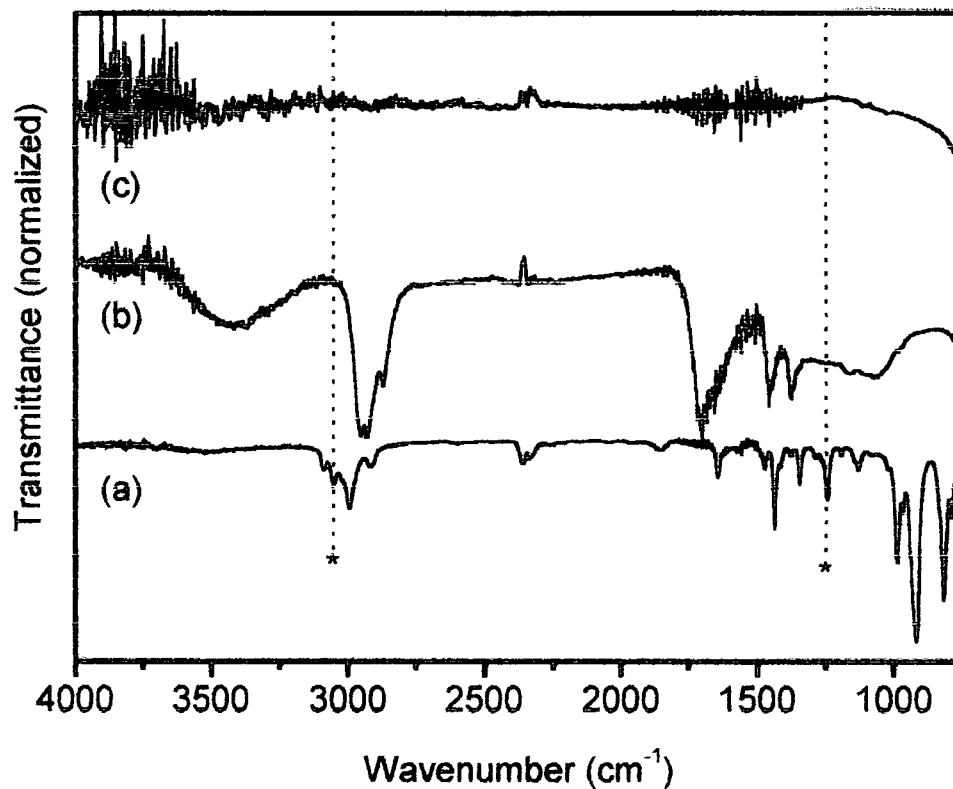


Figure 5.1.

Infrared spectra of (a) butadiene monoxide monomer; (b) 3 W continuous wave plasma polymer; and (c) pulsed plasma polymer (time on = 20 μ s, time off = 20 ms, peak power = 40 W). * denotes epoxide features

5.3.2. Allyl Glycidyl Ether Plasma Polymerization

XPS analysis on the plasma polymer coatings (Table 5.2.) showed depletion in oxygen in the continuous wave plasma polymer with respect to the theoretical value. No Si(2p) peak was observed from the glass substrate. The pulsed plasma environment instead did not produce a polymeric coating as determined by the presence of Si in the 90 min deposited film.

Table 5.2. Elemental analysis of the allyl glycidyl ether coatings as determined by XPS.

Conditions	%C	%O	%Si
Theoretical	75	25	0
CW 3W 30 min	86 ± 2	14 ± 2	0
Pulsed 30 min	49 ± 4	35 ± 3	16 ± 2
Pulsed 90 min	61 ± 2	30 ± 1	9 ± 2
Glass slide	23 ± 2	53 ± 1	24 ± 2

The C(1s) envelope of the continuous wave plasma polymer coating (Figure 5.2.) was characterized by a strong hydrocarbon peak (285.0 eV) but other functionalities are discernible such as $\underline{\text{C}}\text{-O}$ (286.5 eV) and $\underline{\text{C}}\text{=O}$ (288.2 eV).¹⁷ The latter functionality is not present in the monomer and could be due to rearrangement of the molecule in the plasma environment.

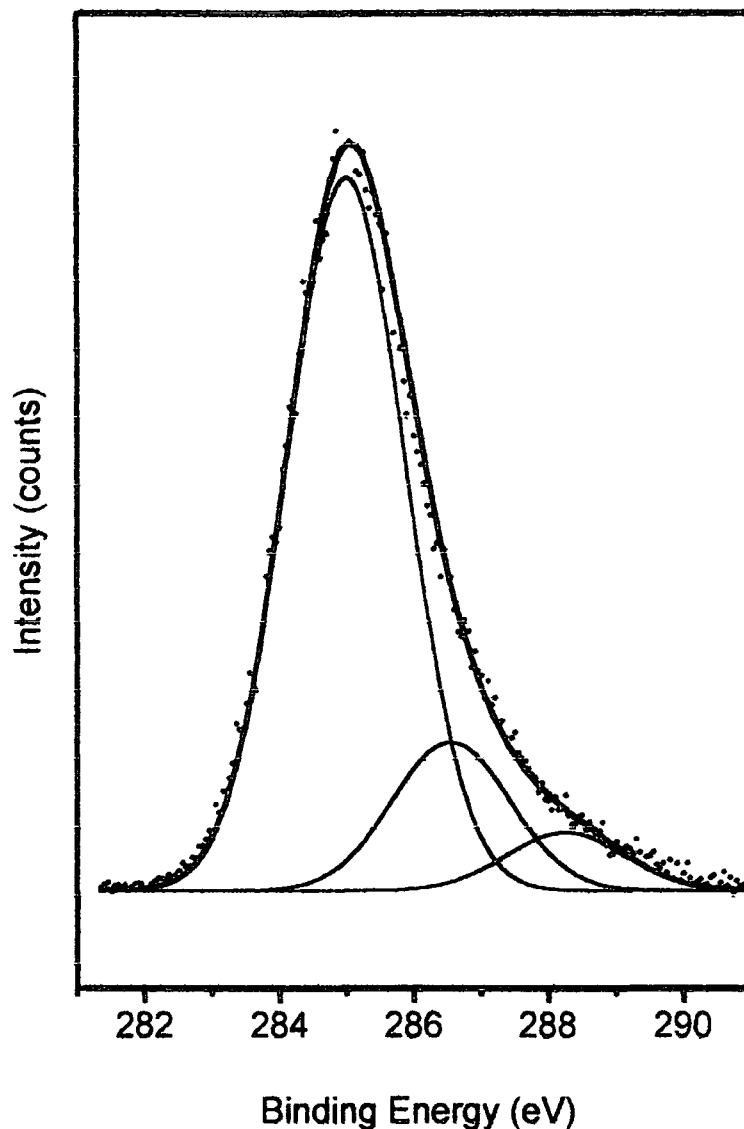


Figure 5.2.

C(1s) XPS spectra of 3 W continuous wave allyl glycidyl ether plasma polymers deposited onto a flat glass substrate.

The infrared spectrum of the monomer showed the following bands(Figure 5.3):¹⁶ allyl C-H stretching (3087 cm^{-1} and 2996 cm^{-1}), epoxide C-H stretching (3054 cm^{-1}), saturated C-H stretching (2926 cm^{-1} and 2855 cm^{-1}), C=C stretching (1658 cm^{-1}), epoxide ring breathing (1252 cm^{-1}), C-O stretching (1096 cm^{-1}), antisymmetric epoxide deformation (923 cm^{-1}), symmetric epoxide deformation (852 cm^{-1}). The continuous wave plasma polymer showed a small retention of epoxide functionality under continuous wave conditions and the presence of C=O at 1728 cm^{-1} .¹⁶ This peak overlaps with the C=C which has not completely disappeared.

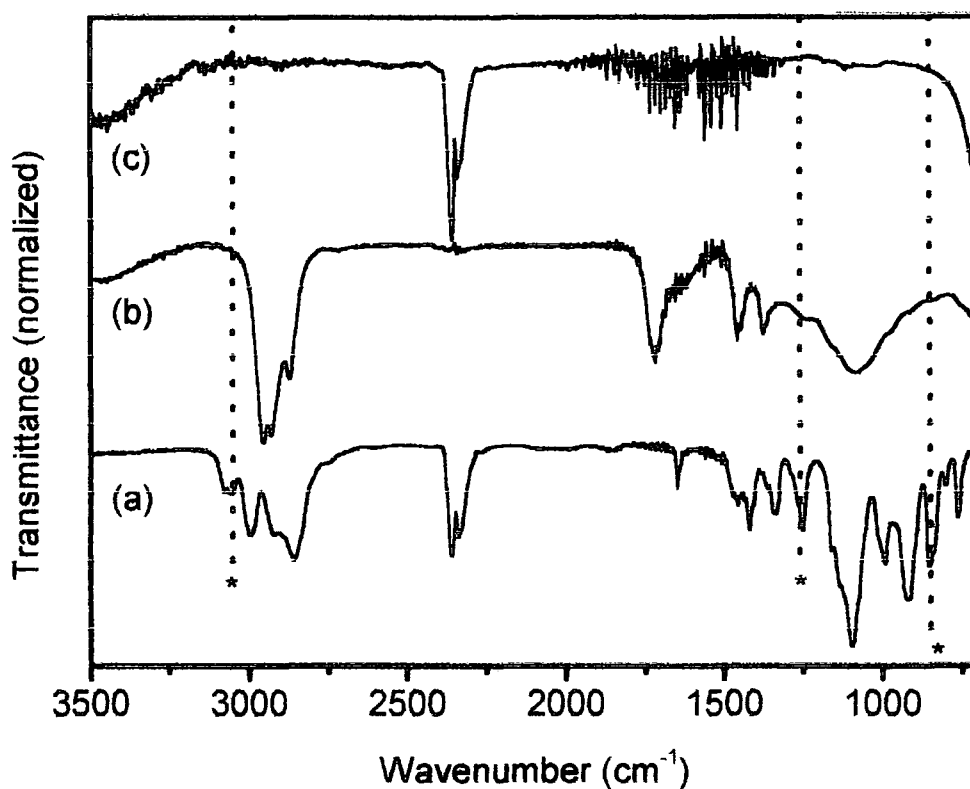


Figure 5.3.

Infrared spectra of (a) allyl glycidyl ether monomer; (b) 3 W continuous wave plasma polymer; and (c) pulsed plasma polymer (time on = 20 μ s, time off = 20 ms, peak power = 40 W).

5.3.3. Glycidyl Methacrylate Plasma Polymerization

XPS analysis of the glycidyl methacrylate plasma polymers shows only carbon and oxygen on the surface, with no Si (2p) signal showing through from the underlying glass substrate. The elemental percentage analysis for the continuous wave plasma polymer indicated a depletion of oxygen compared to the theoretical value expected from the polymerization via the double bond. The pulsed plasma polymer instead has an elemental composition that resembled those values, Table 5.3.

Table 5.3. XPS analysis of glycidyl methacrylate plasma polymers.

Conditions	C(1s)		Atomic %	
	% Epoxide	% (C=O)O	% C	% O
Continuous wave	7.1 ± 0.5	6.5 ± 0.5	77.5 ± 0.5	22.5 ± 0.5
Pulsed	19.1 ± 0.5	10.6 ± 0.3	73 ± 1	27 ± 1
Theoretical	20	10	70	30

The C(1s) envelope, Figure 5.4., contained a variety of carbon functionalities for both the continuous wave and the pulsed plasma polymer layers: $\underline{\text{C}}\text{H}_2$ (285.0 eV), $\underline{\text{C}}(\text{CH}_3)(\text{C}=\text{O})\text{O}$ (285.7 eV), $\text{O}-\underline{\text{C}}\text{H}_2-\text{CO}$ (286.7 eV), epoxide carbons (287.2 eV), $\underline{\text{C}}=\text{O}$ (287.8 eV) and $(\underline{\text{C}}=\text{O})\text{O}$ (289.1 eV). Apart from the carbonyl group at 287.8 eV (associated with the continuous wave plasma polymer), the remaining peak assignments are referenced to XPS spectra obtained from conventional solution phase polymerized glycidyl methacrylate.¹⁷ Pulsed plasma polymerization yielded a greater retention of epoxide and ester groups compared to the continuous wave conditions, when extensive fragmentation occurred.

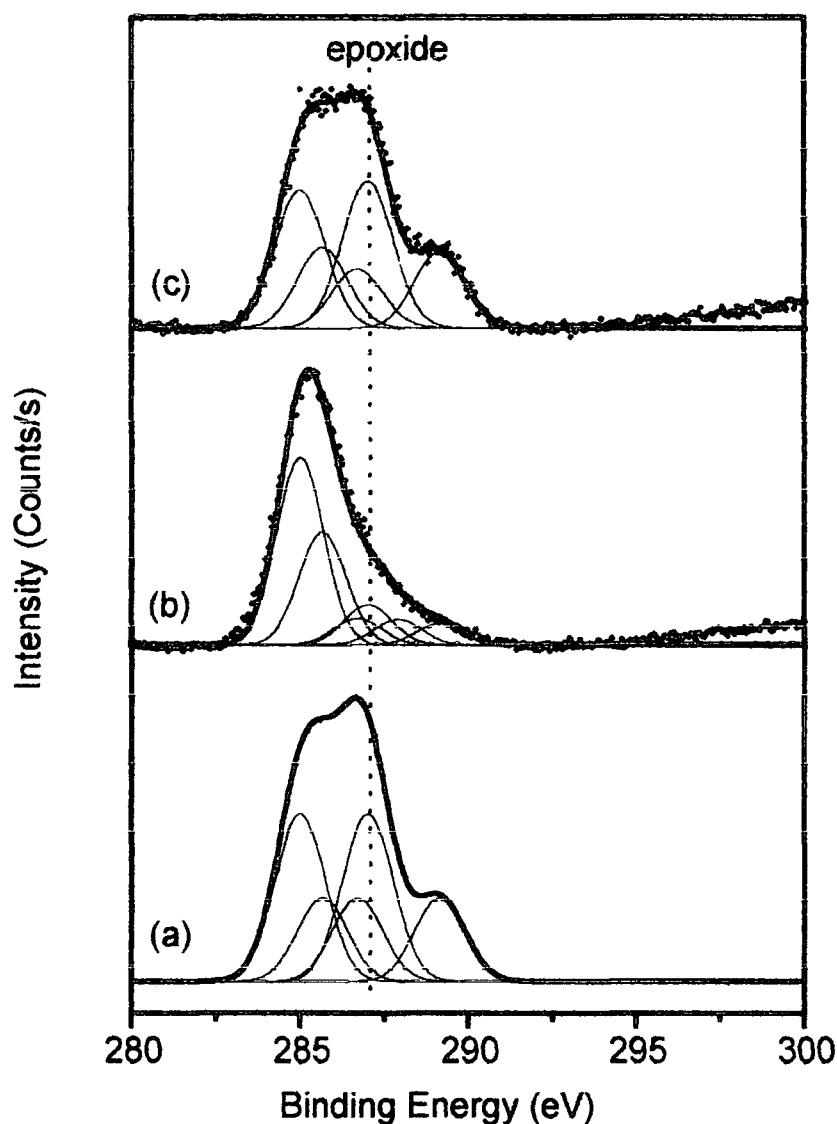


Figure 5.4.

C(1s) XPS spectra of glycidyl methacrylate plasma polymers deposited onto a flat glass substrate: (a) theoretical curve; (b) 3 W continuous wave; and (c) pulsed (time on = 20 μ s, time off = 20 ms, peak power = 40 W).

Infrared spectroscopy was used to probe the molecular structure of the plasma polymer coatings (Figure 5.5.). For the glycidyl methacrylate monomer the following band assignments were made:^{2, 16} epoxide ring C-H stretching (3063 cm^{-1}), C-H stretching ($3000\text{-}2900\text{ cm}^{-1}$), acrylate carbonyl stretching (1720 cm^{-1}), acrylate C=C stretching (1637 cm^{-1}), epoxide ring breathing (1253 cm^{-1}), antisymmetric epoxide ring deformation (908 cm^{-1}), and symmetric epoxide ring deformation (842 cm^{-1}). The weak absorption feature at 2360 cm^{-1} can be attributed to background CO_2 present in the spectrometer. Continuous wave plasma deposition of glycidyl methacrylate gave rise to

broad infrared absorption features: C-H stretching (3063 cm^{-1}), C-H stretching ($3000\text{--}2900\text{ cm}^{-1}$), saturated ester carbonyl stretching (1728 cm^{-1}), epoxide ring breathing (1253 cm^{-1}), antisymmetric epoxide ring deformation (908 cm^{-1}), and symmetric epoxide ring deformation (842 cm^{-1}). The epoxide ring features were much weaker compared to the monomer, whereas the C-H stretching region was more intense. All bands associated with the glycidyl methacrylate monomer were clearly discernible following pulsed plasma polymerization, except for the C=C feature, which had disappeared during polymerization. The more intense infrared adsorption bands belonging to the epoxide ring confirmed that greater structural retention had occurred during pulsed conditions.

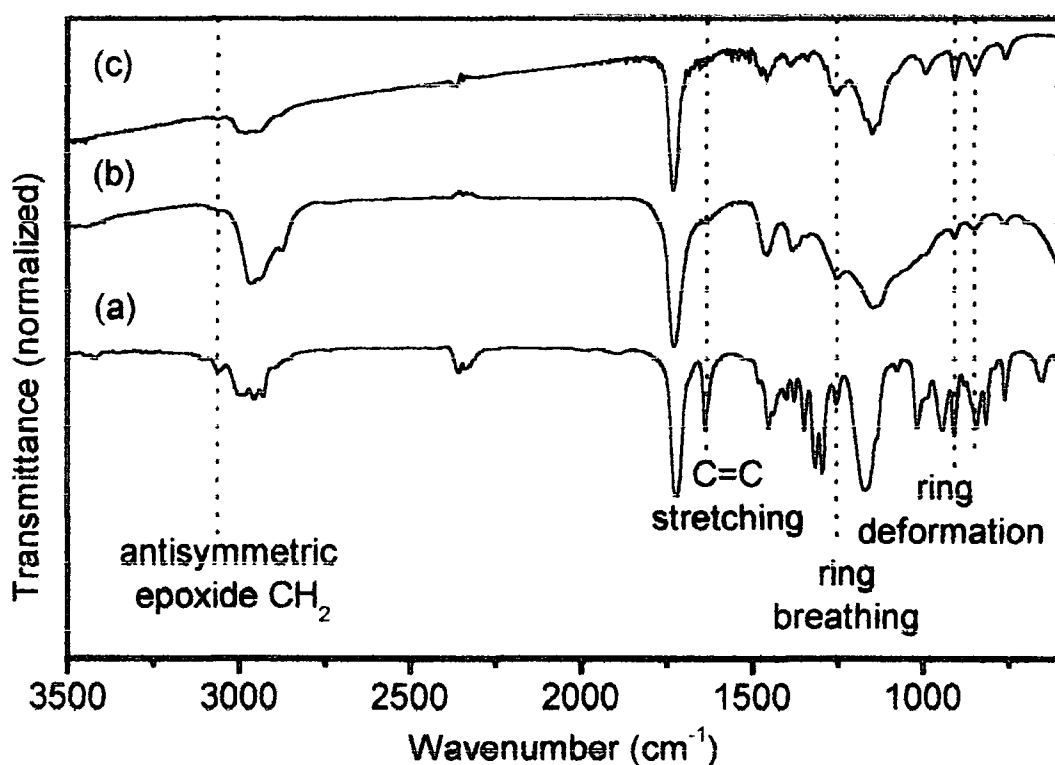


Figure 5.5.

Infrared spectra of (a) glycidyl methacrylate monomer; (b) 3 W continuous wave plasma polymer; and (c) pulsed plasma polymer (time on = $20\text{ }\mu\text{s}$, time off = 20 ms , peak power = 40 W).

Comparison of the positive ions TOF-SIMS spectra for the continuous wave and the pulsed plasma polymer layers confirmed the greater structural integrity of the latter, Figure 5.6. and Figure 5.7. For continuous wave plasma polymerization, a large range of masses was observed, which can be taken as being indicative of extensive monomer

fragmentation and rearrangement during plasma deposition. In contrast, the pulsed plasma counterpart displayed well-defined polymer repeat units, which have been assigned on the basis of the positive ion SIMS spectra obtained for conventionally polymerized methyl methacrylate.¹⁸ Three series of fragments up to five repetition units were detected, Table 5.4.

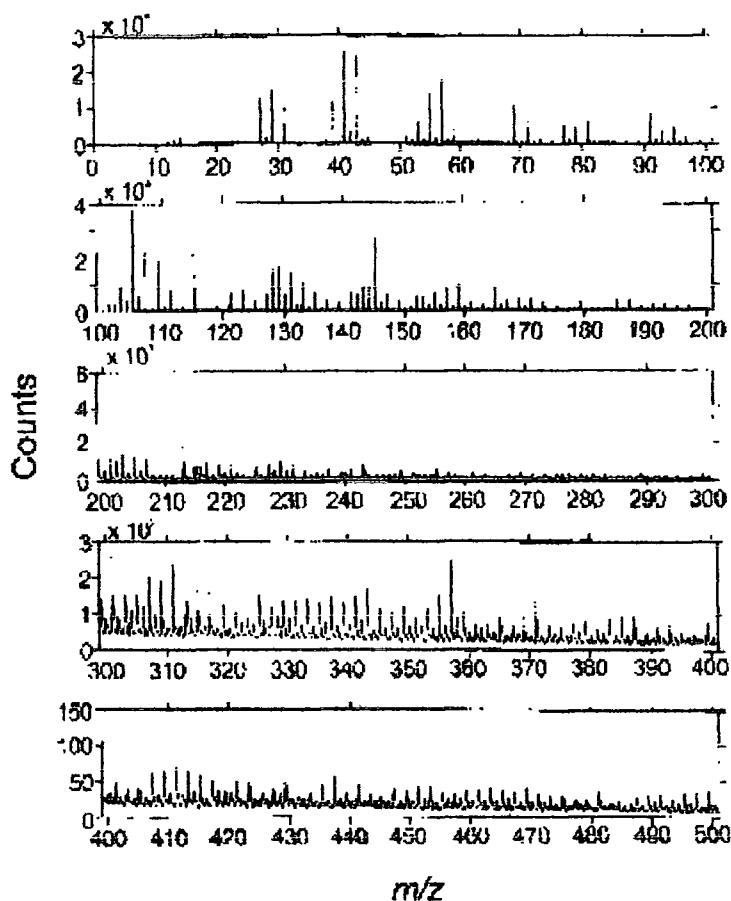


Figure 5.6.

Positive ion TOF-SIMS spectra of glycidyl methacrylate 3 W continuous wave plasma polymer.

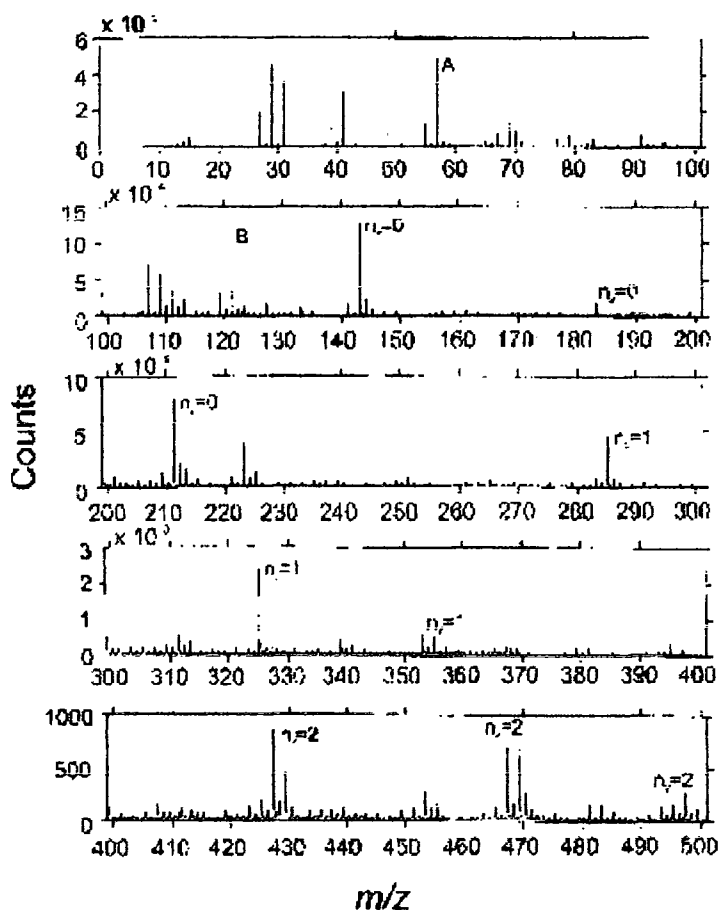
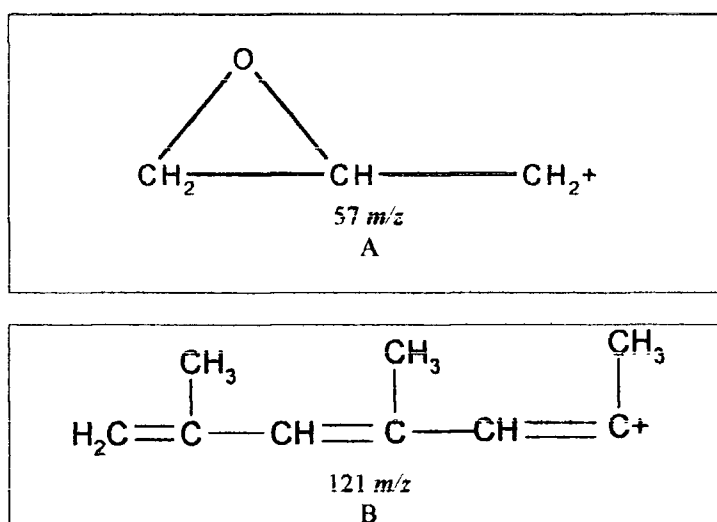
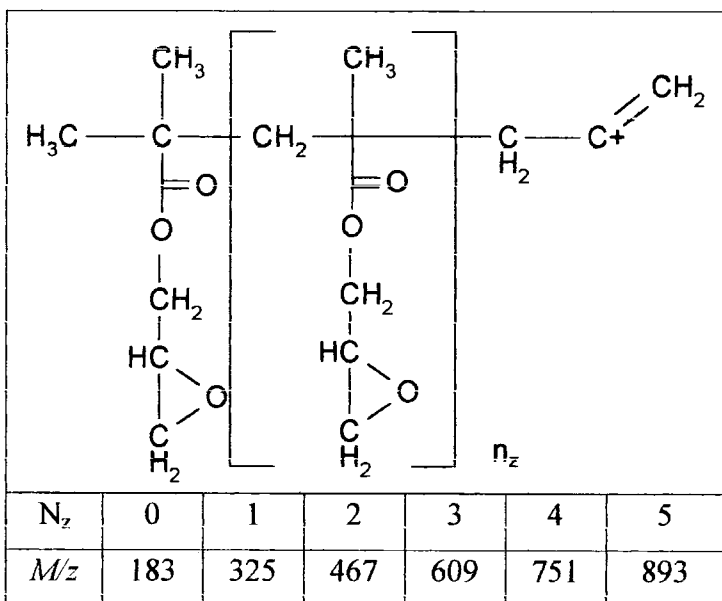
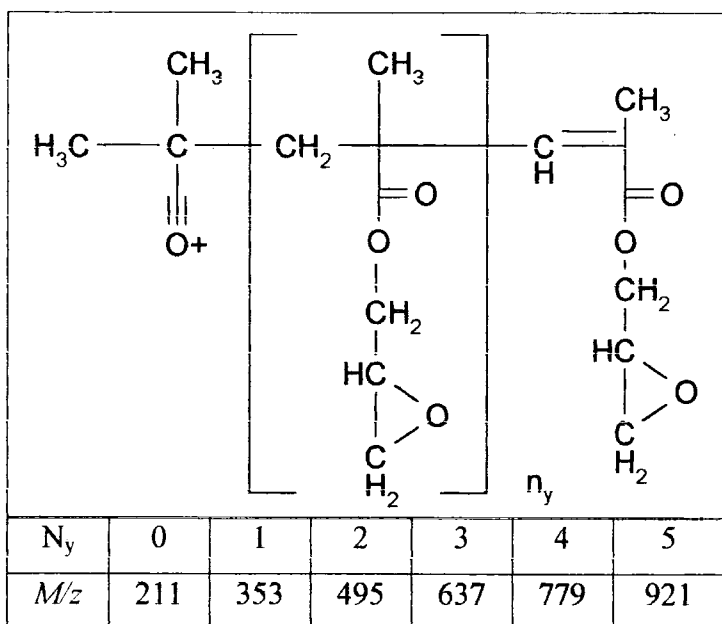
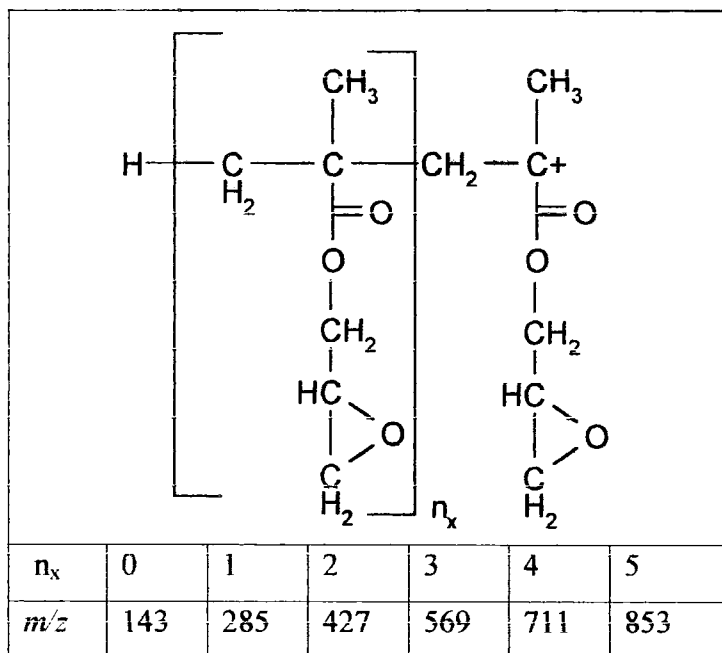


Figure 5.7.

Positive ion TOF-SIMS spectra of glycidyl methacrylate pulsed plasma polymer
(time on = 20 μ s, time off = 20 ms, peak power = 40 W)

Table 5.4. Assignments for positive ions TOF-SIMS of glycidyl methacrylate plasma polymers





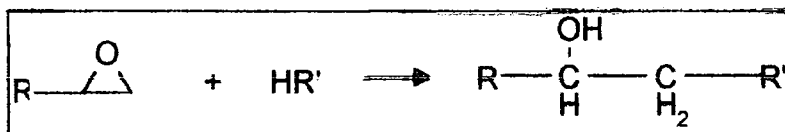
Quartz crystal deposition rate measurements provided values of $19 \pm 3 \cdot 10^{-9}$ and $2.5 \pm 0.5 \cdot 10^{-9} \text{ g s}^{-1} \text{ cm}^{-2}$ for the continuous wave and pulse conditions, respectively. The lower value obtained for pulsed plasma polymerization can be mainly attributed to less energy input. In fact the deposition efficiency was calculated to be $6.3 \cdot 10^{-9}$ and $63 \cdot 10^{-9} \text{ g cm}^{-2} \text{ J}^{-1}$ respectively. This implies that there is greater deposition per quantity of energy input in the case of pulsed plasma polymerization.

5.3.4. Glycidyl Methacrylate Plasma Polymer Coatings Derivatization Reactions

Epoxide functionalized surfaces produced by plasma polymerization of glycidyl methacrylate were employed as substrate for conventional derivatization reactions of epoxide groups.

The most important reactions involving the epoxide ring are the electrophilic attack on the oxygen atom or the nucleophilic attack on one of the ring carbon atoms. In unsymmetrical molecules the nucleophilic attack occurs on the less steric hindered carbon atom to yield the secondary alcohol, Scheme 5.1.¹⁹

Scheme 5.1. Reaction between an epoxide ring and a nucleophilic reagent.



Typical nucleophilic reagents for epoxide ring opening include mineral acids, carboxylic acids, ammonia and amines.

XPS elemental analysis of glycidyl methacrylate plasma polymers following derivatization reactions with a variety of nucleophilic reagents (e.g. carboxylic acids and amines) is reported in Table 5.4.

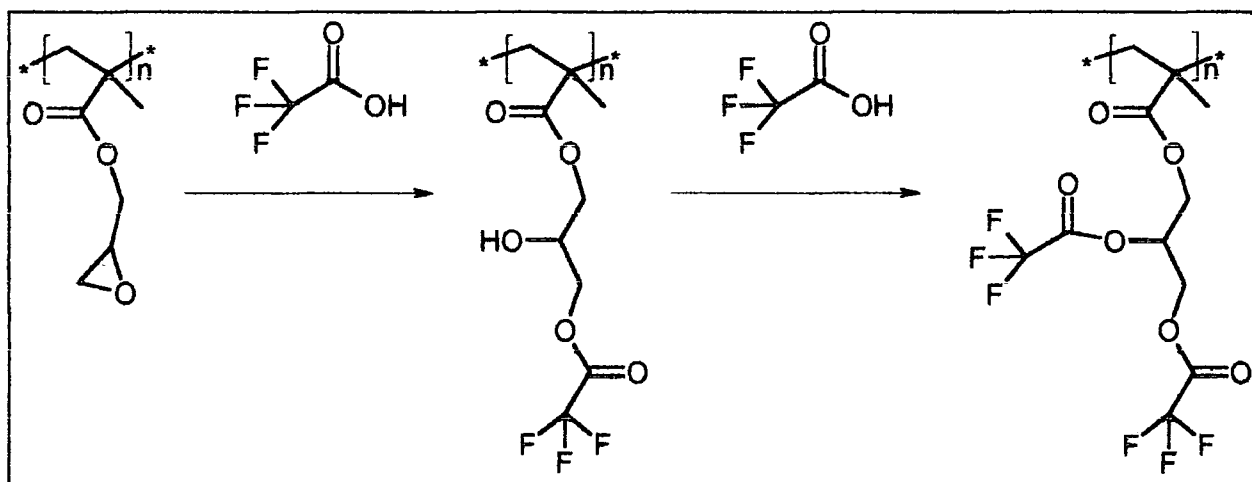
Table 5.4. Elemental analysis of the reacted glycidyl methacrylate plasma polymer coatings as determined by XPS.

Coating	%F	%C	%N	%O
CW + CF ₃ COOH	4.1 ± 0.5	77 ± 1	-	18 ± 1
Pulsed + CF ₃ COOH	16.0 ± 0.8	55 ± 2	-	28.6 ± 0.3
Pulsed + Jeffamine	-	70 ± 3	2.2 ± 0.3	27 ± 2
CW + diethylamine	-	75 ± 3	1.9 ± 0.1	23 ± 2
Pulsed + diethylamine	-	76.0 ± 0.2	4.7 ± 0.4	20 ± 1
Pulsed + ethylenediamine	-	73.1 ± 0.8	5 ± 2	22 ± 2

5.3.4.1. Carboxylic Acids

Trifluoroacetic acid vapour underwent reaction to greater extent with the pulsed plasma polymer films (Scheme 5.2). This enhancement in reactivity for the pulsed plasma polymer layer was confirmed by the identification of the CF₃ functionality at 293.3 eV in the C (1s) envelope,¹⁷ Figure 5.8.

Scheme 5.2. Reaction of poly(glycidyl methacrylate) with trifluoroacetic acid.



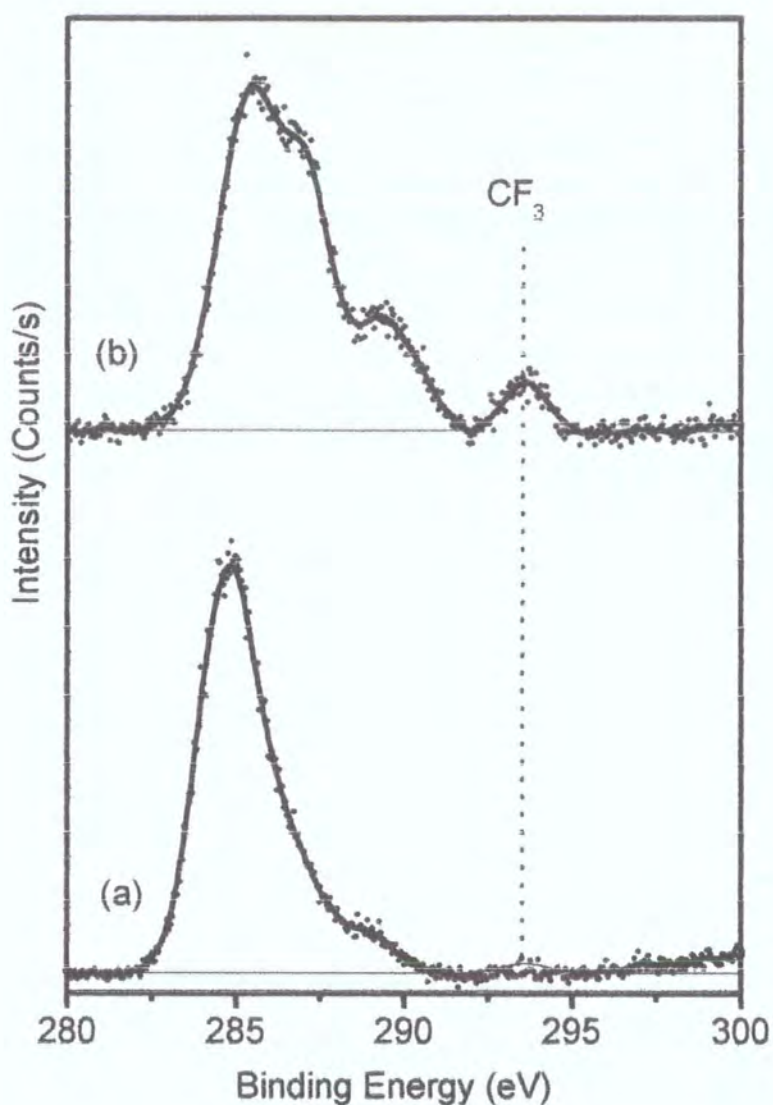


Figure 5.8.

C(1s) XPS spectra of plasma polymers exposed to trifluoroacetic acid vapour: (a) 3 W continuous wave; and (b) pulsed (time on = 20 μ s, time off = 20 ms, peak power = 40 W).

The proportion of epoxide groups which had undergone monoesterification was calculated using the F (1s) peak as follows:^{20, 21}

$$\%[F] = \frac{\frac{3}{2}x[Epoxide]_0}{[C]_0 + [O]_0 + \frac{7}{2}x[Epoxide]_0} \times 100 \quad (5.1.)$$

Where x is the fraction of reacted epoxides, $[Epoxide]_0$ is the initial atomic percentage of carbons belonging to epoxide groups, $[C]_0$ is the atomic percentage of carbon prior to reaction, $[O]_0$ is the atomic percentage of oxygen prior to reaction and $[F]$ is the atomic percentage of fluorine detected on the reacted surface. On this basis $42 \pm 6 \%$ and $89 \pm 5 \%$ of surface epoxide groups were calculated to have undergone reaction for the continuous wave and the pulsed plasma polymer layer respectively. Therefore, it appears that the proportion of epoxide group centers calculated from the C(1s) peak fitting (Figure 5.4. and Table 5.3.) for the continuous wave conditions is probably an overestimation. Other groups such as ethers or alcohols must also be present in the plasma polymer layer contributing to the assigned epoxide component at 287.2 eV. Alternatively, greater cross-linking may hinder reaction throughout the whole XPS sampling depth. Excess trifluoroacetic acid could potentially react further with alcohol groups formed during epoxide ring opening to produce a diester and this may be contributing to slight overestimation in the overall reaction yield.²

5.3.4.2. Amines

The reaction of epoxide groups with ammonia and amines is at the basis of the curing of epoxy resins. Ammonia is capable of attacking three epoxide groups, primary amines two and secondary amines only one.¹⁹

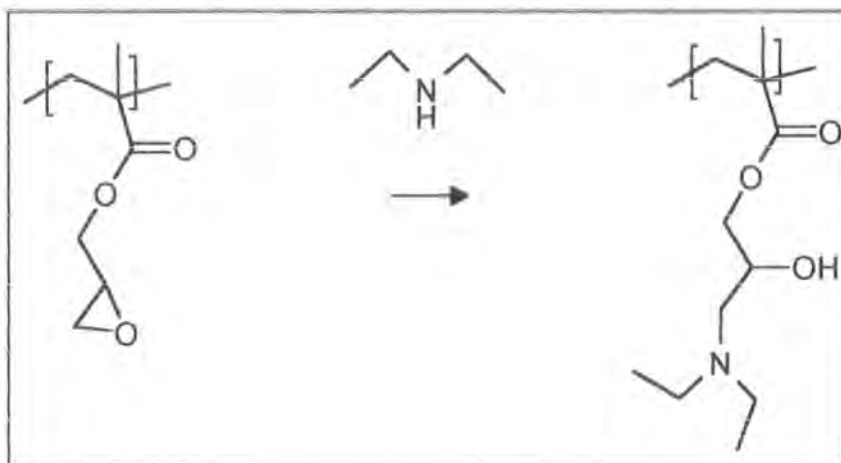
Reaction of glycidyl methacrylate plasma polymer layers with ethylenediamine was first tried for 30 min in the vapour phase. No reaction, as determined by the presence of the N(1s) peak in the XPS spectra, was detected under these conditions. The reaction is believed to be slow at room temperature and would require longer reaction times that are not attainable under these conditions. The reaction with amines is accelerated by compounds that stabilize the alkoxide ion intermediate, e.g. hydroxyl groups.¹⁹ Reactions carried out for longer time in alcoholic solution of the amine gave atomic percentages reported in Table 5.4.

Diethylamine was used to assess the reactivity of surface epoxide groups towards amines. This secondary amine was chosen because it is capable of reacting only once with an epoxide centre (Scheme 5.3), therefore making it much easier to calculate the number of aminated epoxides from the corresponding N(1s) peak area

$$\%[N] = \frac{\frac{1}{2}x[Epoxide]_0}{[C]_0 + [O]_0 + \frac{5}{2}x[Epoxide]_0} \times 100 \quad (5.2.)$$

On this basis 59 ± 5 % of the surface epoxide groups have undergone reaction for both the continuous wave and the pulsed plasma polymer layers.

Scheme 5.3. Reaction of poly(glycidyl methacrylate) with diethylamine.



In all three cases studied the N(1s) envelope presented two peaks: the peak seen at 399.8 eV can be assigned to a neutral nitrogen environment, while the feature at 402.1 eV is due to positively charged nitrogen, Figure 5.9. The latter can be attributed to protonation by atmospheric moisture,¹⁹ rather than the reaction of the newly formed tertiary amine center with an adjacent epoxide group.

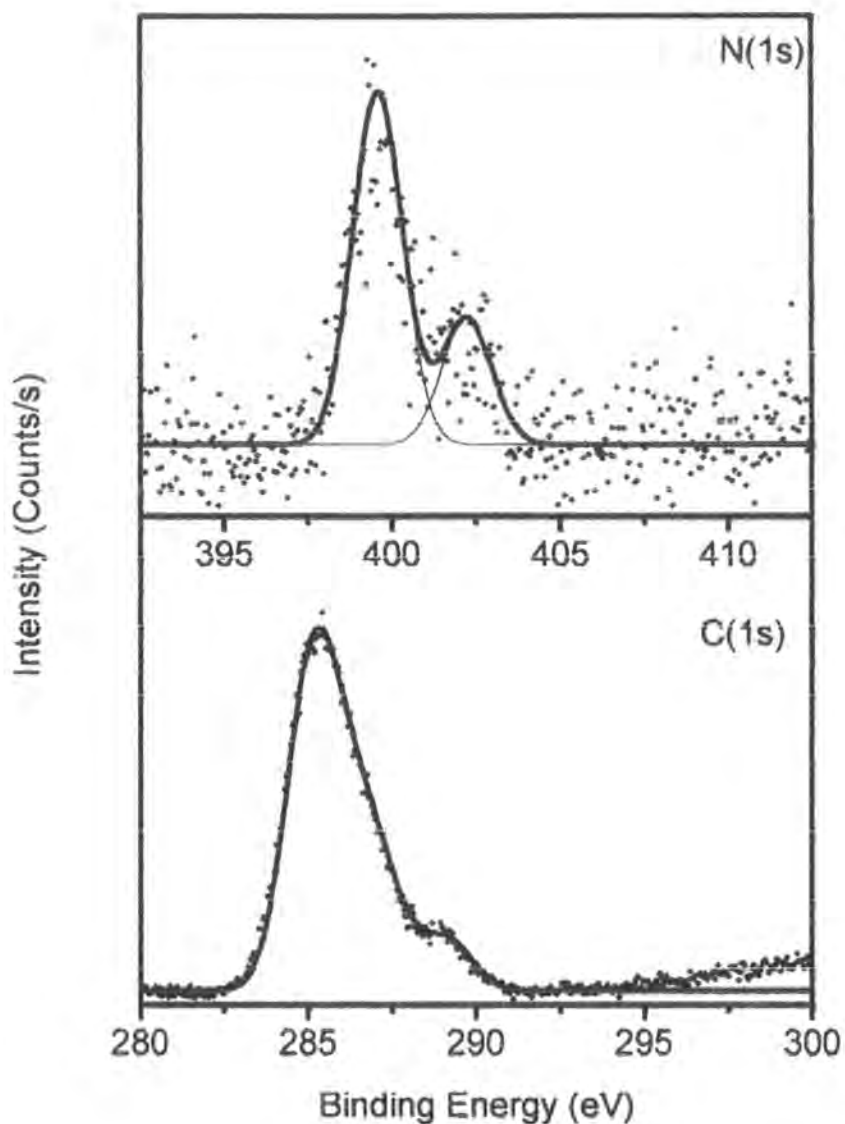


Figure 5.9.

N(1s) and C(1s) XPS spectra of glycidyl methacrylate pulsed plasma polymer reacted with diethylamine (time on = 20 μ s, time off = 20 ms, peak power = 40 W).

5.3.4.3 Dendrimers

Dendrimers are three-dimensional macromolecules. Unlike classical polymers, they are essentially monodisperse and can be synthesized in specific sizes. They are made up of a central core surrounded by repetitive units all enclosed by a terminal group shell. They are prepared by a series of repetitive steps starting with a central initiator core. Each subsequent growth step represents a “new generation” of polymer. Each generation is characterized by a certain number and type of terminal reactive sites.²² The high

controllability in size and chemical nature has made dendrimers appealing for various technological applications. My interest in dendrimers lies in the possibility to react with the epoxide functionalized surface in order to form “activated islands” on the surface capable of complexing noble metals.

Glycidyl methacrylate pulsed plasma polymer surfaces were reacted with Generation 4 Pamam dendrimers. The percentage of nitrogen detected by XPS vs the reaction time is shown in Figure 5.10.

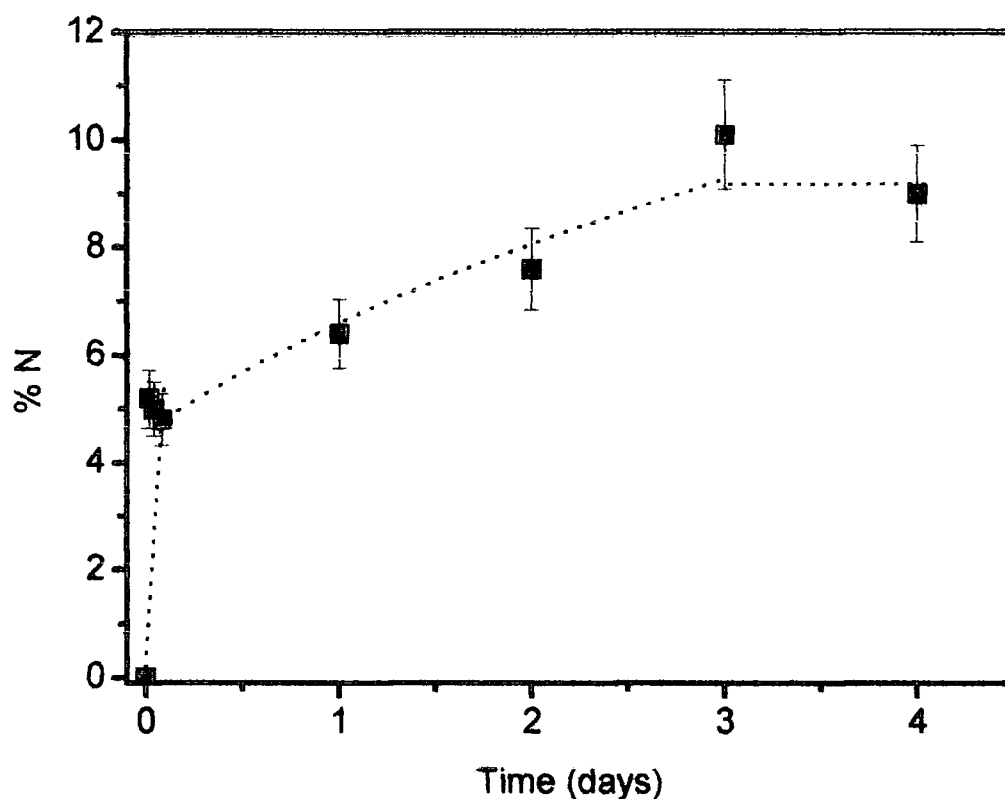


Figure 5.10.

Variation with time of atomic percentage of nitrogen as detected by XPS on glycidyl methacrylate pulsed plasma polymer (time on = 20 μ s, time off = 20 ms, peak power = 40 W) films following reaction with Generation 4 Pamam Starburst dendrimers.

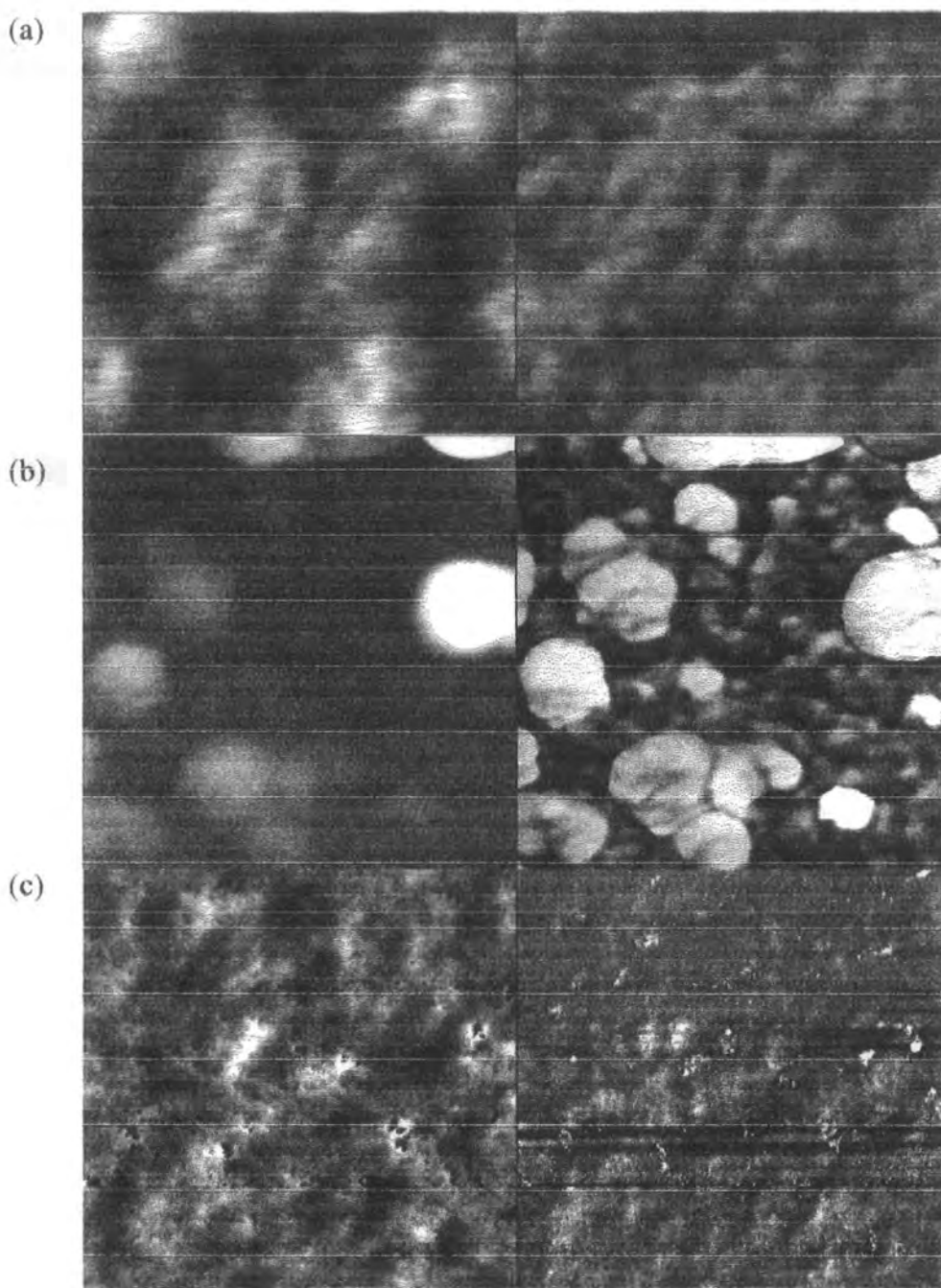


Figure 5.11.

Tapping mode ($1\ \mu \times 1\ \mu$) AFM scans of: (a) glycidyl methacrylate pulsed plasma polymer film (time on = $20\ \mu\text{s}$, time off = $20\ \text{ms}$, peak power = $40\ \text{W}$, z range $5\ \text{nm}$ and $60\ \text{de}$); (b) generation 4 PAMAM dendrimers on glycidyl methacrylate pulsed plasma polymers films ($12\ \text{h}$ reaction in methanol z range $50\ \text{nm}$ and $30\ \text{de}$); and (c) glycidyl methacrylate pulsed plasma polymer films following $12\ \text{h}$ immersion in methanol (z range $10\ \text{nm}$ and $10\ \text{de}$).

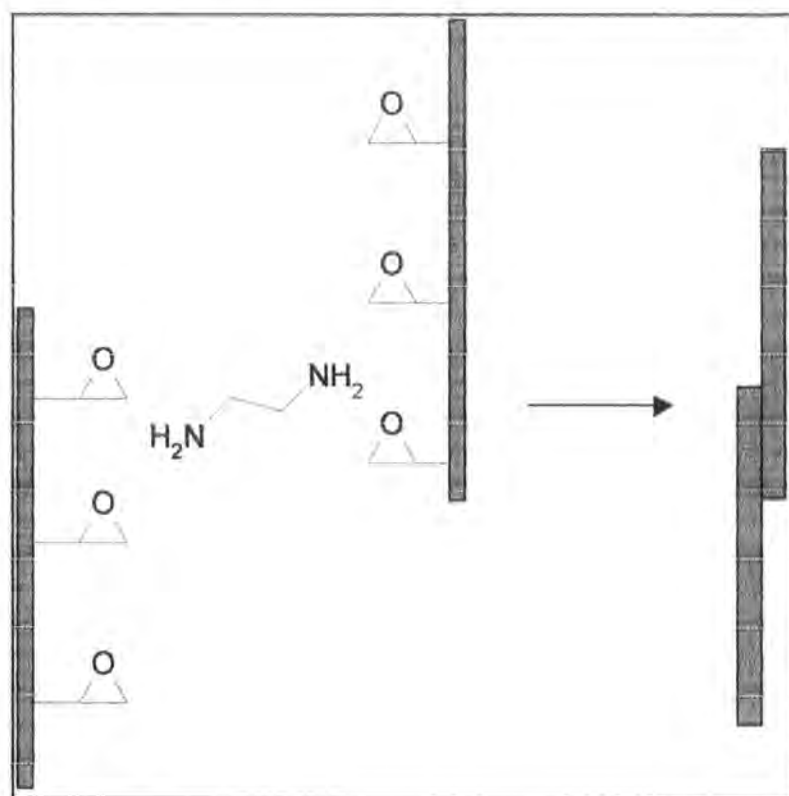
These features are not due to a solvent effect. In fact leaving the glycidyl methacrylate pulsed plasma polymer coated samples in pure methanol for the same time has no effect on the morphology of the plasma polymer layer. These results are in accordance with those of Meier²³ indicating that at high concentration single generation 4 PAMAM dendrimers can not be visualized on the surface.

Dendrimers were used as substrates for the formation of gold domains on the surface. The samples were first reacted with dendrimers and then left in a AuCl_3 solution for 30 min. Upon reduction with 5 min H_2 plasma at 20 W, 1.6 ± 0.3 % gold was detected on the surface. No gold was detected in absence of the dendrimers.

5.3.5. Adhesion

The reaction between surface epoxide groups and amines was further investigated using ethylene diamine as curing agent for adhesion.

Scheme 5.4. Reaction of poly(glycidyl methacrylate) with diethylamine.



A drop of 0.5 M solution of ethylenediamine dissolved in 1,4-dioxane was placed between two pieces of plasma polymer coated polyethylene. The samples were then

annealed overnight at 60° to allow solvent evaporation and bonding. In the case of pulsed plasma polymer layer single lap joint and T-peel adhesion tests resulted in failure of the polyethylene material adjacent to the joint, Figure 5.12, leaving the latter intact. Whereas, the actual joint was found to fail for continuous wave plasma polymerization. No adhesion between polyethylene strips was observed in the absence of either the plasma polymer or the coupling agent.

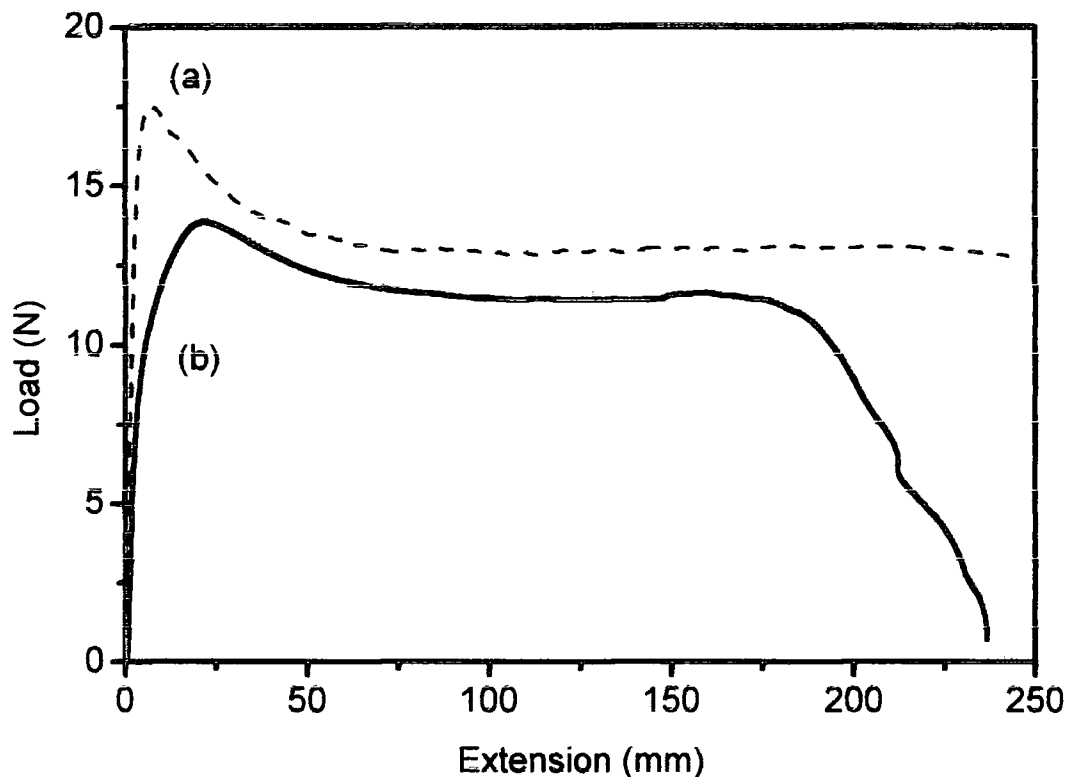


Figure 5.12.

Stress/strain curves of: (a) polyethylene substrate, and (b) glycidyl methacrylate pulsed plasma polymer coated polyethylene single lap joint (time on = 20 μ s, time off = 20 ms, peak power = 40 W).

O₂ plasma roughening^{24, 25} of the PTFE substrate was necessary prior to pulsed plasma deposition of glycidyl methacrylate in order to achieve good adhesion. Here the joint eventually failed rather than the substrate since PTFE was much stronger than PE (bulk failure 45 N). The duration of O₂ plasma pretreatment was found to affect the strength of the adhesive joint, Figure 5.13. Excessively long O₂ plasma exposures were

probably leading to polymer chain scission and the formation of low molecular weight material, which is known to have detrimental effect upon adhesion.

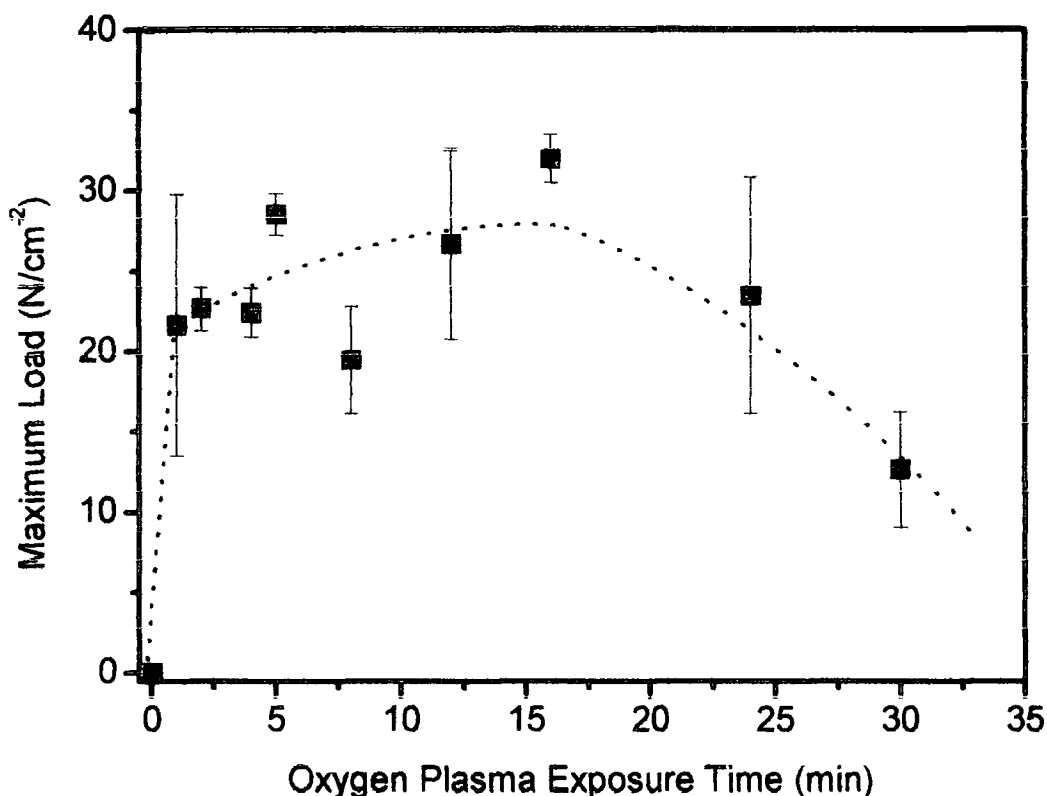


Figure 5.13.

Variation in PTFE joint strength as a function of 20 W oxygen plasma pretreatment time of PTFE followed by pulsed plasma deposition of glycidyl methacrylate (time on = 20 μ s, time off = 20 ms, peak power = 40 W).

5.4. Conclusions

Pulsed plasma polymerization of glycidyl methacrylate is a simple one-step method for functionalizing solid substrates with epoxide groups. These surfaces are amenable to conventional epoxide derivatization chemistry. In addition they have been found to offer excellent adhesion performance.

5.5. References

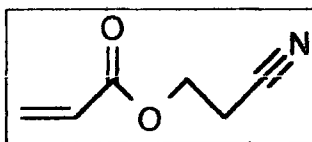
- [1] Gritter, R. J. In *The chemistry of the ether linkage*, ; S. Patai, Ed.; Interscience: New York, 1967.
- [2] Rosowsky, A. In *Heterocyclic Compounds with Three and Four-Membered Rings.*, ; A. Weissberger, Ed.; Interscience Publishers: New York, 1964; Vol. Part 1.
- [3] Zhang, J.; Kato, K.; Uyama, Y.; Ikada, Y. *J. Polym. Sci., Part A: Polym. Chem.* **1995**, *33*, 2629.
- [4] Mori, M.; Uyama, Y.; Ikada, Y. *J. Polym. Sci., Part A: Polym. Chem.* **1994**, *32*, 1683.
- [5] Allmer, K.; Jult, A.; Ranby, B. *J. Polym. Sci., Part A: Polym. Chem.* **1989**, *27*, 1641.
- [6] Allcock, H. R.; Nelson, C. J.; Coggio, W. D. *Chem. Mater.* **1994**, *6*, 516.
- [7] Lee, W.; Furusaki, S.; Saito, K.; Sugo, T. *J. Colloid Interface Sci.* **1998**, *200*, 66.
- [8] Kubota, H.; Ujita, S. *J. Appl. Polym. Sci.* **1995**, *56*, 25.
- [9] Bai, G.; Hu, X.; Yan, Q. *Polym. Bull.* **1996**, *36*, 503.
- [10] Motomura, T.; Moyashita, Y.; Ohwada, T.; Onishi, M.; Yamamoto, N. Eur. Pat. Appl. 679436, 1999.
- [11] Zhang, M. C.; Kang, E. T.; Neoh, K. G.; Han, H. S.; Tan, K. L. *Polymer* **1999**, *40*, 299.
- [12] Wu, S.; Kang, E. T.; Neoh, K. G.; Han, H. S.; Tan, K. L. *Macromolecules* **1999**, *32*, 18
- [13] Yamada, K.; Haraguchi, T.; Kajayama, T. *J. Appl. Polym. Sci.* **1996**, *60*, 1847.
- [14] Wang, T.; Kang, E. T.; Neoh, K. G.; Tan, K. L.; Cui, C. Q.; Lim, T. B. *J. Adhes. Sci. Technol.* **1997**, *11*, 679.
- [15] Lusinov, I.; Julthongpiput, D.; Tsukruk, V. V. *Langmuir* **1999**, *15*, 3029.
- [16] Lin-Vien, D.; Colthup, N. B.; Fateley, W. G.; Grasselli, J. G. *The Handbook of Infrared and Raman Characteristic Frequencies of Organic Molecules*; Academic Press: New York, 1991.
- [17] Beamson, G.; Briggs, D. *High resolution XPS of organic polymers: the Scienta ESCA300 database*; John Wiley & Sons: New York, 1992.
- [18] Briggs, D.; Brown, A.; Vickerman, J. C. *Handbook of Static Secondary Ion Mass Spectrometry*; J. Wiley & Sons: New York, 1989.

- [19] Ashcroft, W. R. In *Chemistry and Technology of Epoxy Resins*, ; B. Ellis, Ed.; Blackie Academic & Professional: Glasgow, 1993.
- [20] Popat, R. P.; Sutherland, I.; Sheng, E.-S. *J. Mater. Chem.* **1995**, *5*, 713.
- [21] Sutherland, I.; Sheng, E.-S.; Brewis, D. M.; Heath, R. J. *J. Mater. Chem.* **1994**, *4*, 683.
- [22] Zeng, F.; Zimmerman, S. C. *Chem. Rev.* **1997**, *97*, 1681.
- [23] Li, J.; Piehler, L. H.; Qin, D.; Baker, J. R.; Tomalia, D. A.; Meier, D. J. *Langmuir* **2000**, *16*, 5613.
- [24] Morra, M.; Occhiello, E.; Garbassi, F. *Surf. Interface Anal.* **1990**, *16*, 412.
- [25] Ryan, M. E.; Badyal, J. P. S. *Macromolecules* **1995**, *28*, 1377.

6. FUNCTIONALIZATION OF SOLID SURFACES WITH CYANO GROUPS

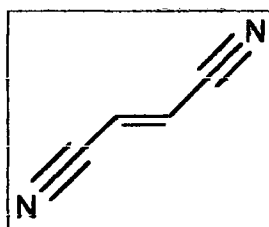
6.1. Introduction

Here is described the pulsed plasma polymerization of 2-cyanoethyl acrylate (Structure 6.1.) and fumaronitrile (Structure 6.2.) to generate cyano functionalized solid surfaces.



Structure 6.1.

2-cyanoethyl acrylate



Structure 6.2.

Fumaronitrile

These monomers contain two potentially reactive groups: the carbon-carbon double bond and the nitrile bond. Preferential activation of the former is necessary in order to attain a simple one-step solventless route to cyano-functionalized thin films. Cyano groups are desirable for many technological applications because they possess a large dipole moment and readily complex metal ions. For instance, incorporation of silver ions at a substrate surface can lead to antibacterial properties.¹⁻⁶ Previous attempts aimed at preparing cyano containing surfaces have included grafting,⁷ gas-phase photochemical reactions involving cyanogen halides,⁸ and also wet chemical functionalization of silica chromatography supports.⁹ Toxicity and the requirement for solvents are considered to be drawbacks for these existing methods.

6.2. Materials and Methods

Plasma polymerization of 2-cyanoethyl acrylate (Aldrich, +85%) was carried out at a pressure of 0.1 torr and 5.2×10^{-9} mol s⁻¹ flow rate for 5 mins.

In the case of fumaronitrile (Aldrich, 99%) plasma polymerization was carried out at a pressure of 0.1 torr for 1 min.

¹³C NMR spectra were acquired on the material collected from the walls of the reactor after the deposition and then dissolved in deuterated acetonitrile (Aldrich, 99.6 atom % D)

Complexation of Ag⁺ ions was undertaken by immersing plasma polymer coated samples in a 1 M aqueous solution of AgNO₃ (Johnson Matthey Chemicals, 99.99% purity) for 24 hrs. The surfaces were then rinsed several times in ultrahigh purity water prior to chemical analysis.

Depth distribution of silver ions was determined acquiring XPS spectra at take off angles of 15°, 45°, 60° and 75° from the substrate normal.

For the adhesion measurements, two 2-cyanoethyl acrylate plasma polymer coated strips of polytetrafluoroethylene (PTFE, Goodfellow, 0.25 mm thickness) were pressed together between two pieces of glass for 10 min. The strips were 1 cm wide and 4 cm long. The overlap was approximately 1 cm².

6.3. Results

6.3.1. Plasma Polymerization of Fumaronitrile

Low power plasma polymerization of fumaronitrile gave rise to a thick black coating following plasma ignition. The plasma rapidly extinguished and pulsed conditions could not be applied.

XPS elemental analysis of the plasma polymer layer showed only carbon and nitrogen on the surface, Table 6.1.

Table 6.1. XPS elemental analysis composition of fumaronitrile plasma polymers

Coating	%C	%N
Theoretical	66.7	33.3
Continuous wave	68 ± 2	32 ± 2

Infrared analysis showed results in accordance with previous works.^{10, 11} The following assignments could be made for fumaronitrile monomer:^{12, 13} unsaturated C-H stretching (3067 cm^{-1}) and $\text{C}\equiv\text{N}$ stretching (2239 cm^{-1}). The plasma polymer spectrum showed absorption due to $\text{C}=\text{N}$ groups at 2205 cm^{-1} (conjugated) and 1617 cm^{-1} ,¹² the $\text{C}\equiv\text{N}$ stretching having disappeared.

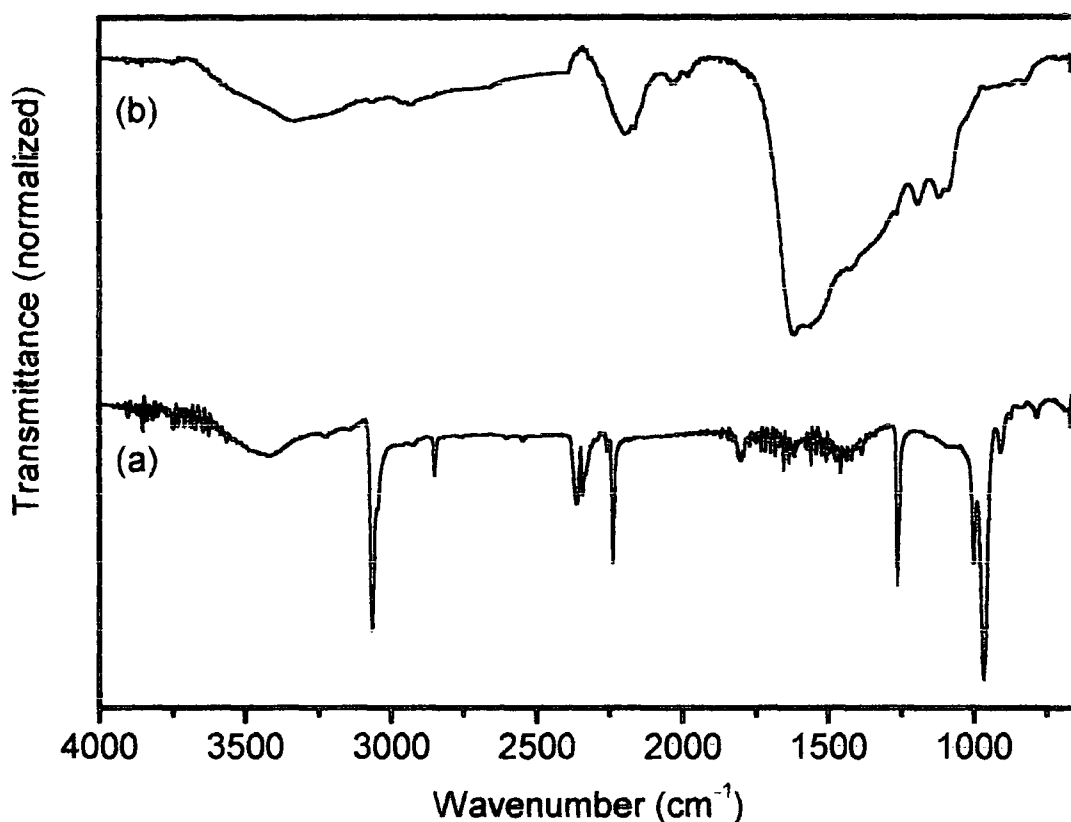


Figure 6.1.

Infrared spectra of (a) fumaronitrile monomer and (b) 3 W continuous wave plasma polymer. (The weak band in the $2360\text{-}2330\text{ cm}^{-1}$ region is due to residual CO_2 in the spectrometer).

These results reflect the reported solution phase polymerization results, where activation of the carbon nitrogen triple bond occurs.¹⁴

6.3.2. Plasma Polymerization of 2-Cyanoethyl Acrylate

Elemental XPS analysis showed that the pulsed plasma deposition yielded films with a chemical composition closely resembling the theoretical values expected from conventional free radical polymerisation of 2-cyanoethyl acrylate via the carbon-carbon double bond, Table 6.2. In contrast some degree of oxygen depletion was evident in the case of continuous wave conditions.

Table 6.2. XPS elemental analysis composition of 2-cyanoethyl acrylate plasma polymers

Coating	%C	%O	%N
Theoretical	66.7	22.2	11.1
Continuous wave	68.8 ± 0.5	19.4 ± 0.1	11.8 ± 0.3
Pulsed	67.7 ± 0.5	21.2 ± 0.3	10.9 ± 0.3

Fourier transform infrared spectroscopy identified the following characteristic structural features for the precursor monomer: ¹²C-H stretching (3000-2900 cm⁻¹), C≡N stretching (2254 cm⁻¹) acrylate C=O stretching (1726 cm⁻¹), acrylate C=C stretching (1637 cm⁻¹), C-O stretching (1185 cm⁻¹), =CH₂ wagging (985 cm⁻¹), =CH₂ twisting (810 cm⁻¹), Figure 6.2. In the case of the pulsed plasma film, it was evident that polymerization had proceeded predominantly via the acrylate carbon-carbon double bond. The C=C stretching at 1637 cm⁻¹ disappeared, whilst the following characteristic structural features remained intact: C=O stretching at 1726 cm⁻¹, C≡N stretching at 2254 cm⁻¹, and C-O stretching at 1180 cm⁻¹.¹⁵ In the case of continuous wave plasma polymerization very little structural definition was evident. For instance, the cyano group feature at 2254 cm⁻¹ is hardly visible, reflecting the extensive rearrangement reactions taking place within the continuous wave plasma discharge.¹⁶

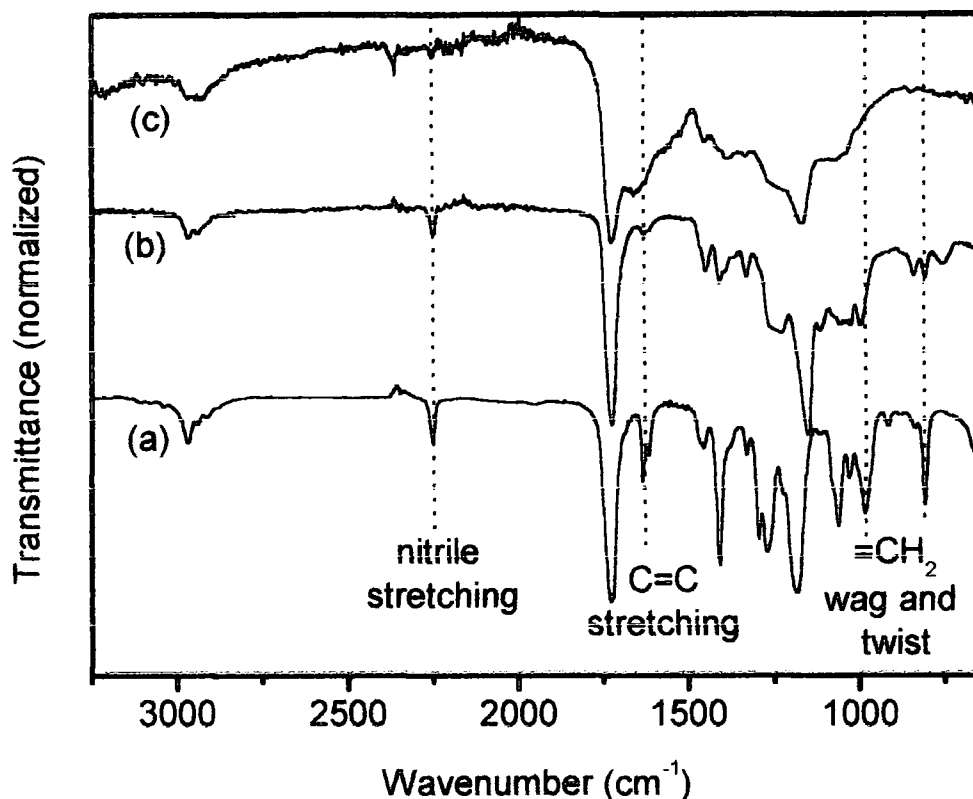


Figure 6.2.

Infrared spectra of (a) 2-cyanoethyl acrylate monomer, (b) pulsed plasma polymer (time on = 20 μ s, time off = 20 ms, peak power = 40 W), and (c) 3 W continuous wave plasma polymer. (The weak band in the 2360-2330 cm^{-1} region is due to residual CO_2 in the spectrometer).

The ^{13}C NMR spectrum obtained for the pulsed plasma polymer film, Figure 6.3, displayed the following shifts: 18.4 ppm ($(\text{CH}_2\text{-CH})_n$), 34.5 ppm ($-\text{CH}_2\text{-CN}$), 41.9 ppm ($(\text{CH}_2\text{-CH})_n$), 60.2 ppm (O-CH_2), 118.8 ppm ($-\text{CN}$) and 174.8 ppm ($(\text{C=O})\text{O}$). These assignments are based on NMR spectra reported for conventional linear poly(2-cyanoethyl acrylate) prepared by solution phase free radical polymerization.¹⁷ The continuous wave plasma polymer product was found to be insoluble in acetonitrile due to its highly cross-linked nature.

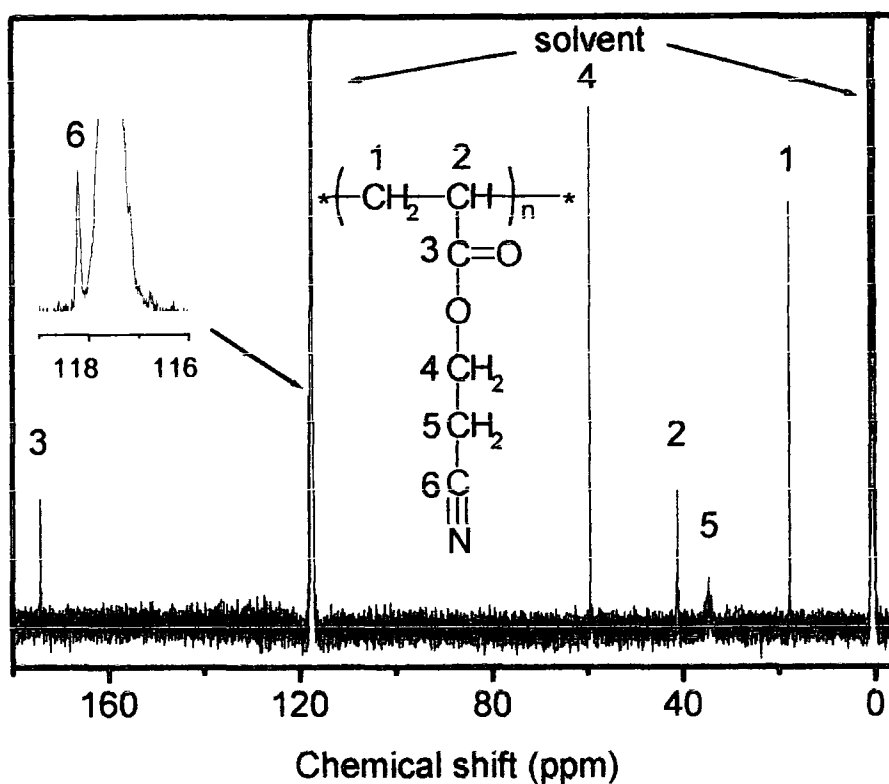


Figure 6.3.

^{13}C NMR spectrum of 2-cyanoethyl acrylate pulsed plasma polymer (time on = 20 μs , time off = 20 ms, peak power = 40 W).

Although the pulsed plasma polymerization conditions were much milder in nature compared to those in continuous wave, the corresponding deposition rate was found to be substantially greater, 194.7 and 8.0 nm min^{-1} respectively.

Soaking substrates coated with the 2-cyanoethyl acrylate pulsed plasma polymer in aqueous AgNO_3 solution followed by rinsing in water gave rise to 1.0 ± 0.2 atom % silver ion complexation to the surface (as measured by XPS ignoring hydrogen). This corresponds to approximately one silver ion for every ten nitrogen atoms. However, angle resolved XPS depth profiling studies showed that the silver to nitrogen ratio increased to 1:4 at shallower sampling depths (Figure 6.4). The absence of trapped nitrate species was checked for by examining the N (1s) envelope (expected at 407 eV); in fact only the $\text{C}\equiv\text{N}$ environment was observed at 399.2 eV.¹⁸ In contrast, the continuous wave plasma polymer deposited layers were found to delaminate upon immersion in aqueous AgNO_3 solution.

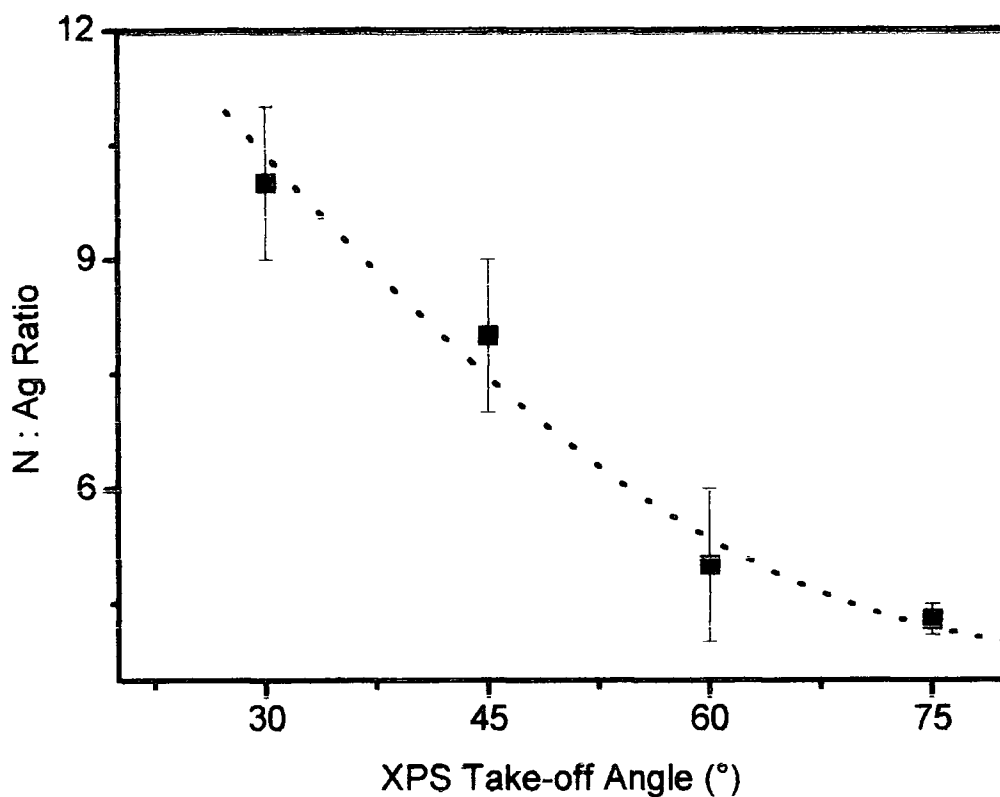


Figure 6.4.

Variation in N:Ag ratio for silver ions complexed to 2-cyanoethyl acrylate pulsed plasma polymer layers as a function of the XPS takeoff angle (time on = 20 μ s, time off = 20 ms, peak power = 40 W).

The adhesive performance of plasma polymer coated PTFE substrates was evaluated using a lap shear test (Figure 6.5). A maximum load of 24 ± 2 N was measured for the pulsed plasma polymer layer, whereas no adhesion was observed in the case of continuous wave deposition. Coating of only one piece of PTFE with pulsed plasma polymer was also found to be insufficient. Interestingly, the adhesive joint could be subsequently reformed following failure by simply repressing the two pieces together. This suggests that the interface fails cohesively. In this case, only a slight deterioration in adhesive performance was observed compared to the original joint (19 ± 2 N).

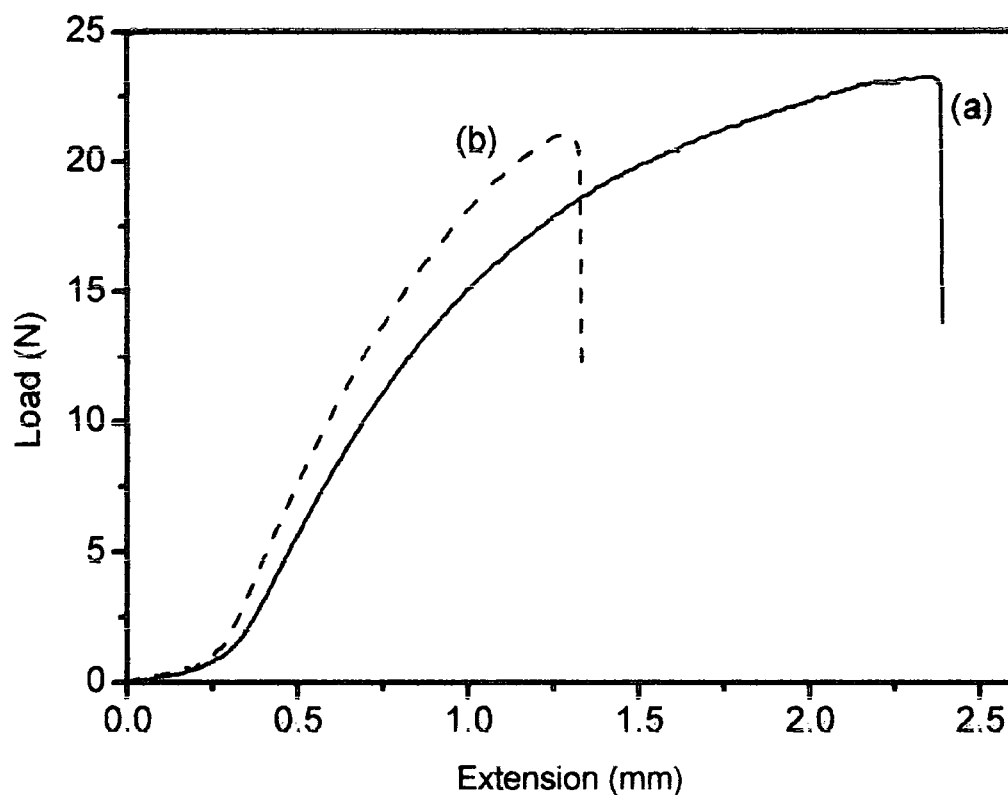


Figure 6.5.

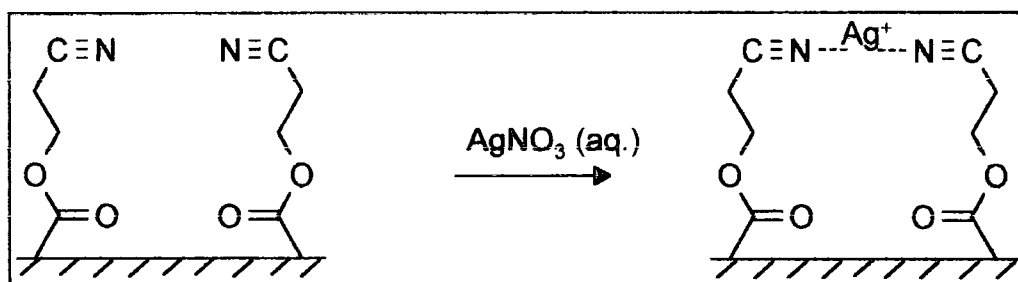
Tensile stress/strain curves of (a) 2-cyanoethyl acrylate pulsed plasma polymer coated PTFE single lap joint (time on = 20 μ s, time off = 20 ms, peak power = 40 W) and (b) repetition of the test after reassembling (the lower strain is due to loss of elasticity of the substrate during the subsequent run).

6.4. Discussion

Continuous wave plasma polymerization of molecules containing cyano groups⁷ (e.g. acrylonitrile,^{10, 11, 16} fumaronitrile,^{10, 11} tetracyanoethylene,^{10, 19} tetracyanobenzene,¹⁹ tetracyanoquinodimethane,¹⁹ acetonitrile,^{16, 19} diaminomaleonitrile,¹⁹ and phthalonitrile¹⁹) has previously been shown to lead to extensive molecular rearrangement reactions and the formation of amide, amino and ketene-imine groups. In the present study, pulsed plasma polymerization of 2-cyanoethyl acrylate gave rise to excellent structural retention of the cyano functionality. This can be attributed to the acrylate bond undergoing selective conventional

polymerization during the off-period of the plasma duty cycle.²⁰

Scheme 6.1. Complexation of Ag^+ ions onto the surface of 2-cyanoethyl acrylate pulsed plasma polymer films.



Complexation of Ag^+ ions (Scheme 6.1.) onto these pulsed plasma polymer surfaces can be attributed to metal coordination by the $\text{C}\equiv\text{N}$ groups via donation of nonbonding electrons from the nitrogen atom.²¹ For instance, silver ions are reported to form 1:2 stoichiometric complexes in acetonitrile.²¹ In the present case, XPS analysis indicated that coordination was limited to the outermost layer of the plasma polymer film, where a 1:4 silver:cyano group ratio was measured. This could be due to either incomplete coordination because of geometrical constraints, or complexation occurring at just the very outer surface.

The adhesive behaviour measured between two pulsed plasma polymer coated surfaces is most likely to originate from polymer chain interdiffusion across the solid-solid interface.²² The large dipole moment of cyano groups will promote strong interactions between the interpenetrating polymer chains.²¹ The slightly lower maximum load measured for the reformed joint can be associated with the loss of tackiness of the surface (i.e. changes in the polymer chains ability to diffuse). Whereas, the absence of adhesion noted for the continuous wave plasma polymer coatings arises from the rigidity (cross-linking) introduced by high energy plasma species bombarding the surface of the growing film throughout deposition, as well as the absence of highly polar cyano groups.

6.5. Conclusions

Solventless functionalization of solid surfaces with cyano groups can be achieved by pulsed plasma polymerization of 2-cyanoethyl acrylate. Variation of the pulsing conditions allows the extent of structural group retention to be controlled. In this way complexation of silver ions to solid surfaces and also their adhesive behaviour can be tailored.

6.6. References

- [1] Feng, Q. L.; Kim, T. N.; Wu, J.; Park, E. S.; Kim, J. O.; Lim, D. Y.; Cui, F. S. *Thin Solid Films* **1998**, 335, 214.
- [2] Thurman, R. B.; Gerba, C. P. *Crit. Rev. Environ. Control* **1988**, 18, 295.
- [3] Rosch, W.; Lugauer, S. *Infection* **1999**, 27, S74.
- [4] Boswald, M.; Lugauer, S.; Regenfus, A.; Braun, G. G.; Martus, P.; Geis, C.; Scharf, J.; Bechert, T.; Greil, J.; Guggenbichler, J. P. *Infection* **1999**, 27, S56.
- [5] Gatter, N.; Kohnen, W.; Jansen, B. *Zbl. Bakt. - Int. J. Med. M.* **1998**, 287, 157.
- [6] Guggenbichler, J. P.; Boswald, M.; Lugauer, S.; Krall, T. *Infection* **1999**, 27, S16.
- [7] Glejbol, K.; Winther-Jensen, B.: Internat. Pat. No. WO 00/20656, April 13, 2000.
- [8] Meyer, U.; Kern, W.; Ebel, M. F.; Svagera, R. *Macromol. Rapid Commun.* **1999**, 20, 515.
- [9] Okusa, k.; Tanaka, H.; ohira, M. *J. Chromatogr., A* **2000**, 869, 143.
- [10] Inagaki, N.; Tasaka, S.; Yamada, Y. *J. Polym. Sci., Part A: Polym. Chem.* **1992**, 30, 2003.
- [11] Inagaki, N.; Tasaka, S.; Ohmori, H.; Mibu, S. *J. Adhes. Sci. Technol.* **1996**, 10, 243.
- [12] Lin-Vien, D.; Colthup, N. B.; Fateley, W. G.; Grasselli, J. G. *The Handbook of Infrared and Raman Characteristic Frequencies of Organic Molecules*; Academic Press: New York, 1991.
- [13] Bellamy, L. J. *The Infrared Spectra of Complex Molecules*; Chapman & Hall: New York, 1980; Vol. 2.
- [14] Woehrle, D.; Knothe, G. *J. Polym. Sci., Part A: Polym. Chem.* **1988**, 26, 2435.
- [15] Bellamy, L. J. *The Infrared Spectra of Complex Molecules*; Chapman & Hall: New York, 1975; Vol. 1.

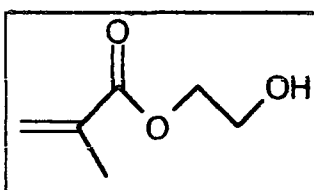
- [16] Lefohn, A. E.; Mackie, N. M.; Fisher, E., R. *Plasmas and Polymers* **1998**, *3*, 197.
- [17] Mehrotra, S.; Nigam, A.; Malhotra, R. *Chem. Commun.* **1997**, *5*, 463.
- [18] Beamson, G.; Briggs, D. *High resolution XPS of organic polymers: the Scienta ESCA300 database*; John Wiley & Sons: New York, 1992.
- [19] Osada, Y.; Yu, Q. S.; Yasunaga, H.; Kagami, Y. *J. Polym. Sci., Part A: Polym. Chem.* **1989**, *27*, 3799.
- [20] Ryan, M. E.; Hynes, A. M.; Badyal, J. P. S. *Chem. Mater.* **1996**, *8*, 37.
- [21] Grundnes, J.; Klaboe, P. In *The chemistry of the cyano group*, ; Z. Rappoport, Ed.; Interscience Publishers: New York, 1970.
- [22] Allen, K. W. In *Handbook of Adhesion*, ; D. E. Packham, Ed.; Longman Scientific & Technical: Essex, UK, 1992.

7. PLASMA DEPOSITION OF 2-HYDROXYETHYL METHACRYLATE

7.1. Introduction

Poly(2-hydroxyethyl methacrylate) (poly(HEMA)) is a hydrophilic, non-toxic and biocompatible polymer. Possible applications include drug release systems, 1-3 separation devices,^{4, 5} biosensors,⁶ and selective transportation membranes.⁷

Widely investigated are also the surface applications of poly(HEMA) and HEMA. Possible uses of HEMA modified surfaces include biocompatibility improvement,⁸ adhesion promotion,⁹ wettability, textile strengthening¹⁰ and adsorption of metal ions.¹¹ HEMA modified surfaces have been produced via graft co-polymerization,¹⁰ spin casting of a solution of the polymer^{8, 12} and plasma polymerization.¹³⁻¹⁵ Conventional continuous wave plasma polymerization of HEMA leads to high fragmentation,¹⁶ and the deposited film differs significantly from poly(HEMA). HEMA functionalised surfaces can be further derivatized by reacting the hydroxyl or the ester group. Surface hydroxyl groups can undergo reactions with metal alkoxides,¹⁷ anhydrides,¹⁸ silane coupling agents¹⁹ and chlorophosphites. The reaction of the ester group with amines can lead to immobilization of proteins.⁶



Structure 7.1.

2-Hydroxyethyl Methacrylate

In this work the growth of poly(HEMA) onto a solid substrate is achieved via pulsed plasma polymerization. Comparison between the low power continuous wave, pulsed plasma and conventional polymers is made on the basis of chemical analysis (X-ray photoelectron spectroscopy, infrared spectroscopy and nuclear magnetic resonance) and reactivity.

The possibility to use 2-hydroxyethyl methacrylate plasma polymer coated surfaces as substrates for catalyst immobilization or multilayer assemblies via derivatization reactions is also investigated.

7.2. Materials and Methods

Plasma polymerization of 2-hydroxyethyl methacrylate (HEMA, Fluka, 99% purity), was carried out at a pressure of 0.1 torr and $4.04 \cdot 10^{-8}$ flow rate, followed by film deposition for 30 min.

Poly(HEMA) (Aldrich, average molecular weight ca. 300,000) spin coated surfaces were prepared with a 4% w/vol solution in methanol (Fisher, + 99.8%).

For transmittance infrared analysis, plasma polymer films were deposited onto NaCl plates. The monomer spectrum was acquired by placing a drop of the liquid between two NaCl plates. The conventional poly(HEMA) spectrum was acquired on a KBr pellet. Silicon wafers were employed as substrate for grazing angle analysis.

The material for NMR analysis was collected from the reactor following deposition (2h) and then dissolved in deuterated methyl sulphoxide (Aldrich, 99.6 atom % D).

The molecular weight values obtained by gel permeation chromatography for the pulsed plasma polymers were divided by the value obtained under the same conditions for conventional free radical polymerized poly(2-hydroxyethyl methacrylate) (Aldrich, Average molecular weight ca. 300,000).

Reaction with trifluoroacetic anhydride (Aldrich, 99%) was carried out by exposing the coated glass slides to the anhydride vapour for 30 min. The samples were then rinsed several times in MeOH prior to analysis.

Reaction with diethyl chlorophosphite (Aldrich 98%) was carried out by exposing the coated glass slides to its vapour in a continuous flow at a pressure of 0.4 torr for 30 min. Unreacted material was pumped off in vacuum for an hour prior to sample analysis. The Rh complexation reaction was performed by immersing the phosphite reacted polymer in a 1% w/v solution of $\text{RhCl}_3 \cdot 3\text{H}_2\text{O}$ (Lancaster, Rh 40%) in 1,4-dioxane (Aldrich, 99%) for 1h. Prior to analysis the slides were rinsed several times in pure 1,4-dioxane and the solvent was evaporated under vacuum (base pressure 0.02 torr).

Reaction with $Zr(OC(CH_3)_3)_4$ (Aldrich, 98% purity) was carried out by exposing the coated glass slides in a flow of the vapour ($P = 0.2$ torr) for 30 min. The samples were then pumped up to the base pressure to remove the excess of the reagent. The following coupling reaction with polyacrylic acid (Aldrich, Average Molecular Weight ca. 450,000) was carried out by immersing the samples in a 5% w/v solution of the polymer in 1,4-dioxane for 15 min. the samples were then rinsed with pure 1,4-dioxane and vacuum dried prior to analysis. The successive coupling reaction with the Zonyl FSD fluorosurfactant (DuPont) was performed by immersing the poly(acrylic acid) reacted samples in a 1: 10 ultra high purity water dilution of the fluorosurfactant for 15 min. The samples were then rinsed in water and vacuum dried prior to analysis.

7.3. Results and Discussion

7.3.1. Plasma Polymerisation of 2-Hydroxyethyl Methacrylate

XPS elemental analysis of the continuous wave plasma polymer showed a depletion in oxygen compared to the theoretical monomer structure, Table 7.1. Whereas, the pulsed plasma polymer coating closely resembled the expected poly(HEMA) chemical composition.

Table 7.1. XPS elemental analysis of 2-hydroxyethyl methacrylate plasma polymers

	%C	%O
Theoretical	66.6	33.3
Conventional	68 ± 1	32 ± 1
CW	76 ± 1	24 ± 0.6
Pulsed	68 ± 0.8	32 ± 0.8

The C(1s) envelope of the conventional polymer could be fitted to the following carbon environments: 20 285.0 eV ($-\underline{C}H_2-$), 285.8 eV ($-\underline{C}H-C=O$), 286.5 eV ($-\underline{C}H_2-OH$), 287.0 eV ($-O-\underline{C}H_2-$) and 289.1 eV ($\underline{C}=O$), Figure 7.1. The peak fitting on the pulsed plasma polymer film C(1s) envelope strongly resembled the conventional polymer; whereas the continuous wave plasma polymer exhibited a more intense hydrocarbon peak at 285.0 eV in conjunction with a lower concentration of oxidized carbon species.

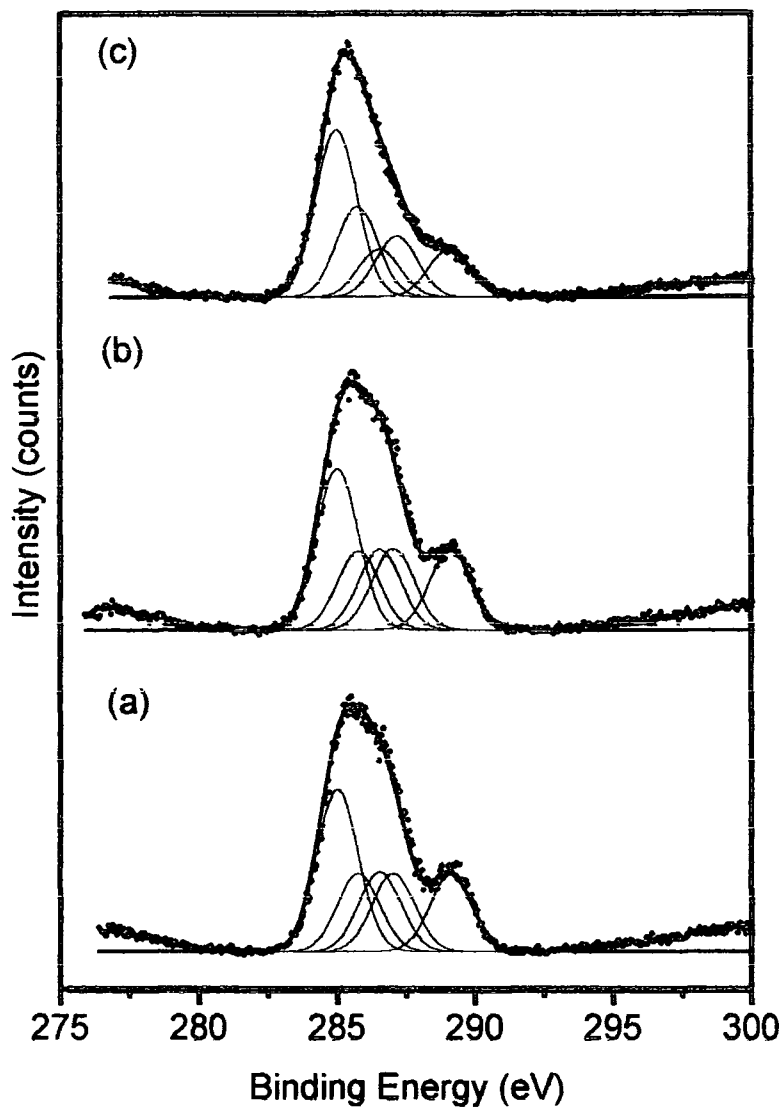


Figure 7.1.

C(1s) XPS spectra of 2-hydroxyethyl methacrylate plasma polymers deposited onto a flat glass substrate: (a) conventional polymer; (b) pulsed (time on = 20 μ s, time off = 20 ms, peak power = 40 W); and (c) 3 W continuous wave.

Infrared analysis confirmed the high retention of the monomer functionalities in the pulsed plasma polymer coating, Figure 7.2. For the 2-hydroxyethyl methacrylate monomer the following peak assignments could be made:²¹ 3500 cm^{-1} O-H stretching, 3112 cm^{-1} acrylate C-H stretching, 2900-2800 cm^{-1} saturated C-H stretching, 1722 cm^{-1} C=O stretching, 1636 cm^{-1} C=C stretching, 942 cm^{-1} =CH₂ wagging, 815 cm^{-1} =CH₂ twisting. The conventional polymer spectrum exhibited all the features of the monomer, except those associated with the C=C double bond. The pulsed plasma polymer spectrum beared a strong resemblance to that of the conventional polymer, presenting

all the peaks well resolved in the fingerprint region. Whereas, poor structural definition was evident for the continuous wave plasma polymer film.

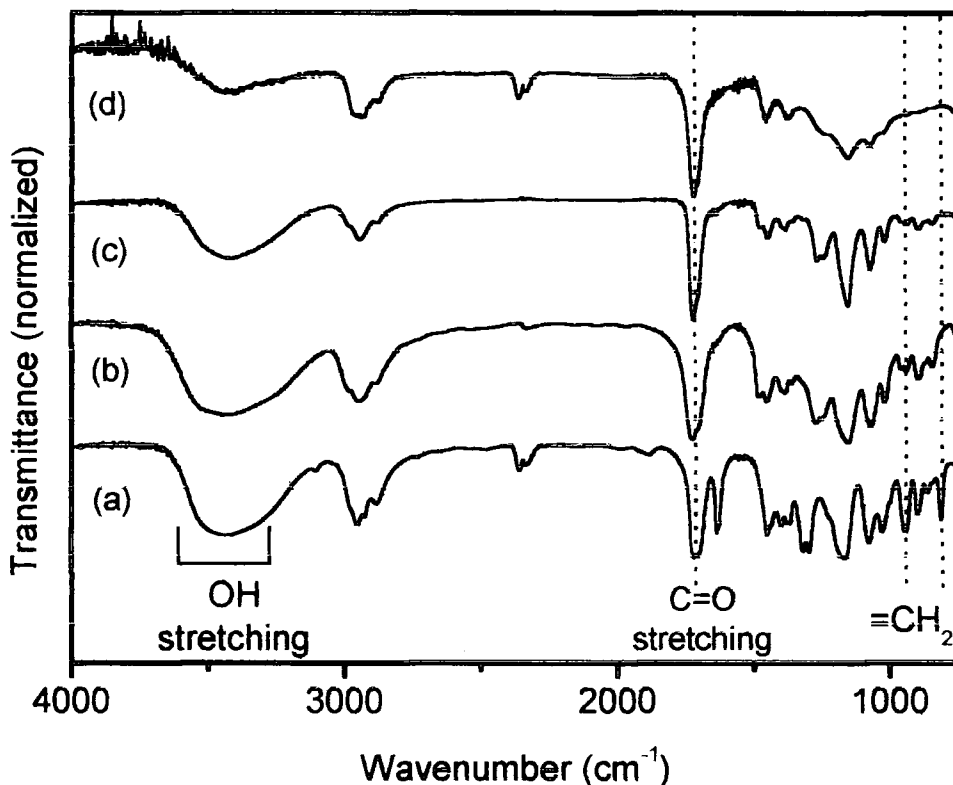


Figure 7.2.

Infrared spectra of (a) 2-hydroxyethyl methacrylate monomer; (b) conventional poly(2-hydroxyethyl methacrylate); (c) pulsed plasma polymer (time on = 20 μ s, time off = 20 ms, peak power = 40 W); and (d) 3 W continuous wave plasma polymer (the weak band in the 2360-2330 cm^{-1} region is due to residual CO_2 in the spectrometer).

The ^1H NMR and ^{13}C NMR spectra of the conventional and the pulsed plasma polymer (Figures 7.3 and 7.4) showed strong similarities. The following assignments could be made. ^1H NMR: 0.74 ppm and 0.91 ppm CH_3 , 1.8 ppm CH_2 , 3.55 ppm $\text{CH}_2\text{-OH}$, 3.87 ppm CH_2O and 4.78 OH ppm.²² ^{13}C NMR: 16.2 ppm and 18.0 ppm CH_3 , 44.1 ppm and 44.5 ppm CH_2 , 58.4 ppm $\text{CH}_2\text{-OH}$, 66.2 ppm CH_2O and 177.1 ppm C=O .²²

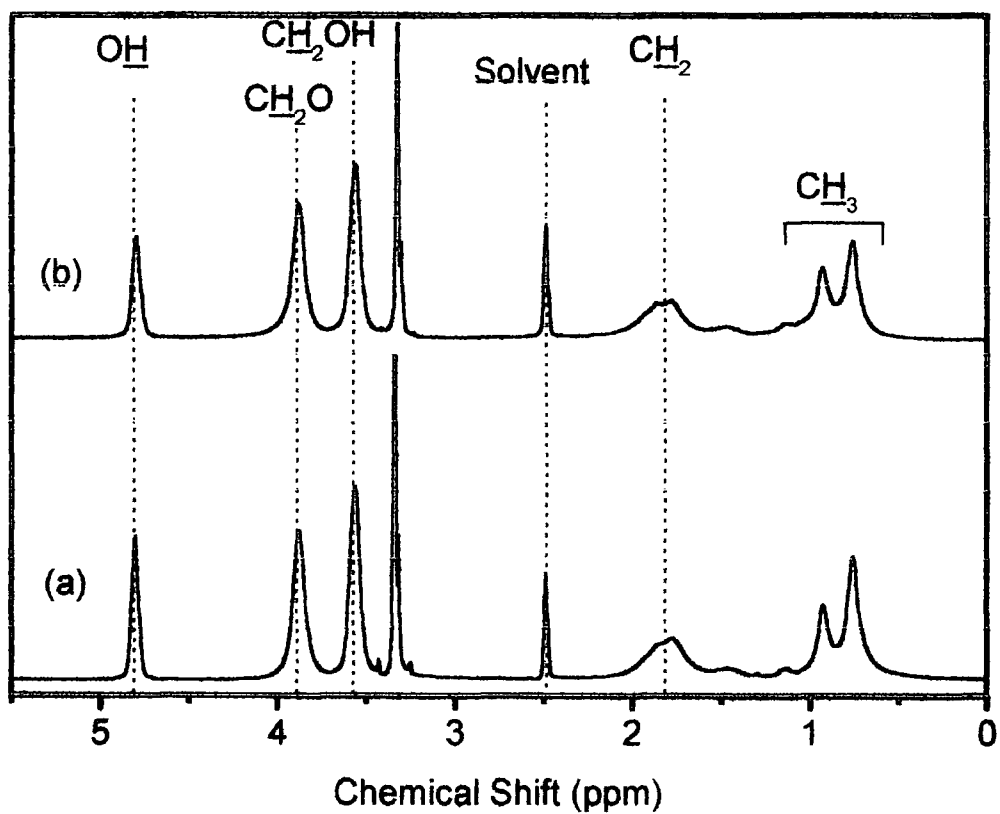


Figure 7.3.

^1H NMR spectra of (a) 2-hydroxyethyl methacrylate conventional polymer and (b) 2-hydroxyethyl methacrylate pulsed plasma polymer.

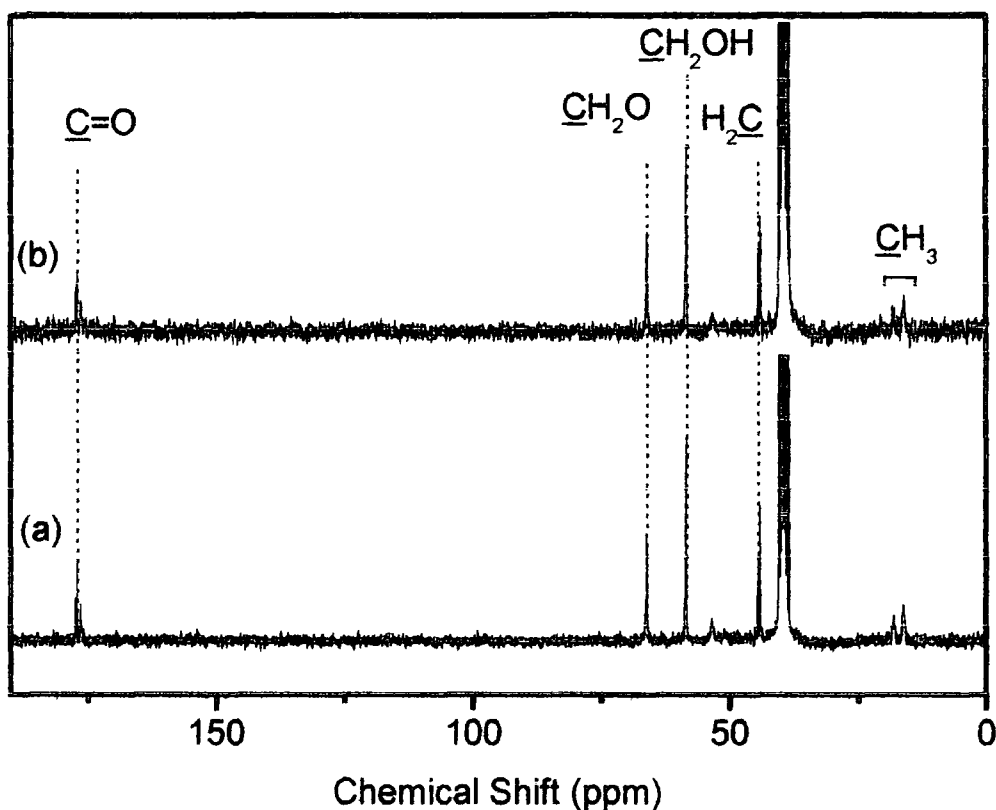


Figure 7.4.

^{13}C NMR spectra of (a) 2-hydroxyethyl methacrylate conventional polymer and (b) 2-hydroxyethyl methacrylate pulsed plasma polymer.

Gel permeation chromatography (GPC) analysis of the pulsed plasma polymer films showed that they generally tended to have lower molecular weight compared to the conventional poly(HEMA) polymer used in this investigation. Besides, the polymer chain length was found to be dependent on the duty cycle, Figure 7.5. Longer time on periods lead to a reduction of the molecules' size. The opposite trend is observed when the time off is increased. This can be explained considering the reaction mechanism occurring in the plasma. The species formed during the time on are allowed to react for longer, without further activation, when the time off is extended. Thus, longer chains result. The number of active species responsible for chain growth is instead reduced when the time on is increased, because the monomer undergoes further fragmentation. Thus, shorter chains originate from an augmentation of the time on.

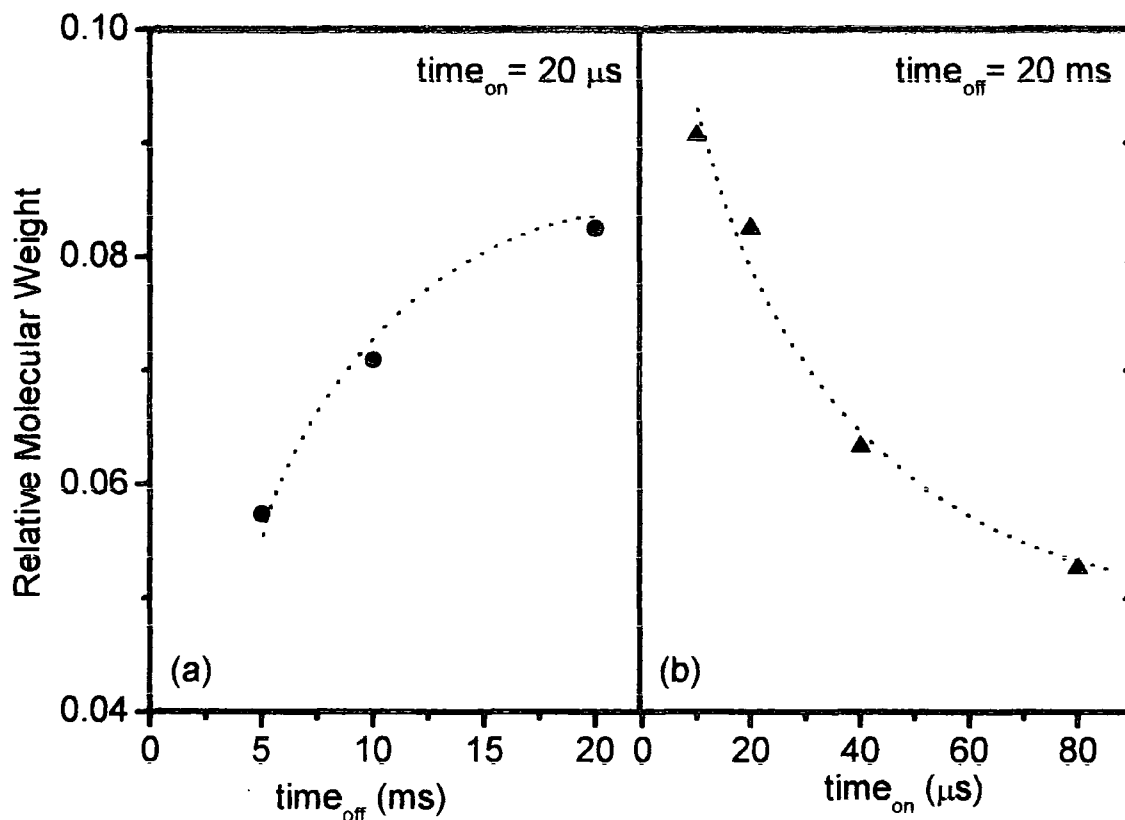


Figure 7.5.

Variation of the average molecular weight relative to the conventional polymer of the pulsed plasma polymers with the duty cycle

Thickness measurements showed a deposition rate of $13.4 \pm 0.3 \text{ nm min}^{-1}$ and $30.0 \pm 0.1 \text{ nm min}^{-1}$ for the pulsed and the continuous wave conditions respectively.

Water contact angle values of $17^\circ \pm 1^\circ$ and $50^\circ \pm 2^\circ$ were measured for the pulsed and the continuous wave plasma polymer layers. This is consistent with greater structural retention in the former case.

The pulsed plasma polymers react with the atmospheric moisture and adsorb water. This is clearly shown by quartz crystal microbalance measurements that indicated a dramatic increase in weight following air exposure, Figure 7.6. This phenomenon is not observed in the case of continuous wave plasma polymer films. Thus, the high concentration of hydroxyl groups in the pulsed plasma polymer films effectively means that this coating can behave as hydrogel.

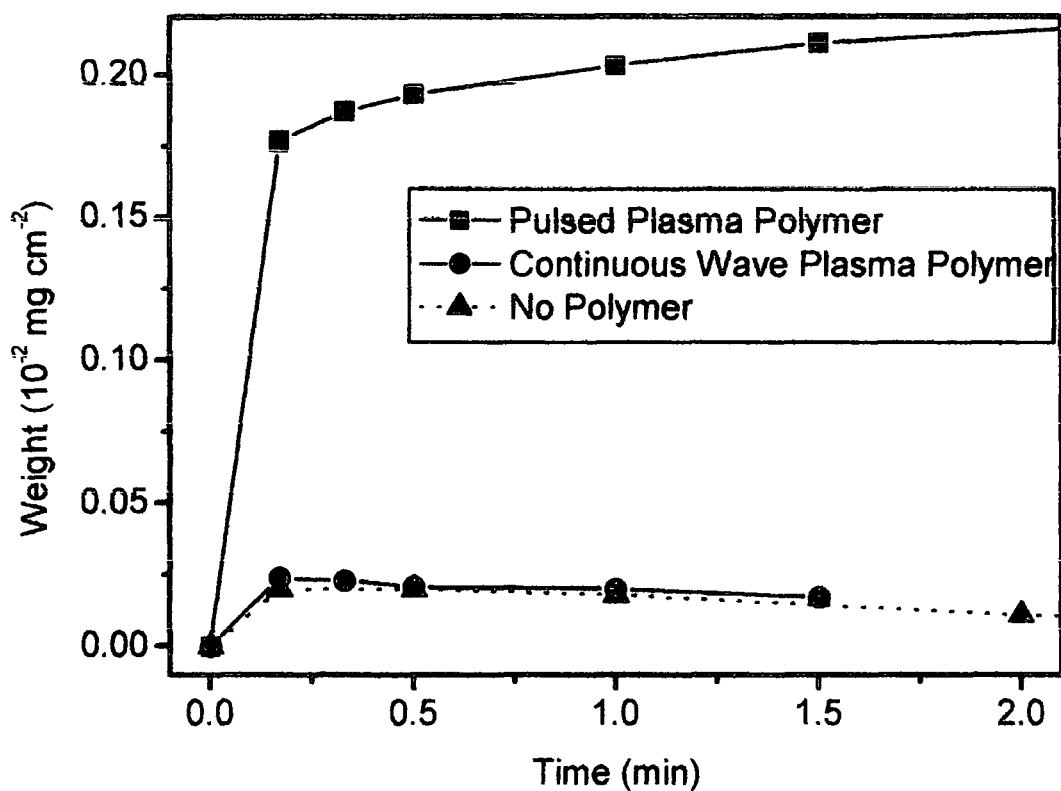


Figure 7.6.

Variation of the weight of the coating during deposition and following air exposure.

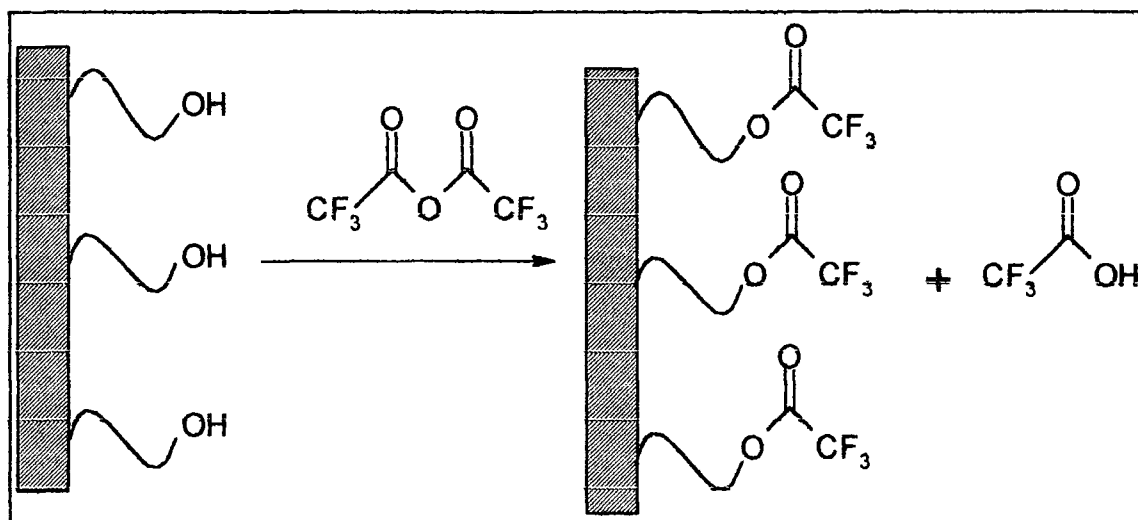
7.3.2. Derivatization Reactions

7.3.2.1 Reaction with Trifluoroacetic Anhydride

Surface hydroxyl groups were reacted with trifluoroacetic anhydride in the vapour phase.

Reaction produces an ester group, Scheme 7.1.

Scheme 7.1. Reaction of surface hydroxyl groups with trifluoroacetic anhydride.



XPS elemental analysis of the plasma polymer layers reacted with trifluoroacetic anhydride (Table 7.2.) showed a reactivity of the pulsed plasma polymer similar to that of the spin coated conventional polymer. Whereas, the continuous wave plasma polymer was less reactive. This can be attributed to a minor amount of OH groups in the coating or to a higher degree of cross linking that reduces its permeability.

Table 7.2. XPS elemental analysis of of 2-hydroxyethyl methacrylate polymers reacted with trifluoroacetic anhydride

	% F	%C	%O	x
Theoretical	20	53.3	26.7	100
Conventional	20 ± 2	54 ± 1	25.2 ± 0.1	100 ± 10
CW	10 ± 2	67 ± 3	23 ± 2	52 ± 16
Pulsed	17 ± 2	56.0 ± 0.2	26 ± 2	80 ± 12

The C(1s) envelope of the conventional polymer reacted with trifluoroacetic anhydride (Figure 7.7) exhibited the CF₃ peak of the anhydride at 293.0 eV. The intensity of the CF₃ peak in the pulsed plasma polymer spectrum is similar to that of the conventional polymer. Whereas it is less prominent in the continuous wave plasma polymer.

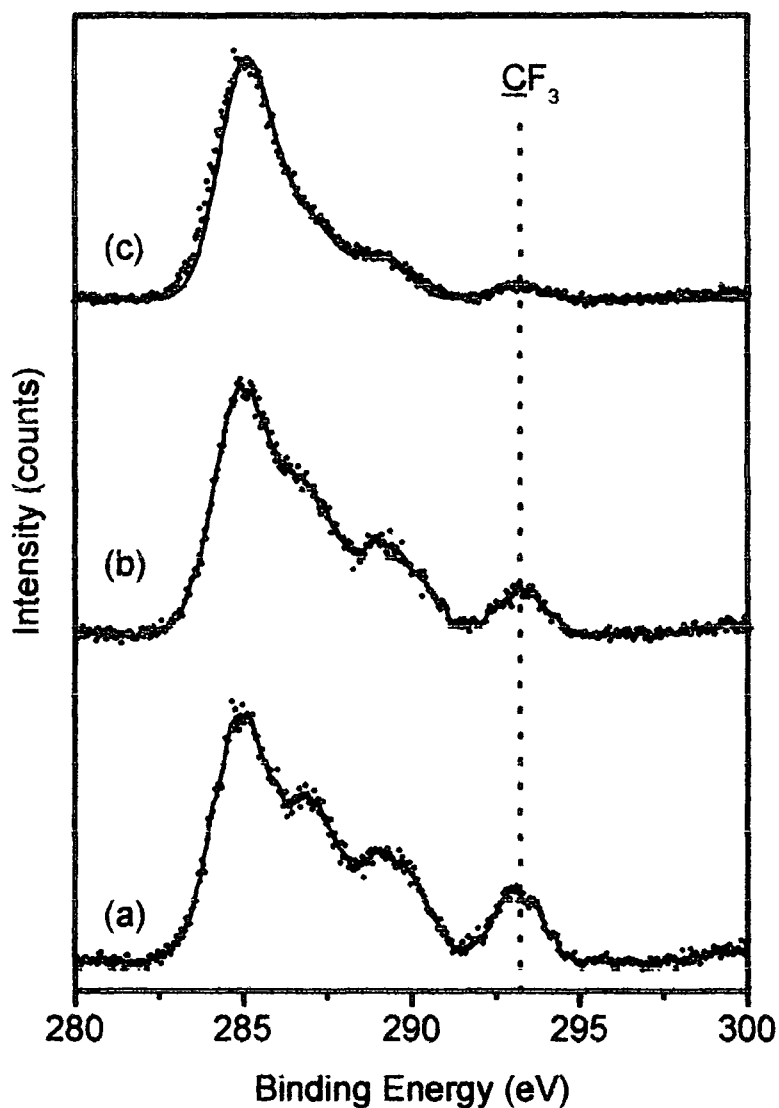


Figure 7.7.

C(1s) XPS spectra of 2-hydroxyethyl methacrylate plasma polymers deposited onto a flat glass substrate and reacted with trifluoroacetic anhydride: (a) conventional polymer; (b) pulsed (time on = 20 μ s, time off = 20 ms, peak power = 40 W); and (c) 3 W continuous wave.

The proportion of hydroxyl group that had undergone esterification was calculated using the F(1s) peak.

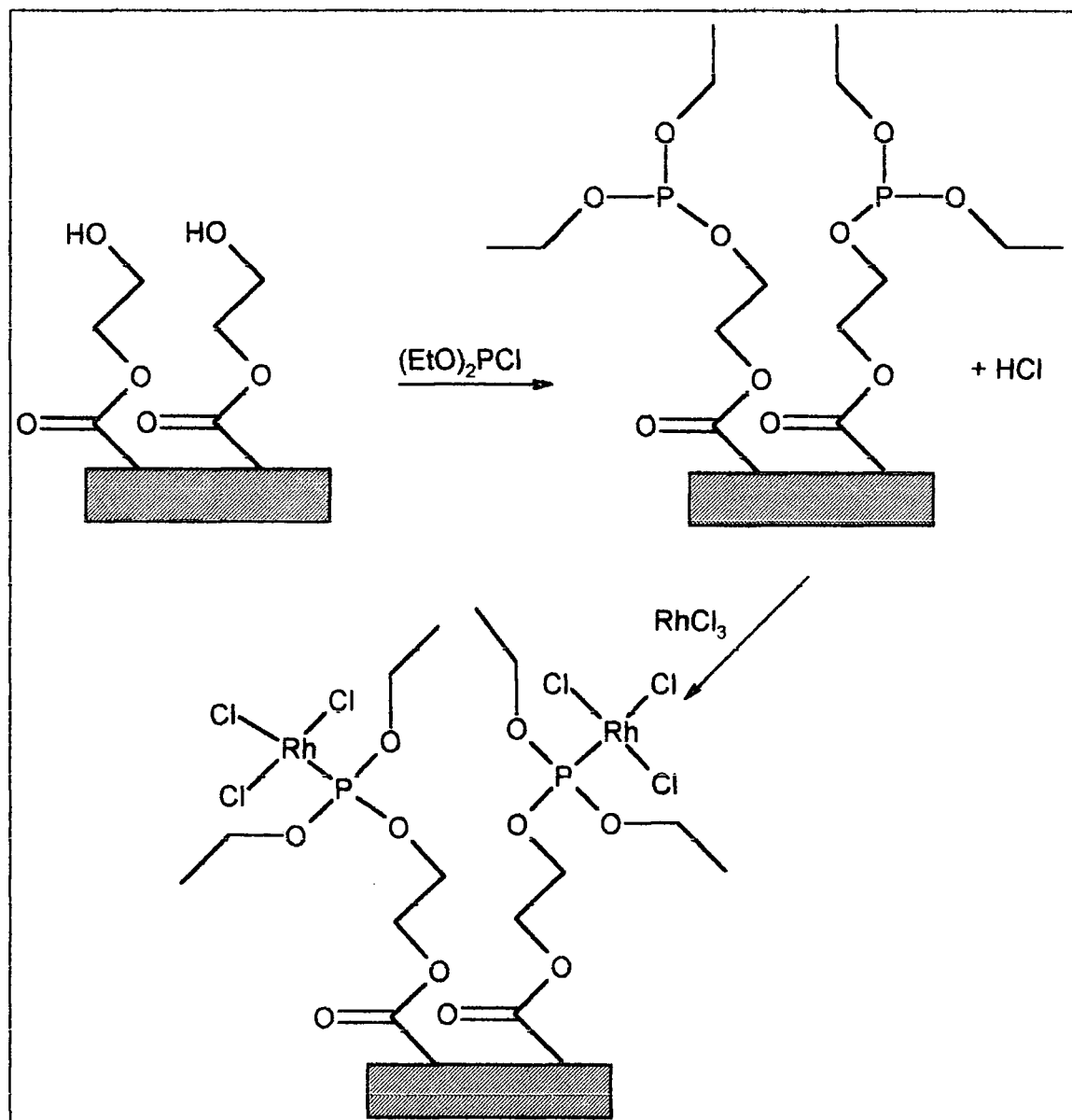
$$\%[F] = \frac{x[O]_0}{[C]_0 + [O]_0 + 2x[O]_0} \times 100 \quad (7.1)$$

where x is the fraction of reacted hydroxyls, $[O]_0$ is the initial concentration of oxygen, $[C]_0$ is the initial concentration of carbon, and $[F]$ is the percentage of fluorine detected at the surface.

7.3.2.2. Diethyl Chlorophosphate and Rh Absorption

Phosphine complexes of rhodium are widely employed for catalytic hydrogenation and hydroformilation reactions.²³ These complexes are often prepared using RhCl_3 as the precursor. In order to anchor such complexes to HEMA functionalized surface a phosphine specie must be introduced, followed by Rh complexation, Scheme 7.2.

Scheme 7.2. Reaction of surface hydroxyl groups with diethylchlorophosphate.



XPS analysis following reaction of diethylchlorophosphate vapour with poly(HEMA) surfaces gave rise to the appearance to the $\text{P}(2p_{3/2})$ at 132.7 eV,²⁰ Scheme 7.2 and Table 7.3. A small amount of residual chlorine was also detected. It was only

partially eliminated upon washing with 1,4-dioxane. It is probably due to HCl byproduct rather than unreacted absorbed reagent. The lower reactivity of the conventional polymer is probably due to its higher molecular weight (lower chain mobility).

Table 7.3. XPS elemental analysis of of 2-hydroxyethyl methacrylate polymers reacted with diethylchlorophosphate

Coating	%C	%Cl	%O	%P	%Rh	%Si
Pulsed + (EtO) ₂ PCl unwashed	60.8 ± 0.6	2.0 ± 0.4	31 ± 1	6 ± 1	-	-
CW + (EtO) ₂ PCl unwashed	74 ± 4	0.35 ± 0.05	24 ± 4	1.0 ± 0.3	-	-
Conventional + (EtO) ₂ PCl unwashed	64 ± 2	0.90 ± 0.01	33 ± 2	2.50 ± 0.01	-	-
Pulsed + (EtO) ₂ PCl washed	64 ± 2	1.5 ± 0.7	30 ± 0.7	4 ± 1	-	-
CW + (EtO) ₂ PCl washed	76 ± 3	-	23 ± 2	0.8 ± 1	-	-
Pulsed + (EtO) ₂ PCl + RhCl ₃	54.2 ± 0.1	12.8 ± 0.3	24 ± 3	3.1 ± 0.3	4.0 ± 0.5	-
CW + (EtO) ₂ PCl + RhCl ₃	72.8 ± 0.6	1.8 ± 0.1	23.0 ± 0.1	-	0.7 ± 0.1	1.1 ± 0.5
Pulsed + RhCl ₃	69 ± 3	5 ± 2	25 ± 1	-	1.4 ± 0.7	-
CW + RhCl ₃	75 ± 3	1.0 ± 0.2	24 ± 3	-	-	-

The percentage of surface hydroxyl groups (x) which had reacted were calculated using the percentage of detected phosphorous ($\%[P]$) following washing in 1,4-dioxane:

$$\%[P] = \frac{\frac{1}{3}x[O]_0}{[Cl]_0 + [O]_0 + \frac{7}{3}x[O]_0} \times 100 \quad (7.2.)$$

This corresponded to $10 \pm 3\%$ and $52 \pm 8\%$ hydroxyl groups for the continuous wave and the pulsed plasma polymer respectively.

It has been reported in the literature that this type of phosphite ligand readily coordinates to catalytic rhodium centres²³. In order to demonstrate the viability of carrying out such reactions at solid surfaces, the diethylphosphite functionalized poly(HEMA) plasma polymer films were reacted with RhCl_3 . XPS analysis showed the appearance of Rh(3d) doublet with the $3d_{5/2}$ peak at 310.6 eV corresponding to Rh(III),²⁴ Figure 7.8. and Table 7.3.

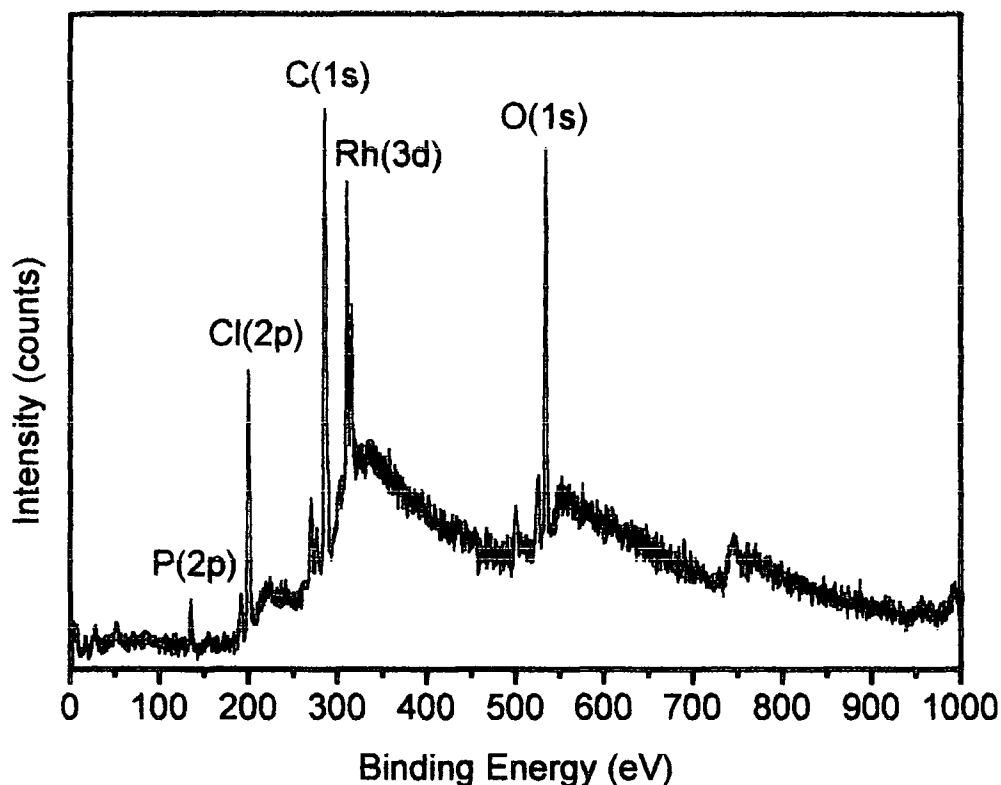


Figure 7.8.

XPS spectra of 2-hydroxyethyl methacrylate pulsed plasma polymer (time on = 20 μs , time off = 20 ms, peak power = 40 W) deposited onto a flat glass substrate and reacted with diethylchlorophosphite followed by complexation of RhCl_3 .

Also it was found that there are 1.3 atoms of Rh for every atom of P, i.e. approximately one as previously reported for grafted phosphite ligands.^{25, 26} A control experiment showed that the plasma polymer layer itself is capable of coordinating Rh species. However, this amount was much lower compared to when the diethylphosphite group is also present on the surface.

7.3.2.3. Zirconium *tert*-Butoxide and Multilayer Assemblies

Anchoring of polymer layers onto solid surfaces is a topic of interest for packaging and electronic applications. It has been shown that alkoxyzirconium compounds are able to bind onto hydroxylated surfaces^{17, 27-33} and provide the binding site for polymers containing carboxylic acid units.³⁴ This leads to a stabilization of the interface. Poly(acrylic acid) can then provide a binding site for positive charged polymers in multilayer assemblies.

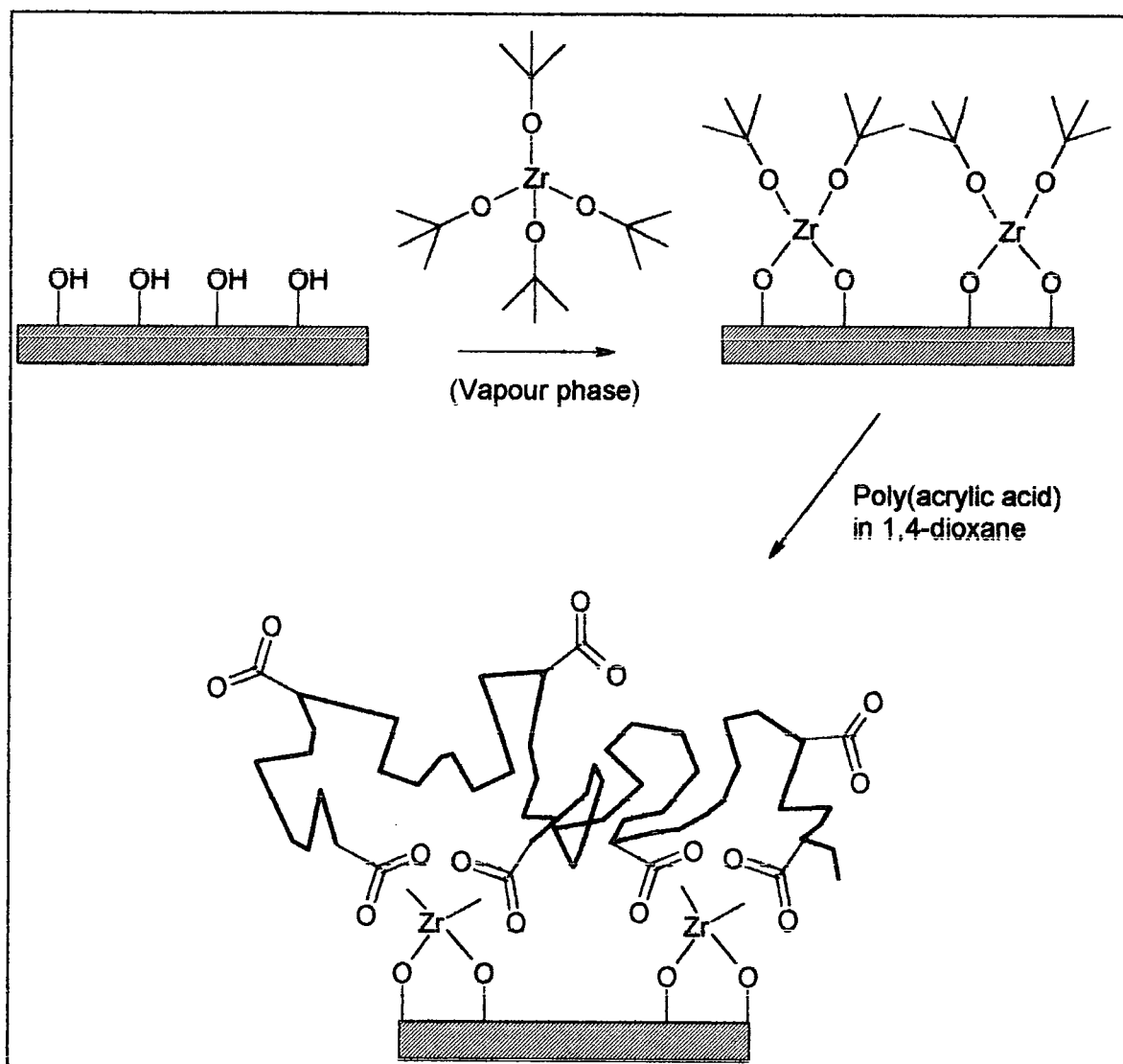
XPS analysis of poly(HEMA) coated samples following reaction with $Zr(OC(CH_3)_3)_4$ is shown on Table 7.4.

Table 7.4. XPS elemental analysis of 2-hydroxyethyl methacrylate plasma polymers multilayer assemblies.

Sample		% Zr	% C	% O	% N	% F
Poly(HEMA) + $Zr(OC(CH_3)_3)_4$	Pulsed	5.0 ± 0.8	72 ± 3	23 ± 4	-	-
	CW	4.5 ± 0.1	74 ± 2	22 ± 2	-	-
	Conv.	6.7 ± 0.7	66 ± 7	27 ± 6	-	-
Poly(HEMA) + $Zr(OC(CH_3)_3)_4$ + Poly(acrylic acid)	Pulsed	1.9 ± 0.5	64 ± 5	34 ± 2	-	-
	CW	2.9 ± 0.6	62 ± 2	34 ± 2	-	-
	Conv.	1.6 ± 0.3	63 ± 4	35 ± 3	-	-
Poly(HEMA) + $Zr(OC(CH_3)_3)_4$ + Poly(acrylic acid) + Fluorosurfactant	Pulsed	-	42 ± 2	6.5 ± 0.5	2.1 ± 0.1	49 ± 2
	CW	0.6 ± 0.2	43 ± 1	6 ± 1	2.0 ± 0.2	49 ± 3
	Conv.	-	42 ± 1	5.5 ± 0.8	2.1 ± 0.1	40 ± 2

The C(1s) envelope (Figure 7.9 (a)) shows an increase in hydrocarbon content following $Zr(OC(CH_3)_3)_4$ exposure, as expected from the introduction of *tert*-butoxide groups on the surface, Scheme 7.3.

Scheme 7.3. Reaction of surface hydroxyl groups with zirconium tert-butoxide followed by poly(acrylic acid) anchoring.



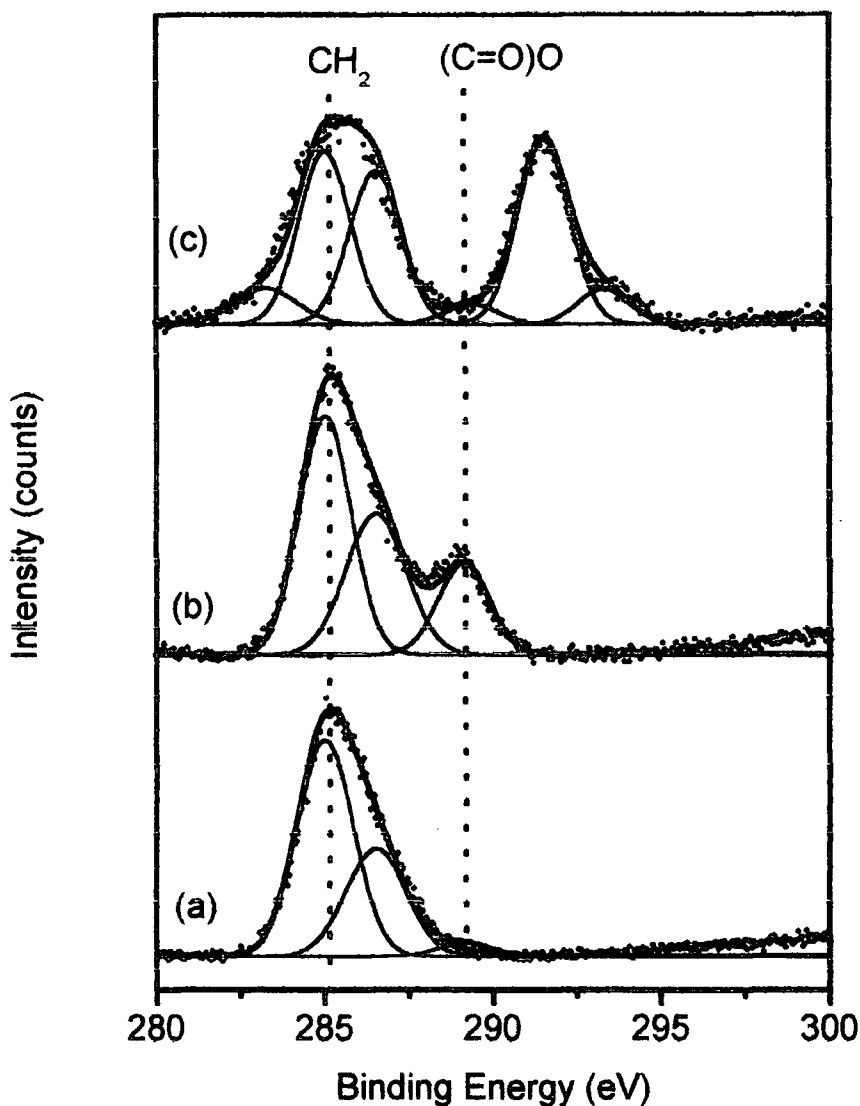


Figure 7.9.

C(1s) XPS spectra of 2-hydroxyethyl methacrylate pulsed plasma polymer (time on = 20 μ s, time off = 20 ms, peak power = 40 W) deposited onto a flat glass substrate: (a) reacted with $\text{Zr}(\text{OC}(\text{CH}_3)_3)_4$; (b) successively coupled with poly(acrylic acid); and (c) successively coupled with Zonyl fluorosurfactant.

Infrared analysis of the 2-hydroxyethyl methacrylate pulsed plasma polymer coating following reaction with $\text{Zr}(\text{OC}(\text{CH}_3)_3)_4$ showed the appearance of the following peaks: 1358 cm^{-1} , 1227 cm^{-1} , 1195 cm^{-1} , 1012 cm^{-1} , 980 cm^{-1} , 902 cm^{-1} and 774 cm^{-1} . This is in accordance with the reflectance infrared spectrum of $(\text{AlO}_x)\text{Zr}(\text{OC}(\text{CH}_3)_3)_2$ as reported by Schwartz et al.³¹ In particular, the absorption at 980 cm^{-1} indicates the presence of the alkoxyzirconium linkage. The peaks of the underlying poly(HEMA) layer are still discernible.

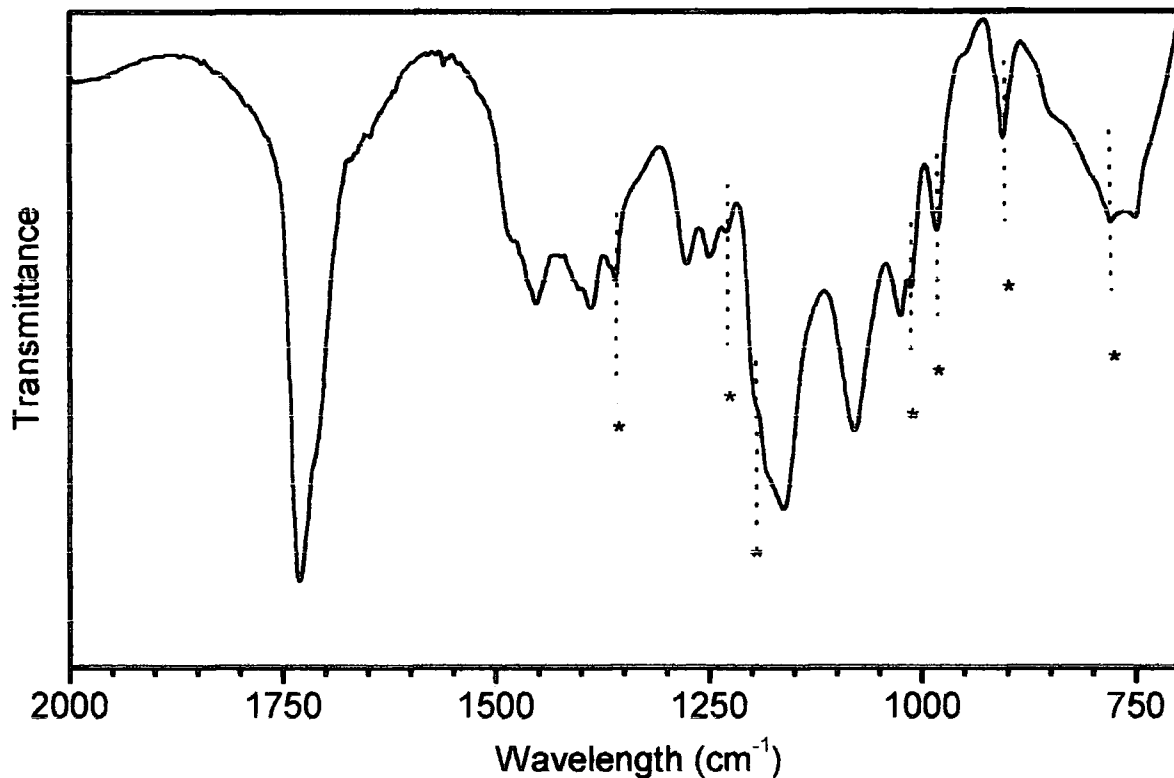


Figure 7.10.

Infrared spectra of 2-hydroxyethyl methacrylate pulsed plasma polymer (time on = 20 μ s, time off = 20 ms, peak power = 40 W) reacted with $Zr(OC(CH_3)_3)_4$.

Immersion of the $Zr(OC(CH_3)_3)_4$ reacted samples into polyacrylic acid dissolved in 1,4-dioxane followed by rinsing in pure solvent, had the effect of attenuating the Zr XPS signal, as well as intensifying the $(C=O)O$ peak in the C(1s) envelope (Figure 7.9 (b)). This can be taken as being evidence for the attachment of polyacrylic acid chains to surface bound Zr complexes via Zr η^2 -carboxylate linkages. In addition, there may also be some binding between poly(HEMA) and poly(acrylic acid).

Subsequent exposure to a cationic fluorinated surfactant solution gave rise to the formation of polyelectrolyte-surfactant complexes anchored onto the surface. This is confirmed by XPS elemental analysis, which showed the appearance of fluorine and nitrogen on the surface. The C(1s) envelope of the pulsed plasma polymer layer following fluorosurfactant adsorption exhibited $C-F$ peaks (Figure 7.9 (c)).

The composition of the final multilayer assembly appeared independent from the original substrate. However, in the case of the continuous wave plasma polymer the Zr from the underlying substrate was still discernible.

7.4. Conclusions

Pulsed plasma polymerization of 2-hydroxyethyl methacrylate provides a one step solventless route for producing well-defined hydroxyl functionalized solid surfaces. The high level of structural retention observed is consistent with polymerization proceeding via a conventional free radical mechanism during the pulsed plasma off-period, in conjunction with monomer activation during the on-period. The observed trend in pulsed plasma polymer molecular weight as a function of electrical discharge duty cycle can be explained on the basis of this reaction mechanism. Longer chains are produced when the species formed during the pulse time on are allowed to react for longer or when the time-off is extended. Whereas, greater chain scission occurs when the time on is increased.

The hydroxyl groups present at the poly(HEMA) plasma polymer surface are found to readily undergo hydration, esterification, and also derivatization with diethylchlorophosphite. The latter reaction is considered to be a useful method for immobilizing precious metal complexes onto solid surfaces for catalytic applications.

7.5. References

- [1] Brazel, C. S.; Peppas, N. A. *Eur. J. Pharm. Biopharm.* **2000**, *49*, 47.
- [2] Ferreira, L.; Vidal, M. M.; Gil, M. H. *Int. J. Pharm.* **2000**, *194*, 169.
- [3] Sun, Y.-M.; Chang, C.-C.; Huang, W.-F.; Liang, H.-C. *J. Controlled Release* **1997**, *47*, 247.
- [4] Denizli, A.; Say, R.; Patir, S.; Arica, M. Y. *React. Funct. Polym.* **2000**, *43*, 17.
- [5] Ibrahim, E.-H.; Denizli, A.; Bektas, S.; Genc, O.; Piskin, E. *J. Chromatogr., B* **1998**, *720*, 217.
- [6] Arica, M. Y.; Senel, S.; Alaeddinoglu, N. G.; Patir, S.; Denizli, A. *J. Appl. Polym. Sci.* **2000**, *75*, 1685.
- [7] Hamilton, C. J.; Murphy, S. M.; Tighe, B. J. *Polymer* **2000**, *41*, 3651.
- [8] Folkman, J.; Moscona, A. *Nature* **1978**, *273*, 345.
- [9] Morra, M.; Occhiello, E.; Garbassi, F. *J. Adhes.* **1994**, *46*, 39.
- [10] Zubaidi; Hirotsu, T. *J. Appl. Polym. Sci.* **1996**, *61*, 1579.
- [11] Osada, Y.; Iriyama, Y. *Thin Solid Films* **1984**, *118*, 197.

- [12] Feng, M.; Morales, A. B.; Beugeling, T.; Bantjes, A.; Van der Werf, K.; Gosselink, G.; De Groot, B.; Greve, J. *J. Colloid Interface Sci.* **1996**, *177*, 364.
- [13] Klee, D.; Hocker, H. *Adv. Polym. Sci.* **1999**, *149*, 1.
- [14] Morra, M.; Cassinelli, C. *J. Biomed. Mater. Res.* **1996**, *31*, 149.
- [15] Morra, M.; Cassinelli, C. *J. Biomed. Mater. Res.* **1995**, *29*, 39.
- [16] Lopez, G. P.; Ratner, B. D.; Rapoza, R. J.; Horbett, T. A. *Macromolecules* **1993**, *26*, 3247.
- [17] Schwartz, J.; Gawalt, E. S.; Lu, G.; Milliron, D. J.; Purvis, K. L.; Woodson, S. J.; Bernasek, S. L.; Bocarsly, A. B.; VanderKam, S. K. *Polyhedron* **2000**, *19*, 505.
- [18] Briggs, D. In *Comprehensive Polymer Science*, ; G. C. Eastmond, A. Ledwith, S. Russo and P. Sigwalt, Ed.; Pergamon Press, 1989; Vol. Volume 1: Polymer characterization.
- [19] Wickson, B. M.; Brash, J. L. *Colloid and Surfaces A: Physicochemical and Engineering Aspects* **1999**, *156*, 201.
- [20] Beamson, G.; Briggs, D. *High resolution XPS of organic polymers: the Scienta ESCA300 database*; John Wiley & Sons: New York, 1992.
- [21] Lin-Vien, D.; Colthup, N. B.; Fateley, W. G.; Grasselli, J. G. *The Handbook of Infrared and Raman Characteristic Frequencies of Organic Molecules*; Academic Press: New York, 1991.
- [22] Hill, D. J. T.; Moss, N. G.; Pomery, P. J.; Whittaker, A. K. *Polymer* **2000**, *41*, 1287.
- [23] Greenwood, N. N.; Earnshaw, A. *Chemistry of the elements*; Pergamon Press: Oxford, 1984.
- [24] Seah, M. P. In *Practical Surface Analysis by X-ray Photoelectron Spectroscopy*; D. Briggs and M. P. Seah, Ed.; John Wiley & Sons: New York, 1983, pp 181.
- [25] Jongma, T.; Kimkes, P.; Challa, G.; VanLeeuwen, P. W. N. M. *Polymer* **1992**, *33*, 161.
- [26] VanLeeuwen, P. W. N. M.; Jongma, T.; Challa, G. *Macromol. Symp.* **1994**, *80*, 241.
- [27] Purvis, K. L.; Lu, G.; Schwartz, J.; Bernasek, S. L. *Langmuir* **1999**, *15*, 7092.
- [28] Purvis, K. L.; Lu, G.; Schwartz, J.; Bernasek, S. L. *J. Am. Chem. Soc.* **2000**, *122*, 1808.
- [29] Bernasek, S. L.; Schwartz, J. *Langmuir* **1998**, *14*, 1367.

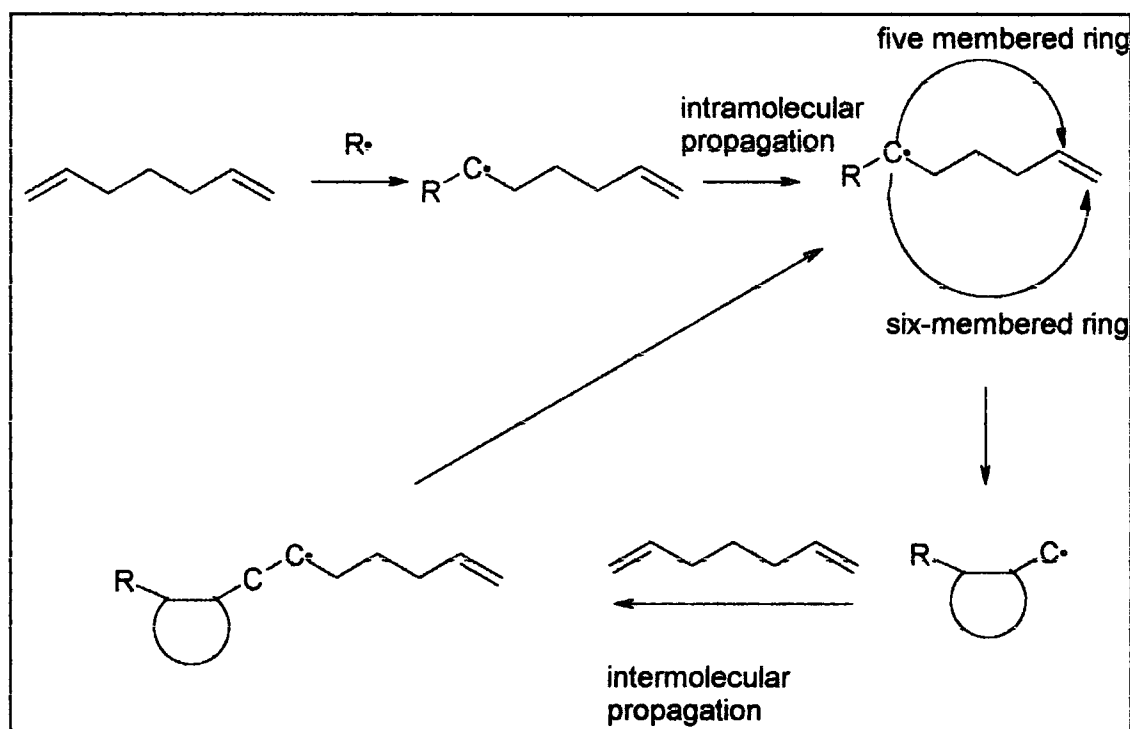
- [30] VanderKam, S. K.; Lu, G.; Bernasek, S. L.; Schwartz, J. *J. Am. Chem. Soc.* **1997**, *119*, 11639.
- [31] Aronoff, Y. G.; Chen, B.; Lu, G.; Seto, C.; Schwartz, J.; Bernasek, S. L. *J. Am. Chem. Soc.* **1997**, *119*, 259.
- [32] Bakiamoh, S. B.; Blanchard, G. J. *Langmuir* **1999**, *15*, 6379.
- [33] Gawalt, E. S.; Lu, G.; Bernasek, S. L.; Schwartz, J. *Langmuir* **1999**, *15*, 8929.
- [34] VanderKam, S. K.; Bocasly, A. B.; Schwartz, J. *Chem. Mater.* **1998**, *10*, 685.

8. PLASMA POLYMERIZATION OF DIFUNCTIONAL MONOMERS

8.1. Introduction

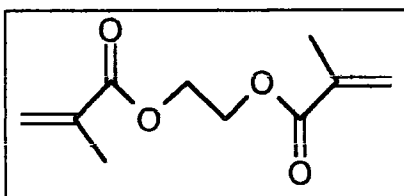
Difunctional monomers (i.e. dienes) lead to crosslinked non-linear polymers. However, it has been found that 1,6-dienes can give rise to soluble linear polymers. This is attributed to cyclopolymerization via an alternating intramolecular-intermolecular chain propagation.¹ The process is favoured by the intramolecular proximity of the vinyl group and the strong driving force of five- or six-membered ring formation, Scheme 8.1.2

Scheme 8.1. Mechanism of cyclopolymerization of 1,6 dienes



In this chapter the plasma polymers originating from three diene molecules are investigated.

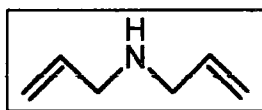
Ethylene glycol dimethacrylate (Structure 8.1.) is a 1,9-diene not capable of cyclopolymerizing. However, it gives rise to highly crosslinked coatings, which possess high chemical and mechanical stability.³



Structure 8.1.

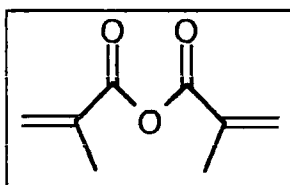
Ethylene glycol dimethacrylate

Diallylamine (Structure 8.2.) and methacrylic anhydride (Structure 8.3.) are typical 1,6-dienes and should undergo cyclopolymerization.^{1,4,5} Infrared spectroscopy and Raman spectroscopy have been employed in order to assess the existence of cyclic structures in the plasma polymer films.



Structure 8.2.

Diallylamine



Structure 8.3.

Methacrylic anhydride

8.2. Experimental

Plasma polymerization of ethylene glycol dimethacrylate (Aldrich, 99% purity) was carried out in at 0.1 torr pressure for 30 min onto NaCl discs for infrared analysis and onto Si wafers for thickness and swelling measurement.

In the case of methacrylic anhydride (Aldrich, 99% purity) plasma polymerization was carried out in at a pressure of 0.2 torr onto KBr discs. Deposition times of 30 min and 120 min were employed for continuous wave and pulsed plasma conditions respectively.

The third series of experiments entailed plasma polymerization of diallylamine (Aldrich, 99% purity) was carried out at 0.1 torr pressure for 30 min and 120 min for the

continuous wave and pulsed plasma conditions respectively. In this case NaCl discs were used for infrared analysis, glass slides for XPS analysis, and roughened silver for surface enhanced Raman spectroscopy.

Infrared spectra of plasma polymer films were acquired in transmittance mode at a resolution of 4 cm^{-1} and averaged over 32 scans. Reference spectra of monomers were obtained by placing a drop of liquid between two NaCl or KBr plates.

Swelling experiments were carried out by placing the samples in tetrahydrofuran (Rectapur, 99%) for 18 h, followed by thickness measurement.

8.3. Results and Discussion

8.3.1. Ethylene Glycol Dimethacrylate Plasma Polymerization

The following infrared band assignments could be made for the monomer (Figure 8.1.): δ unsaturated C-H stretching (3106 cm^{-1} and 2981 cm^{-1}), methyl C-H stretching (2960 cm^{-1} antisymmetric, 2929 cm^{-1} symmetric), ethylene C-H stretching (2930 cm^{-1} antisymmetric, 2894 cm^{-1} symmetric), acrylate C=O stretching (1725 cm^{-1}), acrylate C=C stretching (1638 cm^{-1}), CH_3 bending (1453 cm^{-1} antisymmetric and 1368 cm^{-1} symmetric), ester C-O stretching (1160 cm^{-1}) = CH_2 wagging (943 cm^{-1}) and = CH_2 twist (814 cm^{-1}).

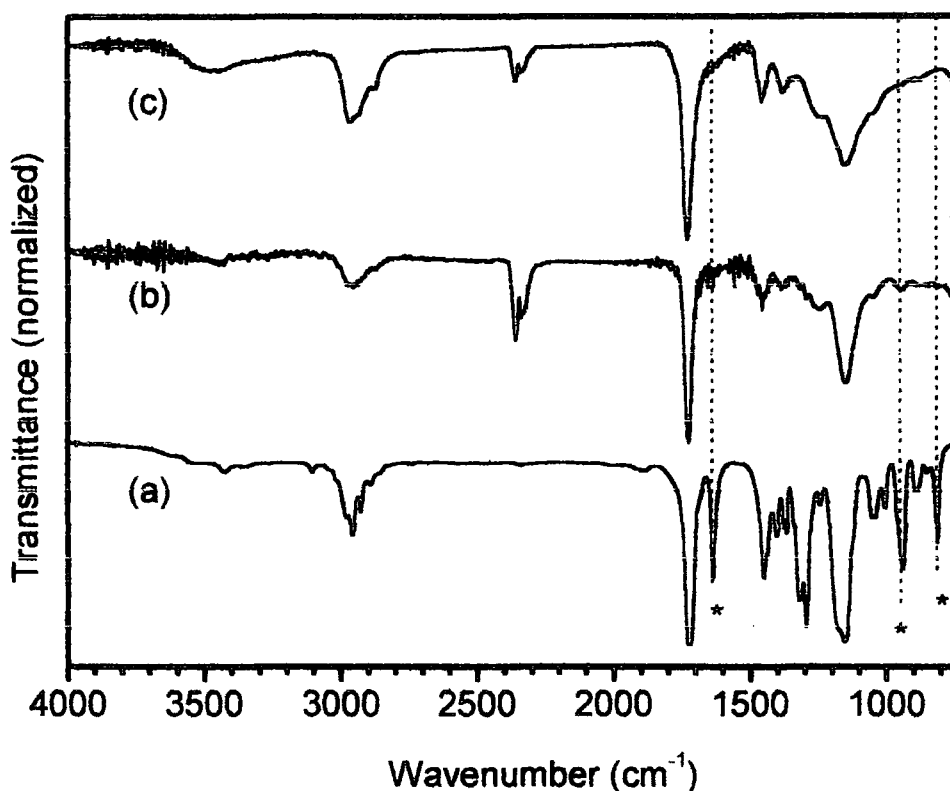


Figure 8.1.

Infrared spectra of (a) ethylene glycol dimethacrylate monomer; (b) pulsed plasma polymer (time on = 20 μ s, time off = 20 ms, peak power = 40 W); and (c) 3 W continuous wave plasma polymer. * corresponds to C=C features in the monomer. The bands around 2300 cm^{-1} are due to residual CO_2 in the spectrometer.

The pulsed plasma polymer spectrum shows all the bands of the monomer with the exception of those attributed to the carbon-carbon double bond (1638 cm^{-1} , 943 cm^{-1} , 814 cm^{-1}). The C-O stretching band at 1150 cm^{-1} is narrow compared to the continuous wave plasma polymer. The continuous wave plasma polymer spectrum shows unresolved broad peaks.

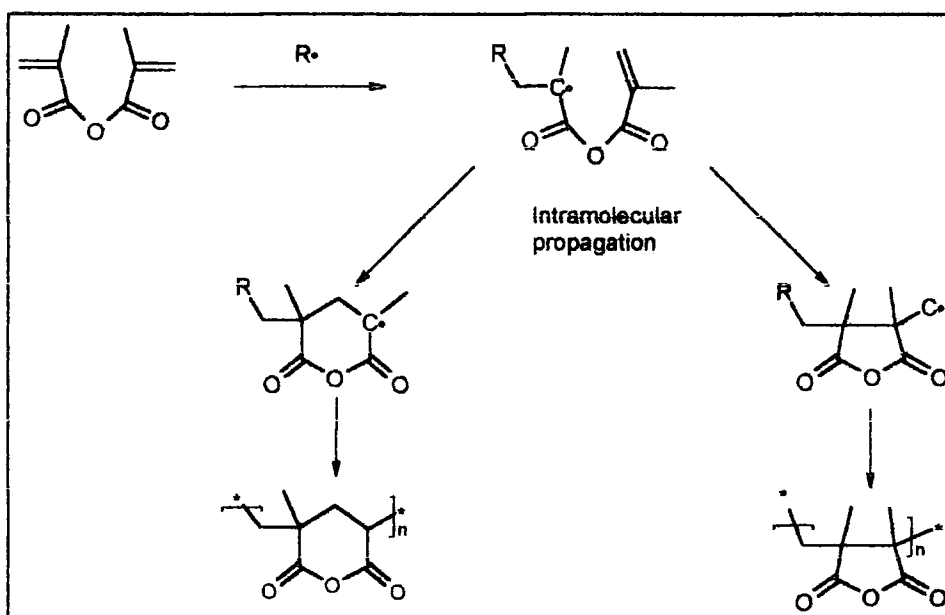
Plasma polymerization gave rise to an unsaturated highly cross-linked polymer coating. However, due to monomer fragmentation the degree of cross-linking is higher in the pulsed plasma polymer. Swelling experiment showed that a 234 ± 3 nm thick pulsed plasma polymer film increased to 258 ± 5 nm when swollen in tetrahydrofuran, whereas a 180 ± 4 nm thick continuous wave plasma polymer film increased to 350 ± 5 nm under identical conditions. A 220 nm thick conventionally polymerized

poly(ethylene glycol dimethacrylate) layer is reported to increase in thickness to 280 nm.³

8.3.2. Methacrylic Anhydride Plasma Polymerization

Methacrylic anhydride is a 1,6-diene capable of cyclopolymerization. It has been found that varying the conditions employed during homopolymerization it is possible to control the ring size. Temperature, polarity of the solvent, and monomer concentration are the factors that govern the process and determine the ring size.^{2,5,7-11}

Scheme 8.2. Mechanism of cyclopolymerization of methacrylic anhydride



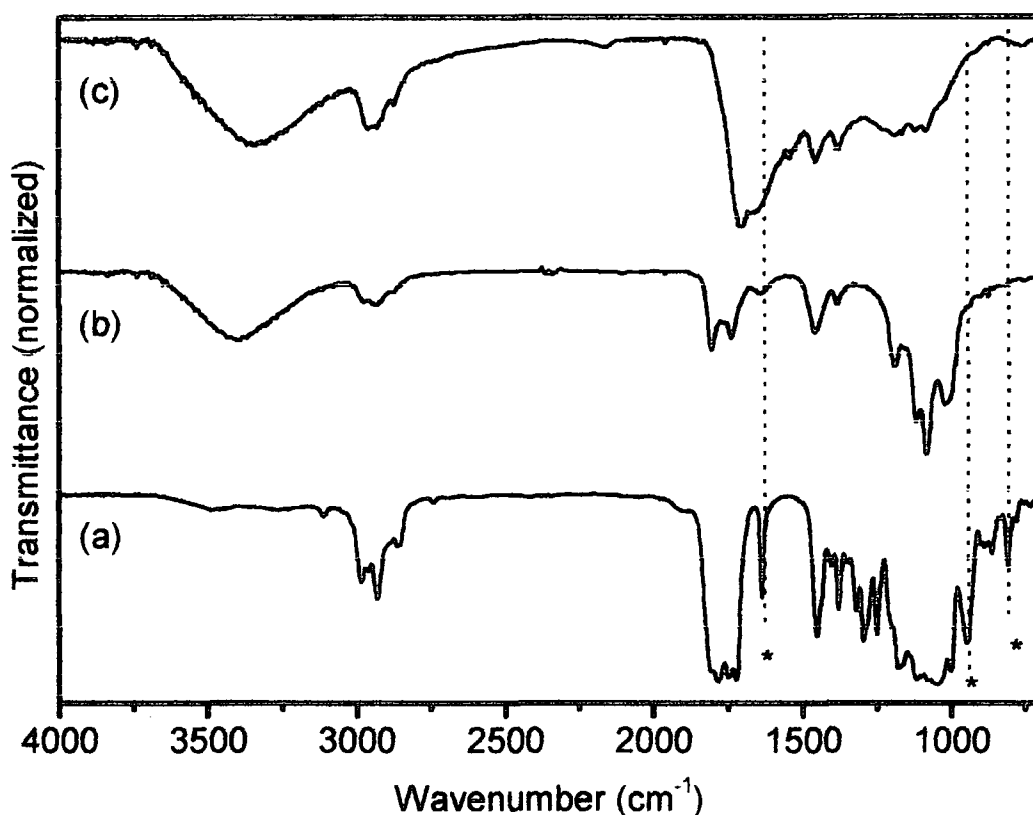


Figure 8.2.

Infrared spectra of (a) methacrylic anhydride monomer; (b) pulsed plasma polymer (time on = 20 μ s, time off = 20 ms, peak power = 40 W); and (c) 3 W continuous wave plasma polymer. * denotes C=C bond features in the monomer.

The following band assignments can be made for the methacrylic anhydride monomer (Figure 8.2):⁶ unsaturated C-H stretching (3111 cm^{-1} and 2986 cm^{-1}), saturated C-H stretching (2931 cm^{-1} and 2963 cm^{-1}), anhydride C=O stretching (1800 cm^{-1} , 1785 cm^{-1} , 1749 cm^{-1} , and 1723 cm^{-1}), acrylate C=C stretching (1637 cm^{-1}), =CH₂ wagging (948 cm^{-1}) and =CH₂ twisting (808 cm^{-1}).

Pulsed plasma polymerization of methacrylic anhydride gave rise to the following bands: C-H stretching (2978 cm^{-1} , 2936 cm^{-1} and 2879 cm^{-1}), anhydride C=O stretching (1858 cm^{-1} , 1804 cm^{-1} , 1762 cm^{-1} and 1737 cm^{-1}). Some absorbed water was also present (O-H stretching at 3397 cm^{-1} and O-H bending at 1641 cm^{-1})

Whereas in the case of continuous wave plasma polymerization spectrum broad unresolved peaks were observed. The presence of only one broad peak at 1710 cm^{-1} in the $1800\text{-}1700\text{ cm}^{-1}$ region indicates that the anhydride functionality is completely destroyed in the plasma.

The precise assignment of the C=O stretching bands belonging to the anhydrides can be used to distinguish linear from cyclic anhydrides, and also it is possible to determine the ring size, Figure 8.3.

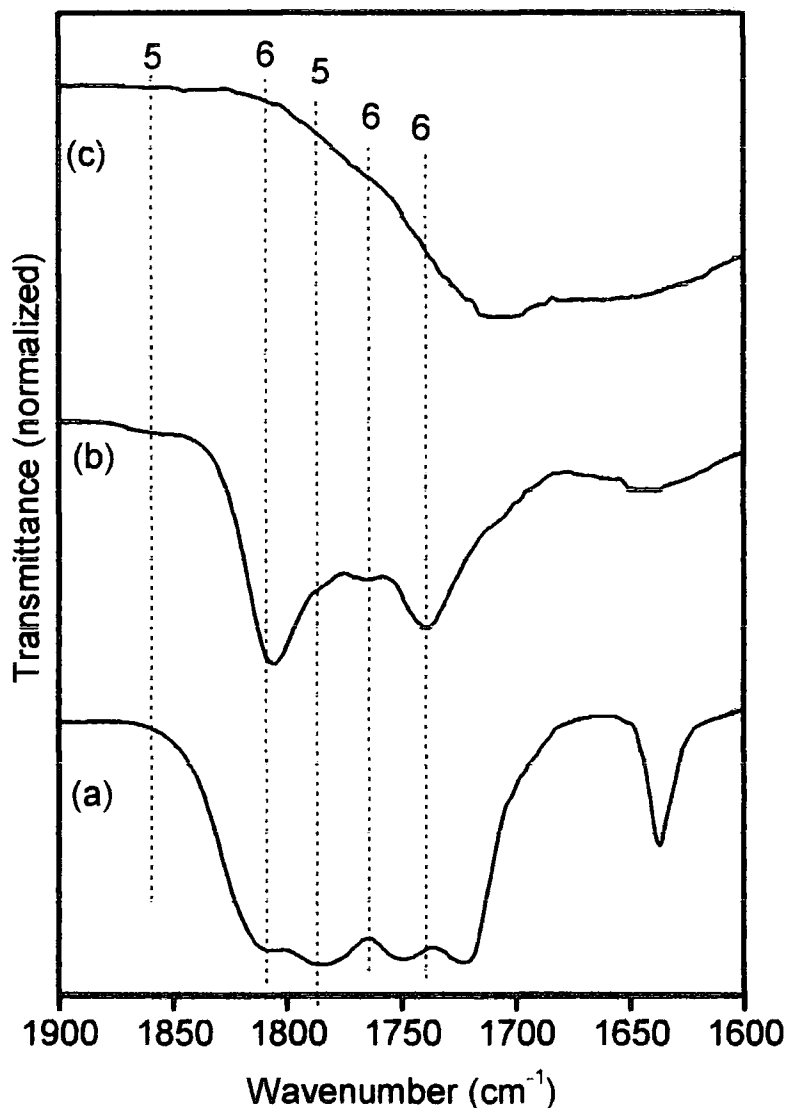


Figure 8.3.

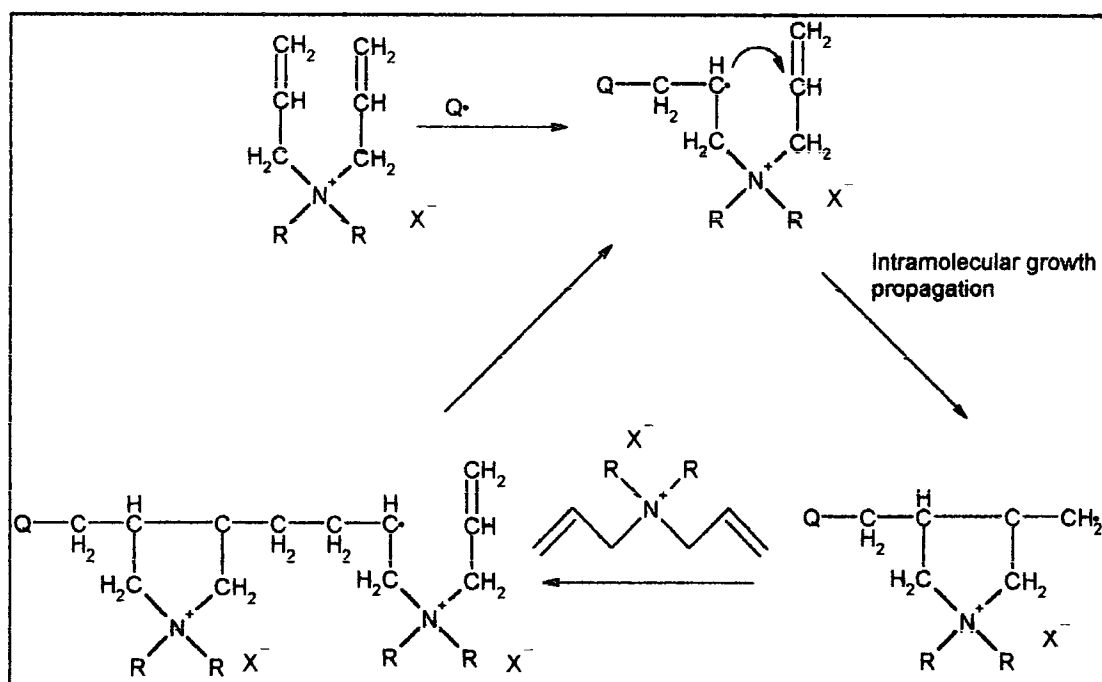
Particular in the 1900 cm^{-1} - 1600 cm^{-1} region of the infrared spectra of (a) methacrylic anhydride monomer; (b) pulsed plasma polymer (time on = $20\text{ }\mu\text{s}$, time off = 20 ms , peak power = 40 W); and (c) 3 W continuous wave plasma polymer.

The peaks at 1805 cm^{-1} , 1765 cm^{-1} and 1740 cm^{-1} are reported to be the C=O stretching of a six-membered ring poly(methacrylic anhydride).⁵ The presence of multiple peaks for six membered rings is due to different stereoisomers.⁷ The small shoulders at 1860 cm^{-1} and 1780 cm^{-1} are the two C=O stretching of a five membered ring poly(methacrylic anhydride).

8.3.3. Diallylamine Plasma Polymerization

Diallylamine is usually polymerized as quaternary ion in aqueous media. The nitrogen cation of a quaternary ammonium salt polarizes the electron density of the double bond, and favours the intramolecular propagation.¹² The possibility of cyclopolymerization of diallylamine under plasma conditions is investigated. It is believed that plasma polymerization occurs mainly via free radical mechanism. However, in the plasma ions are also present and sustain the glow discharge.¹³

Scheme 8.3: Mechanism of cyclopolymerization of diallyl quaternary ammonium salts
(Where Q is a radical initiator and X⁻ is the counteranion)



XPS elemental analysis, Table 8.1, shows oxygen incorporation in both CW and pulsed plasma polymers. In the case of the pulsed plasma polymer the elemental percentage of oxygen corresponds to that of nitrogen. The O(1s) region shows only one peak at 532.8 eV.

Table 8.1. XPS elemental analysis of diallylamine plasma polymers.

Polymer	%C	%N	%O
Conventional	85.7	14.3	0
Continuous Wave	85 ± 1	11 ± 1	3.3 ± 0.3
Pulsed	76 ± 1	11 ± 1	11.7 ± 0.8

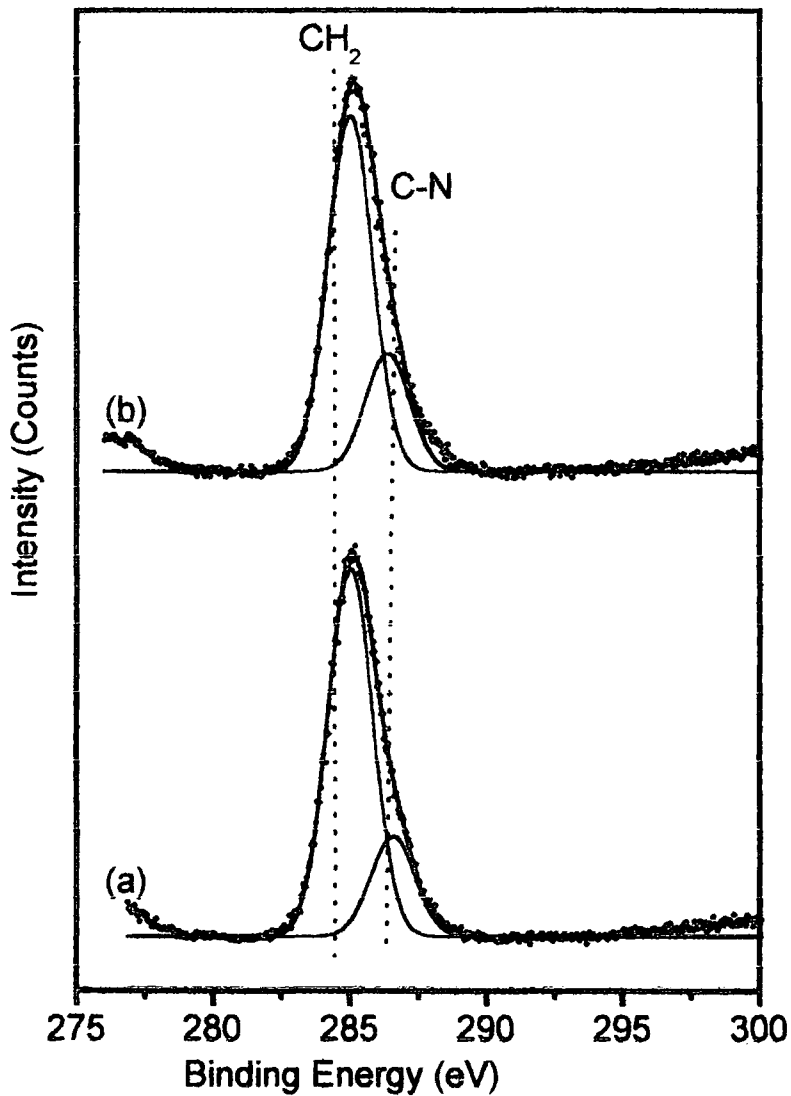


Figure 8.4.

C(1s) XPS spectra of diallylamine plasma polymers deposited onto a flat glass substrate: (a) 3 W continuous wave; and (b) pulsed (time on = 20 μ s, time off = 20 ms, peak power = 40 W).

The N (1s) envelope presents only one peak at 399.5 eV, attributed to uncharged

nitrogen,¹⁴ for both continuous wave and pulsed plasma polymers. The C (1s) envelope presents only the $\underline{\text{C}}\text{H}_2$ and the $\underline{\text{C}}\text{-N}$ peaks, and no carbon-oxygen functionalities are present in the plasma polymer layers.

For these reasons the presence of oxygen is attributed to adsorption of atmospheric moisture following air exposure of the samples. The water might be bonded to the polymer via hydrogen bonding with the secondary amino group.

Infrared analysis shows the disappearance of the C=C features (3077 cm^{-1} , C-H stretching, 1416 cm^{-1} , CH_2 scissoring, 993 cm^{-1} , CH in phase wagging, 917 cm^{-1} , CH_2 wagging) in both the plasma polymer spectra.⁶ Water absorption is confirmed by the presence of a broad band around 3400 cm^{-1} and at 1638 cm^{-1} . The continuous wave and the pulsed plasma polymer have strong resembling IR spectra. However the weak peak at 878 cm^{-1} is present only in the pulsed plasma polymer spectrum. This is attributed to the pyrrolidine ring stretching.¹⁵

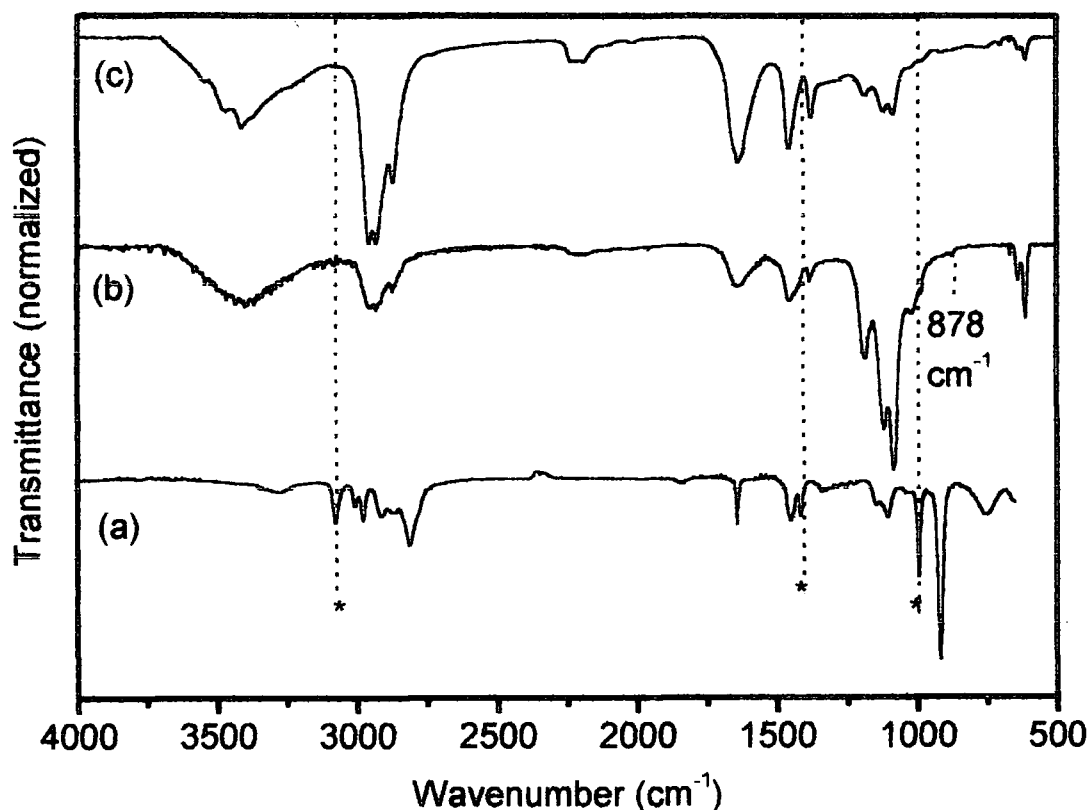


Figure 8.5.

Infrared spectra of (a) diallylamine monomer; (b) pulsed plasma polymer ($t_{\text{on}} = 20\ \mu\text{s}$, $t_{\text{off}} = 20\ \text{ms}$, peak power = 40 W); and (c) 3 W continuous wave plasma polymer.

The peak has a correspondence in the Raman at 890 cm^{-1} .⁶ No such peak is observed in the Raman of the continuous wave plasma polymer, Figure 8.6. The latter is characterized by poor resolution due to background noise.

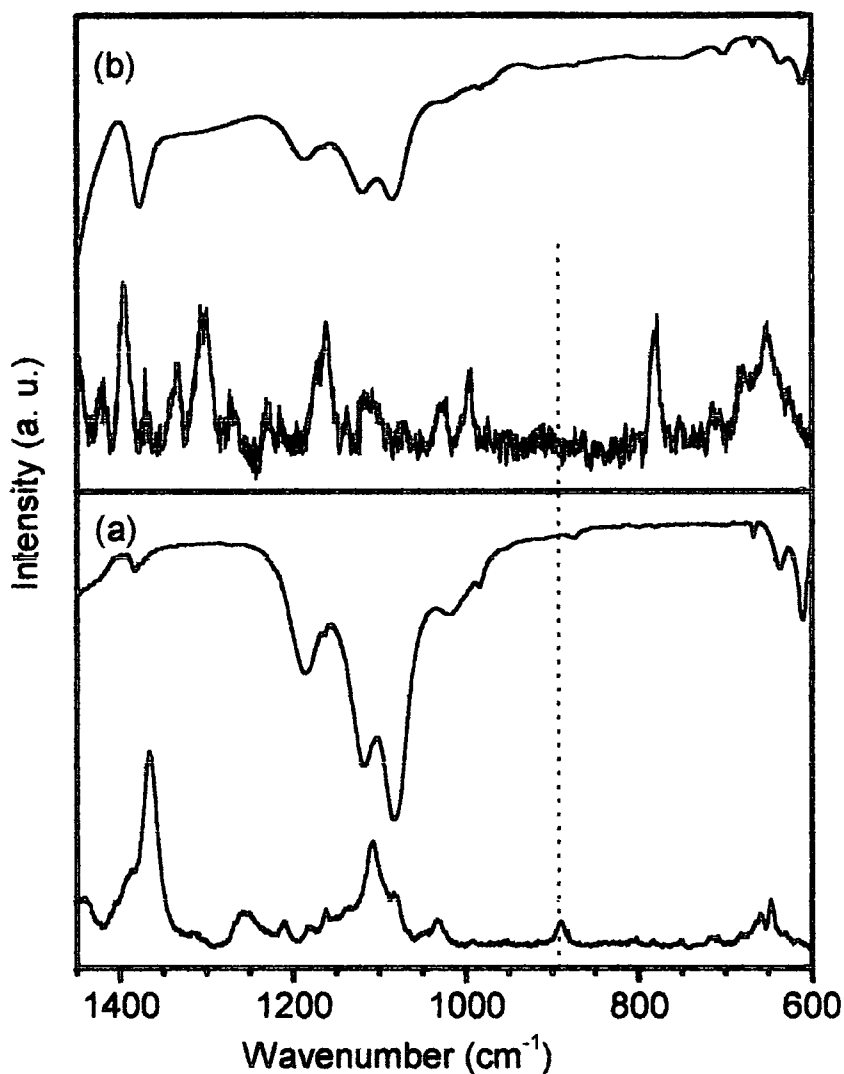


Figure 8.6.

Surface enhanced Raman spectra (below) in comparison with the infrared (above) of (a) diallylamine pulsed plasma polymer (time on = 20 μs , time off = 20 ms, peak power = 40 W); and (b) 3 W continuous wave plasma polymer.

8.4. Conclusions

Ethylene glycol dimethacrylate plasma polymerization leads to cross-linked polymers.

Vibrational spectroscopy instead suggests ring formation under pulsed plasma conditions for both diallyl amine and methacrylic anhydride.

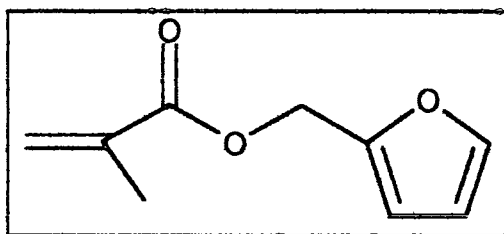
8.5. References

- [1] Butler, G. B. In *Comprehensive Polymer Science*, ; G. C. Eastmond, A. Ledwith, S. Russo and P. Sigwalt, Ed.; Pergamon Press, 1989; Vol. Volume 4: Chain Polymerization.
- [2] Jones, J. F. *J. Polym. Sci.* **1958**, *33*, 15.
- [3] Huang, W.; Baker, G. L.; Bruening, M. L. *Angew. Chem., Int. Ed.* **2001**, *40*, 1510.
- [4] Butler, G. B.; Bunch, R. L. *J. Am. Chem. Soc.* **1957**, *79*, 3128.
- [5] Butler, G. B.; Matsumoto, A. *J. Polym. Sci. Polym. Lett. Ed.* **1981**, *19*, 167.
- [6] Lin-Vien, D.; Colthup, N. B.; Fateley, W. G.; Grasselli, J. G. *The Handbook of Infrared and Raman Characteristic Frequencies of Organic Molecules*, Academic Press: New York, 1991.
- [7] Mercier, J.; Smets, G. *J. Polym. Sci., Part A: Polym. Chem.* **1963**, *1*, 1491.
- [8] Matsumoto, A.; Kitamura, T.; Masayoshi, O. *J. Polym. Sci., Polym. Chem. Ed.* **1981**, *19*, 2531.
- [9] Matsumoto, A.; Kitamura, T.; Masayoshi, O. *Makromol. Chem., Rapid Commun.* **1981**, *2*, 683.
- [10] Ohya, T.; Otsu, T. *J. Polym. Sci., Polym. Chem. Ed.* **1983**, *21*, 3503.
- [11] Crawshaw, A.; Butler, G. B. *J. Am. Chem. Soc.* **1958**, *80*, 5464.
- [12] Jang, T.; Rasmussen, P. G. *J. Polym. Sci., Part A: Polym. Chem.* **1998**, *36*, 2619.
- [13] Yasuda, H. *Plasma Polymerization*, Academic Press: New York, 1985.
- [14] Beamson, G.; Briggs, D. *High resolution XPS of organic polymers: the Scienta ESCA300 database*, John Wiley & Sons: New York, 1992.
- [15] Katritzky, A. R.; Ambler, A. P. *Physical Methods in Heterocyclic Chemistry*, Academic Press: New York, 1963; Vol. 2.

9. DIELS-ALDER CHEMISTRY AT FURAN RING FUNCTIONALIZED SOLID SURFACES

9.1. Introduction

Pulsed plasma polymerization has been proven to be a practical route to deposit coatings containing aromatic rings.¹⁻³ In this chapter the pulsed plasma polymerization of furfuryl methacrylate is investigated in order to functionalize surfaces with diene moieties that can undergo Diels-Alder reactions. Furfuryl methacrylate (Structure 9.1.) is a monomer containing a polymerizable double bond and a furan ring.

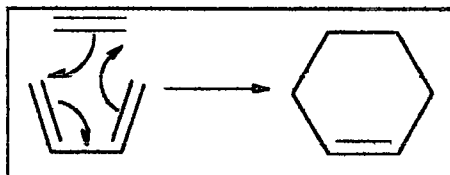


Structure 9.1.

Furfuryl Methacrylate

Furan behaves as diene in Diels-Alder reactions. Diels Alder reactions are [4+2] cycloadditions, in which a molecule containing two conjugated double bonds (a conjugated diene) reacts with a simple alkene (dienophile) to form a six membered ring (Scheme 9.1.).

Scheme 9.1. [4+2] Cycloaddition



Solution phase Diels-Alder reactions on polymers containing furan moieties are reported as a suitable method for the production of new classes of compounds or to cross-link the polymer.⁴⁻⁶ Surface Diels-Alder reactions have been investigated on various semiconductor surfaces for their possible uses in microelectronic applications.⁷⁻¹³ or to fix dyes onto solid surfaces.¹⁴

9.2. Materials and Methods

Plasma polymerization of furfuryl methacrylate (Aldrich, 97% purity) was carried out at a pressure of 0.2 mbar and 1.5×10^{-7} mol s⁻¹ flow rate, followed by film deposition for 30 min.

Subsequent Diels-Alder surface reaction with maleic anhydride (Aldrich, 99%) or maleimide (Fluka, 98%) were carried out by immersing the coated glass slides in a 1% w/v solution of the reagent in toluene (Fisher, 99.8%) for 18 hours. The substrate was then rinsed several times in toluene prior to analysis.

Transmission infrared spectra of plasma polymer films deposited onto KBr plates averaged over 16 scans. A reference spectrum of the monomer was acquired by placing a drop of liquid between two KBr plates. Whilst the maleic anhydride spectrum was acquired in ATR mode. The Diels-Alder reacted polymer was analysed in grazing angle mode. In this case, a silicon wafer was employed as the substrate.

9.3. Results and Discussion

Furfuryl methacrylate plasma polymer films deposited onto glass slides were analysed by XPS, Table 9.1.

Table 9.1. XPS elemental percentage analysis of furfuryl methacrylate plasma polymers

Coating	%C	%O	%N	%Si
Theoretical	75	25	-	-
Continuous Wave	80 ± 1	20 ± 1	-	-
Pulsed	75 ± 2	25 ± 2	-	-
Pulsed washed in toluene	76 ± 2	24 ± 2	-	-
Pulsed reacted with maleic anhydride	70 ± 3	30 ± 1	-	-
Pulsed reacted with maleimide	71 ± 3	25 ± 2	1.8 ± 0.2	2 ± 1

A depletion of oxygen was noted under continuous wave conditions; whereas pulsed plasma deposition yielded a close match to the expected theoretical value. Also the C(1s) envelope for the latter could be fitted to three carbon environments, in accordance with the monomer structure: 285.0 eV ($-\underline{\text{C}}\text{H}_2-$), 286.4 eV ($-\underline{\text{C}}-\text{O}$), and 288.9 eV ($(\underline{\text{C}}=\text{O})\text{O}$) (in the ratio of 5.4: 3.4: 1.0 compared to the theoretical values of 5: 3: 1)

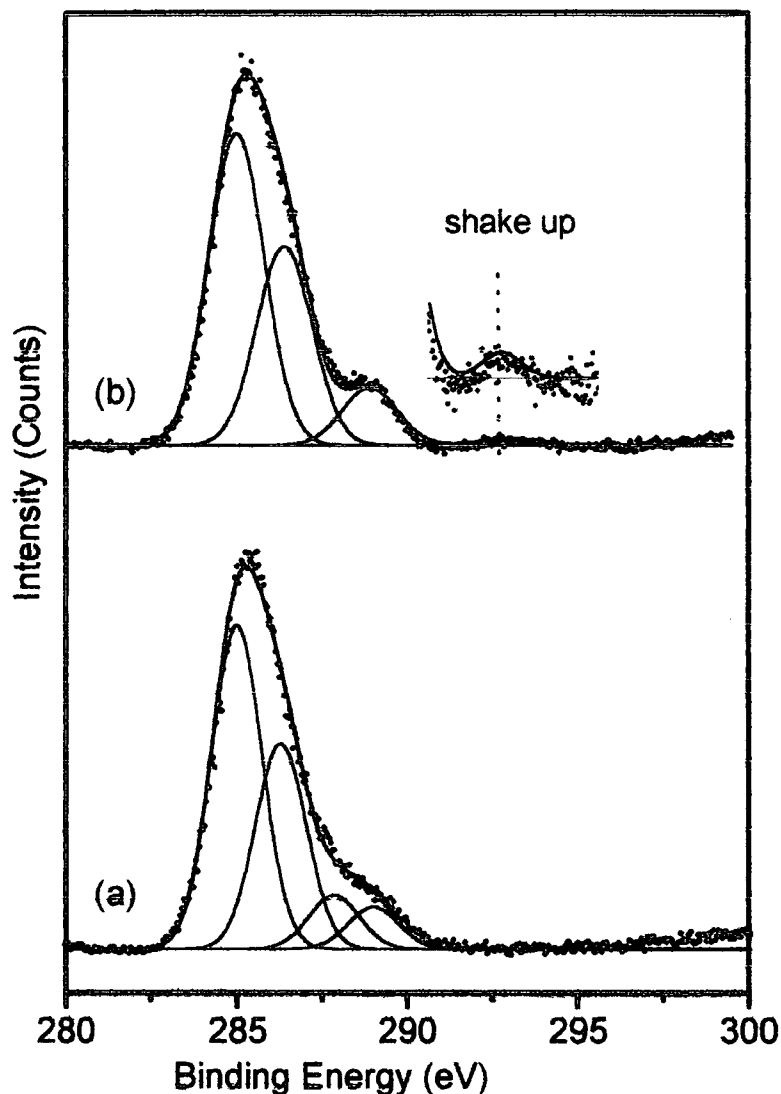


Figure 9.1.

C(1s) XPS spectra of furfuryl methacrylate plasma polymers deposited onto a flat glass slide: (a) pulsed (time on = 20 μs , time off = 20 ms, peak power = 40 W) and (b) 3 W continuous wave.

A $\pi-\pi^*$ shake-up satellite indicative of conjugation provided further evidence for structural retention of the furan ring during pulsed plasma deposition. In the case of continuous wave plasma polymerization, the oxidised carbon region in the C(1s)

envelope was attenuated, and also the π - π^* shake-up satellite was absent, thereby reflecting greater fragmentation of the precursor under these harsher conditions.

Infrared analysis gave further evidence for high levels of structural retention during pulsed plasma polymerization, Figure 9.2.

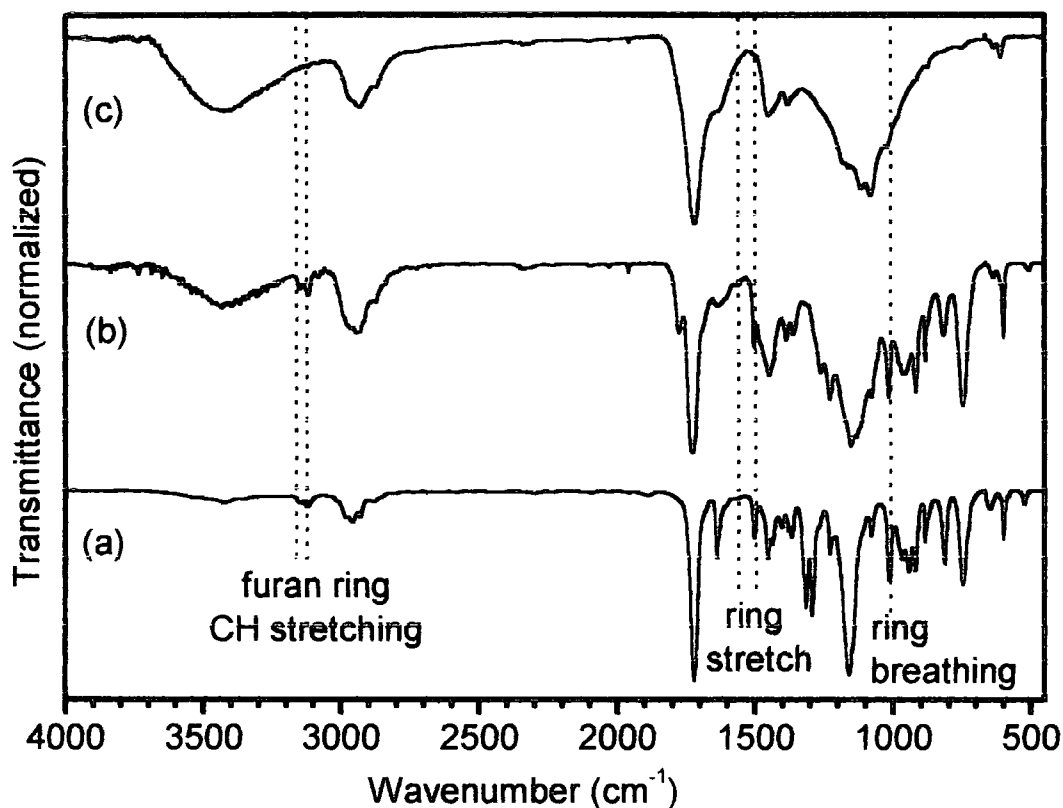
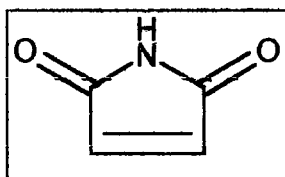


Figure 9.2.

Infrared spectra of (a) furfuryl methacrylate monomer; (b) pulsed plasma polymer (time on = 20 μ s, time off = 20 ms, peak power = 40 W); and (c) 3 W continuous wave plasma polymer.

First of all, the spectrum of the furfuryl methacrylate monomer could be assigned as follows:¹⁵⁻¹⁷ 3122 cm^{-1} and 3152 (furan ring C-H stretching), 2900-2800 cm^{-1} (saturated C-H stretching), 1718 cm^{-1} (methacrylate C=O stretching), 1636 cm^{-1} (methacrylate C=C stretching), 1560 cm^{-1} and 1501 cm^{-1} (furan ring stretching), and 1013 cm^{-1} (furan ring breathing). There were also a variety of other fingerprint bands below 1000 cm^{-1} . The pulsed plasma polymer film exhibited all of these characteristic monomer absorption features, except those associated with the methacrylate C=C double bond (e.g. 1636 cm^{-1} (methacrylate C=C stretching)). Also, the strong C=O stretch shifted to 1725 cm^{-1} , due to the loss of conjugation for the methacrylate carbonyl

group following polymerization via its double bond (the weak shoulder at 1772 cm^{-1} can be attributed to other types of carbonyl environment formed under plasma polymerization conditions). Much broader absorption bands were measured for the continuous wave plasma polymer and the characteristic furan ring features were absent.



Structure 9.2.

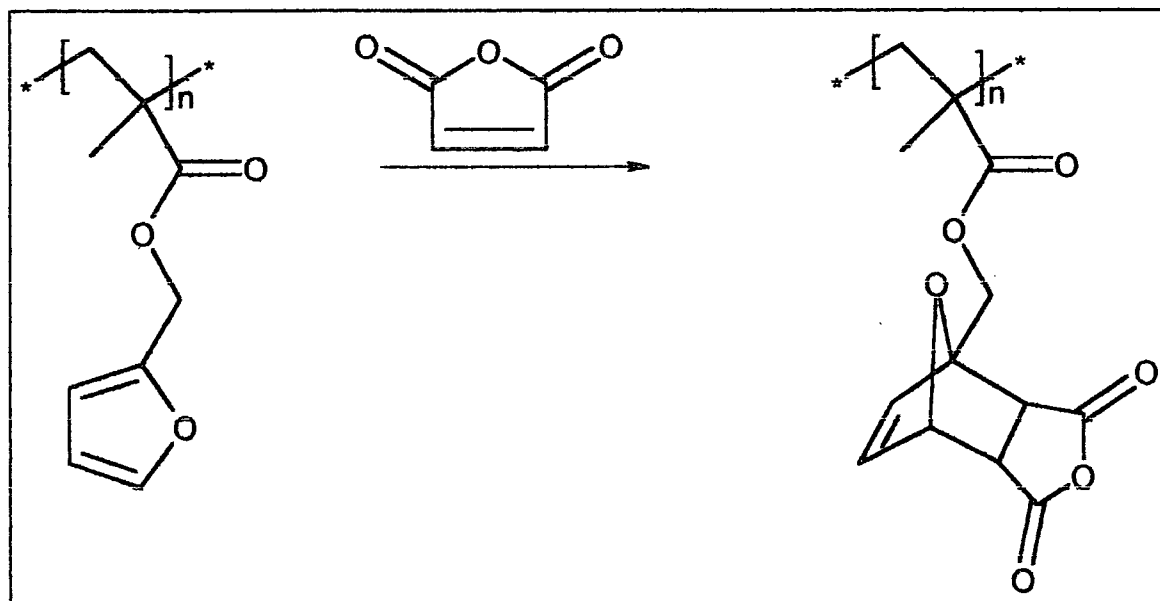
Maleimide

XPS elemental analysis of furfuryl methacrylate pulsed plasma polymer layers following reaction with maleimide (Structure 9.2) showed the appearance of the N(1s) peak at 399.0 eV. However, Si (2p) from the underlying substrate was also detected. Test experiment performed by immersing the sample in toluene for 18 h followed by XPS analysis showed no change in the elemental composition. There must be a partial delamination of the polymer film following Diels Alder reaction.

Following reaction of the furfuryl methacrylate pulsed plasma polymer layers with maleic anhydride, XPS elemental analysis indicated an increase in oxygen content, Table 9.1. This can be attributed to the incorporation of three additional oxygen atoms at the surface for each maleic anhydride molecule undergoing Diels-Alder chemistry with a furan ring, Scheme 9.2.



Scheme 9.2. Reaction of furfuryl methacrylate pulsed plasma polymer surface with maleic anhydride.



Grazing angle infrared spectroscopy of the Diels-Alder derivatized pulsed plasma polymer film (Figure 9.3.), indicated the presence of new peaks attributable to: anhydride C=O stretching (1860 cm^{-1}), C=C stretching (1636 cm^{-1}), and an intense broad band due to C-O-C ether stretching (1070 cm^{-1}).¹⁵ The Diels-Alder reaction also gave rise to an enhancement in the shoulder at 1772 cm^{-1} due to overlap with the maleic anhydride C=O stretching feature in this region. The overall predominance of the underlying pulsed plasma polymer film infrared absorption features following [4+2] cycloaddition chemistry with maleic anhydride is consistent with the reaction taking place at just the outer surface of the deposited layer.

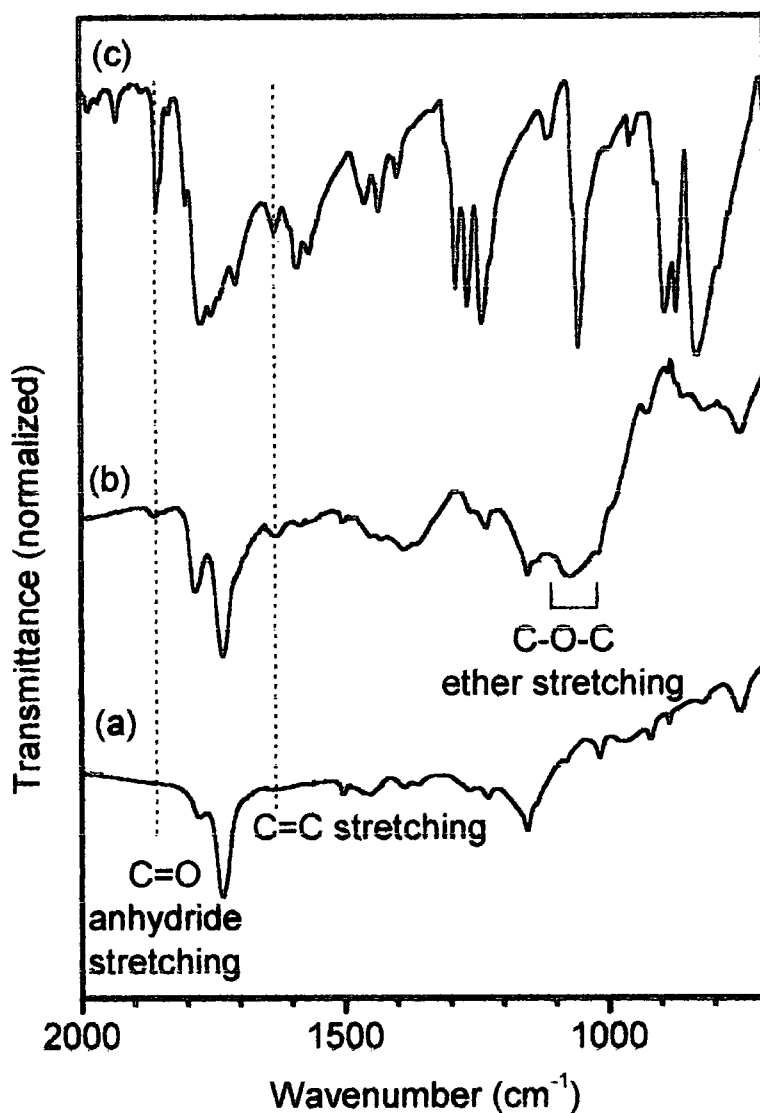


Figure 9.3.

Infrared spectra of (a) furfuryl methacrylate pulsed plasma polymer (grazing angle FTIR, time on = 20 μ s, time off = 20 ms, peak power = 40 W); (b) furfuryl methacrylate pulsed plasma polymer reacted with maleic anhydride (grazing angle IR); and (c) maleic anhydride (diamond ATR accessory).

9.4. Conclusions

To conclude, it has been shown that the surfaces of furfuryl methacrylate pulsed plasma polymer films readily undergo the [4+2] Diels-Alder cycloaddition reaction with maleic anhydride. A major benefit of this methodology is that it is easily adaptable to a whole variety of substrate materials.

9.5. References

- [1] Hynes, A.; Badyal, J. P. S. *Chem. Mater.* **1998**, *10*, 2177.
- [2] Han, L. M.; Timmons, R. B.; Bagdal, D.; Pielichowski *Chem. Mater.* **1998**, *10*, 1422.
- [3] Han, L. M.; Timmons, R. B. *J. Polym. Sci., Part A: Polym. Chem.* **1998**, *36*, 3121.
- [4] Laita, H.; Boufi, S.; Gandini, A. *European Polymer Journal* **1997**, *33*, 1203.
- [5] Kusefoglu, S. H. *J. Polym. Sci. Polym. Chem. Ed.* **1984**, *22*.
- [6] Boudevska, H. *Izv. Otk. Nauki Bulg. Akad. Nauk.* **1970**, *3*, 303.
- [7] Hossain, M. Z.; Aruga, T.; Takagi, N.; Tsuno, T.; Fujimori, N. *Jpn. J. Appl. Phys.* **1999**, *38*, L1496.
- [8] Teplyakov, A. V.; Kong, M. J.; Bent, S. F. *J. Am. Chem. Soc.* **1997**, *119*, 11100.
- [9] Teplyakov, A. V.; Kong, M. J.; Bent, S. F. *J. Chem. Phys.* **1998**, *108*, 4599.
- [10] Hovis, J. S.; Hamers, R. J. *J. Phys. Chem. B* **1998**, *102*, 687.
- [11] Hovis, J. S.; Liu, H.; Hamers, R. J. *Surf. Sci.* **1998**, *402-404*, 1.
- [12] Yousaf, M. N.; Chan, E. W. L.; Mrksich, M. *Angew. Chem. Int. Ed.* **2000**, *39*, 1943.
- [13] Hamers, R. J.; Coulter, S. K.; Ellison, M. D.; Hovis, J. S.; Podowitz, D. F.; Schwartz, M. P.; Greenlief, M. C.; Russel, J. N. J. *Acc. Chem. Res.* **2000**, *33*, 617.
- [14] Tanaka, M. Eur. Pat. Appl. 655345, 1995.
- [15] Lin-Vien, D.; Colthyp, N. B.; Fateley, W. G.; Grasselli, J. G. *The Handbook of Infrared and Raman Characteristic Frequencies of Organic Molecules*; Academic Press: New York, 1991.
- [16] Katritzky, A. R.; Ambler, A. P. *Physical Methods in Heterocyclic Chemistry*; Academic Press: New York, 1963; Vol. 2.
- [17] Bird, C. W.; Cheeseman, G. W. H. In *Comprehensive Heterocyclic Chemistry*; Pergamon Press: Oxford, 1984; Vol. 4.

10. CONCLUSIONS

In the recent years plasma processing has found several applications in various industrial fields, including adhesion technologies, biomedical applications, microelectronics and packaging. Great interest has been focussed on plasma polymerization process, a method, which consists on the deposition of a thin polymer film onto a surface in contact with an ionized gas (plasma). Compared to other processes, such as spin coating or graft polymerization, the advantages of a plasma treatment include environmental aspects (plasma treatment occurs in the gas phase and does not require solvents), single step processing, surface sensitivity and substrate independence. However, plasma polymerization has not found the same interest yet. This is mainly due to the uncontrollability of the plasma reactions and as a consequence of the properties of the resulting coating. The polymers produced under plasma state mechanism differ from conventional polymers mainly because they lack in repeat units. Extensive monomer fragmentation in the plasma produces highly cross-linked molecules. Recently, the possibility of increasing the retention of monomer structure by pulsing the electric discharge (pulsed plasma) has increased the interest and the efforts around these processes.

In this work the plasma polymerization of several monomers has been presented by following two ways, a continuous wave plasma process and a pulsed plasma process. The latter one has been achieved by pulsing the electric discharge of an inductively coupled low pressure RF reactor. The comparison between the two methods clearly demonstrate that using pulsed plasma it is possible to selectively activate C-C double bonds retaining the other molecule functionalities in the polymer film. It is believed that this effect is caused by the very low average powers and reduced ion bombardment achievable under these conditions.

In continuous wave plasma, the monomers' molecules are essentially randomized, breaking down into all conceivable fragments (ions or radicals). This results in uncontrollability of the process. When very short bursts of plasma are instead provided, the molecules are allowed to react without further fragmentation. As a result, the chemical functionalities of the monomer are retained in the polymer film.

It should be noted that despite the increasing use of pulsed plasma polymerization no explanation on the mechanism has been found yet. It is not clear whenever radicals or ions are involved in the reactions. However, some considerations can be drawn.

Firstly, a dependence of film properties on the duty cycle has been observed. For example, the chain length of 2-hydroxyethyl methacrylate pulsed plasma polymer coatings, is related to the duty cycle. The shorter the time on, the longer the chains. The longer the time off the longer the chains. This evidence suggests a mechanism in which the activated species produced by the plasma during the time on react during the time off.

In the time on period radicals or ions are quickly formed. This step could be thought as the initiation step in the conventional polymerization. The plasma replaces conventional initiators, such as peroxides, strong acids or bases. A short time on period reduces the fragmentation of the monomers, because the average power delivered by the system and the ion bombardment is drastically reduced.

The species formed during the time on can undergo conventional polymerization pathways during the time off, as it is confirmed by the fact that longer period gives rise to an increment of the polymer length chain.

Obviously, the molecular structure of the monomer plays an important role in the final result. As shown in this thesis, acrylates and methacrylates generally work better than their allylic or vinylic homologues. This can be explained considering the stability of the intermediates. Due to the resonance with the ester carbonyl group (meth)acrylic ions or radicals are much more stable than the allyl or vinyl analogues.

On these bases, the actual process that occurs in the pulsed plasma polymerization should not be very different from those of the conventional polymerization. For example, methacrylic anhydride or allyl amines have showed to give ring formation, with a mechanism that resembles the conventional one.

However, these considerations do not want to be exhaustive as explanation of a very broad topic. Only the direct observation of the species in the plasma would provide enough information to elucidate the mechanism of pulsed plasma polymerization. These would require a deep study on several monomers and the use of plasma diagnostic tools to detect the intermediates involved in the process.

The monomers used in this work have been chosen on the basis of the functionalities present in their structures, since they are responsible of the properties of the resulting polymer films. So, for example, fluorinate monomers, such as 2,2,3,4,4,4-hexafluorobutyl methacrylate (HFBMA), are expected to give hydrophobic coatings with excellent non-wettability properties, whereas hydroxyl monomers, such as 2-hydroxyethyl methacrylate (HEMA), are expected to give hydrophilic coatings. On this

basis, the properties of a given coating can be predicted by choosing the suitable monomer.

This has been the main purpose of this thesis, a pulsed plasma application's approach rather than an attempt to understand the real mechanism of the process.

In general the importance of plasma polymer coatings lies in the fact that they provide the treated materials with unique properties, without changing their bulk characteristics. An example is given by the non-wettable, non-gluable Teflon, which can adhere after plasma treatment when it is coated with a glycidyl methacrylate or a 2-cyanoethyl acrylate plasma polymer.

In addition, it has been demonstrated that the functionalities retained in the polymer films can undergo conventional chemical reactions, such as nucleophilic attack on epoxide carbons, Diels Alder coupling of furan ring, complexation of metal ions from aqueous solution. This allows further functionalization of plasma polymer surfaces and the broadening of their possible applications. For example, epoxide functionalized surfaces have been successfully reacted with carboxylic acid and amine. The second case is particularly important in adhesion as it is at the basis of the curing of epoxy resins.

The reaction of epoxide functionalized surfaces with Jeffamine and Pamam Dendrimers has demonstrated that it is possible to couple pulsed plasma polymers even with high molecular weight compounds. This opens the applications of the process to a wide range of fields. For example, proteins could be immobilized on the surface for the creation of biosensors in diagnostic devices, or they could be use in catalysis. Cyclodextrins could instead be used for the selective entrapment of small molecules. Complexation of metal ions is also possible onto the surface. For example, cyano plasma polymer films have been used to complex silver ions onto the surface, providing it with antibacterial properties. This approach could be applied to other ions, for catalytic applications.

To conclude I can say that compared to low power continuous way, pulsed plasma polymerization allows the retention of several, even complex, carbon functionalities in the plasma polymer coating. This leads to "tailor-made" surfaces for several applications. Compared to other methods of surface functionalization, i.e. grafting or spin coating, pulsed plasma polymerization has the advantage to be single step and substrate independent. In addition, the coating generally presents good adhesion to the substrate, and the whole process is completely dry. The main disadvantage of the process is the necessity to operate under vacuum. This raises the cost of the process in

view of industrial applications, and makes it difficult for those substrates, which would require long pumping times before it is possible to reach in the plasma chamber the pressure desired. Another disadvantage is the dependence of the plasma on a variety of parameters, such as frequency of exciting potential, excitation power, monomer flow rate, plasma pressure and geometry, which are not always controllable. This makes the transfer and as a consequence the spread of this technology very difficult, in particular from an industrial point of view.

However, it is reasonable to think that in the view of its advantages, particularly the solvent less and the single step aspects, pulsed plasma polymerization will receive more and more attention in the future.

